Implications of gravitational instantons for the strong CP problem and axions

ZHE CHEN

THE UNIVERSITY OF SYDNEY

Supervisor: Prof Archil Kobakhidze

A thesis submitted in fulfilment of
the requirements for the degree of
Doctor of Philosophy

School of Physics
Faculty of Science
The University of Sydney
Australia

5 February 2024

Declaration

I, Zhe Chen, declare that this thesis is submitted in partial fulfillment of the requirements for the conferral of the degree Doctor of Philosophy (Ph.D) from the University of Sydney is wholly my work unless otherwise referenced or acknowledged. This document has not been submitted for qualifications at any other academic institution.

Zhe Chen
5 October 2023

Abstract

The thesis investigates quantum gravity effects on the topological $\theta-$vacua in Yang-Mills theories and their implications for the problem of violation of combined CP parity in strong interactions. Namely, we argue that a new set of Yang-Mills instantons on Eguchi-Hanson spaces (the coloured Eguchi-Hanson instantons) are responsible for the violation of CP in strong interactions in addition to the CP violation due to the Yang-Mills instantons on flat spacetime. This additional CP violation, like the standard one is dominated by large-size instantons. Being dominated by infrared physics, it is only marginally suppressed relative to the standard strong CP and hence provides a sizable contribution to the physical observables, most notably to the electric dipole moment of the neutron. Consequently, we find that the standard one-axion Peccei-Quinn mechanism is insufficient to enforce CP symmetry in strong interactions to the level that is consistent with experimental bounds on the neutron electric dipole moment.

We have proposed an extension of the standard Peceei-Quinn mechanism to provide a genuine solution to the strong CP problem. This extension introduces an additional axion field, a companion to the standard QCD axion. Our model offers a rich and interesting phenomenology that is studied in this thesis. In particular by reviewing constraints on axion-photon couplings, quite remarkably we find that future axion searches with haloscopes and helioscopes may well discover two QCD axions, perhaps even within the same experiment.

We also study the cosmological production of companion-axion dark matter in order to predict windows of preferred axion masses and calculate the relative abundances of the two particles. Additionally, we show that the presence of a second axion solves the cosmological domain wall problem automatically in the scenarios in which one or both of the axions are post-inflationary. We also suggest unique cosmological signatures of the companion-axion model, such as the production of a ~ 10 nHz stochastic gravitational wave background, and $\sim 100\ M_{\odot}$ primordial black holes.

Publication list and attribution statement

This thesis is based on the following papers:

(1) Zhe Chen and Archil Kobakhidze. Coloured gravitational instantons, the strong CP problem and the companion axion solution. *The European Physical Journal C*, 82(7):1– 6, 2022.

(2) Zhe Chen, Archil Kobakhidze, Ciaran A. J. O'Hare, Zachary S. C. Picker, and Giovanni Pierobon. Cosmology of the companion-axion model: dark matter, gravitational waves, and primordial black holes. *arXiv preprint* arXiv:2110.11014, 2021.

(3) Zhe Chen, Archil Kobakhidze, Ciaran A. J. O'Hare, Zachary S. C. Picker, and Giovanni Pierobon. Phenomenology of the companion-axion model: photon couplings. *The European Physical Journal C*, 82(10):940, 2022.

Chapter 6 is published as (1). Chapter 7 and 8 are published as (2) and (3), but the order of the content has been adjusted for legibility. Authors lists are alphabetical in all cases. All of these publications resulted from a true collaboration between all authors. My contribution to all publications was essential both idea-wise and in technical implementation. In particular, most of the calculations in (1) were done by me with guidance from my supervisor. I contributed with my theoretical expertise and model building in projects (2) and (3), performed analytical calculations, and provided input into the physical interpretation of the obtained results.

Zhe Chen, 5 October 2023

I confirm that the thesis was written by Mr Zhe Chen. I also confirm Mr Zhe Chen's contribution to the original work as described above.

Prof Archil Kobakhidze, 5 October 2023

Acknowledgements

First and foremost, I must express my deepest gratitude to my supervisor, Professor Archil Kobakhidze, for all his professional guidance and encouragement. He guided me to the heart of theoretical physics: field theory, particle, and general relativity. With his support, I could glimpse physics's vast and profound world. From him, I see enthusiasm, persistence, and rigor. I believe these spirits will influence me all my life. Secondly, I would like to thank Ciaran, Zac, and Giovanni for all their indispensable efforts in our collaborative papers. Thirdly, I would like to thank the University of Sydney for its safe, comfortable, and decent environment. Finally, I thank my family for your steadfast support and love.

The journey ahead is long, my friends, take care.

Contents

CHAPTER 1

Introduction

1.1 Overview

Quantum theory and general relativity form the two cornerstones of modern physics. Although many reliable experiments have verified them, the two are incompatible. We apply quantum theory on smaller scales relevant to particle physics. However, general relativity, such as astronomy and cosmology, is essential on larger scales. The strength of gravitational interactions is so small that we usually ignore them when we study particle interactions. This is not always the case due to the existence of complex vacuum structures with transitions between vacua mediated by instantons.

Instantons usually refer to the (anti) self-dual solutions to the Yang-Mills equations[1]. They are closely related to the topology of the gauge field vacua. Later, the (anti) self-dual solutions to the Einstein field equation were also found and are known as *gravitational instantons*[2]. Yang-Mills and gravitational instantons induce topological interaction terms and contribute to neutron electric dipole moment. The instantons effects are *non-perturbative* and led to the well-known strong CP problem [3].

The strong CP problem has not been solved yet. A hypothetical particle called *axion* is a widely accepted and desirable resolution. The axion comes from the spontaneous breaking of a new global $U(1)$ symmetry called the *Peccei-Quinn symmetry*, which Roberto Peccei and Helen Quinn originally proposed in 1977[4, 5]. The Peccei-Quinn solution essentially promotes the θ parameter as a field, explaining why the CP violation effect is so tiny in strong interactions.

Besides solving the strong CP problem, axion is also a compelling candidate for dark matter [6, 7, 8, 9]. The axion is exceptionally light, non-relativistic, and weakly interacting, which aligns with the characteristics of dark matter particles. Numerous experiments, such as the Axion Dark Matter Experiment (ADMX)[10, 11, 12, 13, 14], are actively searching for axions to confirm their existence and shed light on the nature of dark matter.

This thesis focuses on gravitational instanton contribution to the big CP problem and relevant implications on various topics. The rest of this chapter will briefly review general relativity and some basics of quantum field theory and the Standard Model. In Chapter 2, we will review the path integral of the derivation of chiral anomaly. We will introduce instanton in Chapter 3. In Chapter 4, we will present the well-known strong CP problem and its resolution: axion. Chapter 6 will introduce the companion-axion model. Chapter 7 and 8 are implications of the companion-axion model.

1.2 General Relativity

1.2.1 Special Relativity

Special relativity was formulated by Einstein, Lorentz, and Poincare and applied to the inertial reference frame of spacetime theory. This is an extension and modification of Newtonian spacetime theory. By the end of the 19th century, Maxwell's theory had been verified by many experiments, but it did not transform covariantly under the Galilean transformation of classical mechanics. Covariance means that the laws of physics have the same form in different reference frames. To solve this issue, physicists proposed the "aether hypothesis" to abandon the relativity principle and hold that Maxwell's equations only fit for an absolute reference frame (aether). According to this hypothesis, the speed of light in a vacuum calculated by Maxwell's equations is relative to the absolute reference frame (aether). The speed of light has different values in the reference frame of motion relative to the "aether". But Michelson-Morley's experiments [15] negated the aether hypothesis. The experiment results showed that the speed of light is independent of the motion of the reference frame. Einstein realized that a new theory of time and space could be established if the experimental fact that "the speed of light in a vacuum is independent of the reference frame" was accepted as the basic principle. In 1905, Einstein published his famous paper "On the Electrodynamics of Moving Bodies" [16], which established the theory of special relativity, successfully describing the motion of macroscopic objects. The basic principles of special relativity include the following two postulates [17]:

(1) Special principle of relativity: the laws of physics take the same form in *all* inertial systems.

(2) Principle of the invariant speed of light: the speed of light in a vacuum is the same in *all* inertial systems.

Special relativity also holds that there is no absolute space and time and that space and time are not independent. Still, they should be described as a unified four-dimensional space-time, like Minkowski. This can be seen from the well-known Lorentz transformation of special relativity. The Lorentz transformation states that an event with spacetime coordinates (t, x, y, z) in reference S and another event (t', x', y', z') in a reference frame S' moving at a velocity v along the x-axis are related in the following way:

$$\begin{aligned} t' &= \frac{t - vx/c^2}{\sqrt{1 - v^2/c^2}} \\ x' &= \frac{x - vt}{\sqrt{1 - v^2/c^2}} \\ y' &= y \\ z' &= z. \end{aligned} \tag{1.1}$$

It can be seen that if one changes the reference frame, the time of the events he observed changes accordingly. A relatively simple conclusion is that when we see two events happening simultaneously in an inertial frame, they might not co-occur by changing the inertial frame. So, simultaneity is relative. This is different from Newtonian mechanics. Except for the relativity of simultaneity, we can also conclude the *time dilation* and *length contraction* from Lorentz transformation. Time dilation means that when an object moves, everything about it slows down from the point of view of the frame of reference. According to Lorentz transformation, the dilation factor is $1/\sqrt{1-v^2/c^2}$. Length contraction means that the length of the moving axis observed by an observer moving relative to an object gets a factor $\sqrt{1-v^2/c^2}$ and is shorter than the same length observed by an observer at rest close to the thing.

1.2.2 The birth and development of General Relativity

After special relativity was established, Einstein began to think about how gravity could fit into the framework of special relativity. He conceived two thought experiments:

(1) stationary elevator on the ground versus upward accelerating elevator in deep space.
(2) freely falling elevator on the ground versus still standing elevator in deep space.

Assuming someone is in a closed elevator for the first experiment. Scenario one: This person is standing still on Earth and feels gravity. Another scenario: The elevator is accelerating upward through space (meaning without the gravitational pull of any star). As a man in an elevator, he felt a force pulling down. Still, he couldn't tell whether it was an inertial system in a gravitational field (a stationary elevator on the ground) or a non-inertial system without a gravitational field (an upward accelerating elevator in deep space). We have similar conclusions for the second thought experiment by the same analysis. Einstein then proposed the famous *weak equivalence principle* as a fundamental postulate of general relativity: locally, gravity has the same effect as an accelerating reference frame (non-inertial frame). This means that we cannot distinguish gravitational and non-inertial systems in a *local* region. Local region means that this region is small enough to have a uniform gravitational field. We can view the gravitational field as the dynamic effect of a non-inertial frame or vice versa.

The weak equivalence principle also gives profound insight into another puzzle: Why does inertial mass m_I equal gravitational mass m_G? Inertial mass m_I is the mass that measures the net force on an object, while gravitational mass m_G measures the gravitational force. When there only exists gravity, the acceleration a of an object is then $a = (m_G/m_I)g$. Two objects with different m_G/m_I will have different accelerations. But it's not weird to have different accelerations, like in an electric field: two charged bodies usually have different charge-to-mass ratios and, therefore, have different accelerations. There is no doubt about that. However, numerous experiments have shown that m_G/m_I is the same for every object and can be adjusted to 1, that is, $m_I = m_G$. Why does $m_I = m_G$ hold for *every* object? This universal phenomenon shows that gravity is something *intrinsic* of spacetime itself. Spacetime is like a table. If one bottle falls on the table, something may be wrong. But the problem could be the table itself if all the bottles fall. So it's reasonable to think that gravity doesn't exist as a force but as spacetime bends, changing how things move. Therefore, two free particles with the same initial state must have the same four-dimensional spacetime trajectory (worldline), so they must have the same acceleration, and it can be deduced that the inertial mass is equal to the gravitational mass. With this level of understanding, geometry is a natural tool for describing spacetime: we regard spacetime as a manifold and relate its curvature to gravity.

In addition to the weak equivalence principle, Einstein also proposed the *strong equivalence principle*. The strong equivalence principle states that *any* physical experiment cannot distinguish between gravity and acceleration in a local region. In the weak equivalence principle, the motion of a free-falling body cannot distinguish between gravity and acceleration, while the strong equivalence principle emphasizes that all experiments cannot distinguish between them, not just dynamics. In other words, in any small enough free-falling local reference frame, all the laws of physics should be the same as in an inertial reference frame without gravitational fields. Another point is that the weak equivalence principle is concerned with point-like masses; the strong equivalence principle extends this to encompass all types of matter, even self-gravitating.

Another pillar of general relativity is the *general covariance*, which states that the laws of physics take the same form in *all* reference frames. The essential idea is that coordinates do not exist innately in nature but are merely a trick to help formalism. It should, therefore, play no role in formulating the fundamental laws of physics. Regarding this principle, physical quantities are expressed as tensor fields on spacetime, treated as a manifold. This way, when two tensors T and T' are equal, their components are equal under any coordinate system. This point also holds for equations. For example, Newton's equations of gravity

$$\nabla^2\Phi = 4\pi\rho \tag{1.2}$$

is not invariant under arbitrary coordinates transformation and must be modified. General relativity dramatically changed the study of physics, and its effects were profound. Two important objects of study are black holes and gravitational waves.

A black hole is a region of spacetime where gravity is so strong that nothing, including light, can escape. The boundary of a black hole is called the event horizon. Despite black holes' complex and mysterious structure, only three variables must be specified to classify them: mass, electric charge, and angular momentum. This is known as *no-hair conjecture*. Human scientists took the first image of a black hole in 2019 for the first time.

As matter moves through spacetime, the warping of spacetime moves with it. The twisting changes caused by these accelerating objects spread like waves at the speed of light. This propagation is known as *gravitational waves*. In 2015, the LIGO Scientific and Virgo Collaboration observed transient gravitational wave signals from merging two black holes. Since then, many more gravitational wave events have been observed, such as GW170817, the first gravitational wave event from the merger of two neutron stars, detected on August 17, 2017. In 2017, Reiner Weiss, Barry Clark Barish, and Kip Stephen Thorne won the Nobel Prize in Physics for their successful observation of gravitational waves.

1.2.3 Mathematics of General Relativity

In this subsection, we briefly review the mathematical elements of general relativity [**18**, **19**, **20**, **21**]. Four-dimensional spacetime is treated as a manifold M. Physical quantities are treated as tensor fields on M. A tensor field is a map T that smoothly assigns each point p of M a tensor T_p. T can be expanded under M's local coordinate chart $x^\mu = (x^0, x^1, x^2, x^3)$ as

$$T = T^{\mu_1..\mu_l}_{\nu_1\nu_2...\nu_m} \partial_{\mu_1} \otimes \partial_{\mu_2} ... \otimes dx^{\mu_l} \otimes dx^{\nu_2} ... \otimes dx^{\nu_m}, \tag{1.3}$$

where $T^{\mu_1..\mu_l}_{\nu_1\nu_2...\nu_m}$ is called T's components. 'Local' means this expansion only holds in an open subset of M. When we choose a new coordinate system or expand it in another local coordinate chart, $x'^\mu = (x'^0, x'^1, x'^2, x'^3)$, $T^{\mu_1..\mu_l}_{\nu_1\nu_2...\nu_m}$ must change correspondingly to keep T

invariant. Let $x'^{\mu} = f^{\mu}(x)$ be the transformation between two coordinate systems, we have

$$\partial_\mu = \frac{\partial x'^{\lambda}}{\partial x^{\mu}}\partial'_\lambda, \quad dx^\nu = \frac{\partial x^\nu}{\partial x'^{\alpha}}dx'^{\alpha}. \tag{1.4}$$

Expanding T in another coordinates system x'^{μ}:

$$T = T'^{\lambda_1..\lambda_l}_{\alpha_1...\nu_m}\partial'_{\lambda_1} \otimes \partial'_{\lambda_2}... \otimes dx'^{\alpha_1} \otimes dx'^{\alpha_2}... \otimes dx'^{\alpha_m}. \tag{1.5}$$

Using Eq.1.4, we have the following *covariant* transformation rule between components under different coordinate systems

$$T'^{\lambda_1..\lambda_l}_{\alpha_1...\nu_m} = T^{\mu_1...\mu_l}_{\nu_1...\nu_m}\frac{\partial x'^{\lambda_1}}{\partial x^{\mu_1}}...\frac{\partial x'^{\lambda_l}}{\partial x^{\mu_l}}...\frac{\partial x'^{\nu_1}}{\partial x^{\alpha_1}}...\frac{\partial x'^{\nu_m}}{\partial x^{\alpha_m}}. \tag{1.6}$$

The physical laws and equations are expressed in terms of relationships between tensors (field), and these relationships are independent of the coordinate system. This means if we have $T = 0$, then all its components are zero under any coordinate system.

Spacetime manifold M is usually equipped with a second-order tensor field called *metric*, denoted as g or ds^2. Metric smoothly assigns each point a symmetric bilinear form that takes two tangent vectors there as input. In particular, taking two basis vectors ∂_μ, ∂_ν from a given coordinate chart as input gives the metric's components:

$$g_{\mu\nu} = g(\partial_\mu, \partial_\nu). \tag{1.7}$$

Just as we use derivatives to study functions, we also need some derivatives to study tensor fields on a manifold. This kind of derivative is called *connection*. Further, we require it to be *compatible* with metric and *torsion-free*. The fundamental theorem of (pseudo) Riemannian geometry states that there is a unique such connection ∇ called the Levi-Civita connection that satisfies two conditions. Components of ∇ are written as $\Gamma^\alpha_{\beta\lambda}$, which is not a tensor but simply an object carrying three indices:

$$\Gamma^\alpha_{\beta\lambda} = \frac{1}{2}g^{\alpha\mu}(\partial_\beta g_{\mu\alpha} + \partial_\alpha g_{\mu\beta} - \partial_\mu g_{\alpha\mu}). \tag{1.8}$$

Differentiating a tensor $T^{a_1 a_2..a_l}_{b_1 b_2..b_m}$ along a direction given by vector field $X = X^\mu \partial_\mu$ gives a new tensor $T' = \nabla_X T$ whose component is given by

$$\begin{aligned} T'^{\alpha_1\alpha_2...\alpha_l}_{\beta_1\beta_2...\beta_m} &= X^\mu (\nabla_\mu T)^{\alpha_1\alpha_2...\alpha_l}_{\beta_1\beta_2...\beta_m} \\ &= X^\mu (\partial_\mu T^{a_1 a_2..a_l}_{b_1 b_2..b_m} + \Gamma^{\alpha_1}_{\mu\tau} T^{\tau\alpha_2...\alpha_l}_{\beta_1\beta_2...\beta_m} + \Gamma^{\alpha_2}_{\mu\tau} T^{\alpha_1\tau...\alpha_l}_{\beta_1\beta_2...\beta_m} + .. + \Gamma^{\alpha_l}_{\mu\tau} T^{\alpha_1\alpha_2...\tau}_{\beta_1\beta_2....\beta_m} \\ &- \Gamma^\tau_{\mu\beta_1} T^{\alpha_1\alpha_2...\alpha_l}_{\tau\beta_2....\beta_m} - \Gamma^\tau_{\mu\beta_2} T^{\alpha_1\alpha_2...\alpha_l}_{\beta_1\tau....\beta_m} - ... - \Gamma^\tau_{\mu\beta_m} T^{\alpha_1\alpha_2...\alpha_l}_{\beta_1\beta_2....\tau}). \end{aligned} \tag{1.9}$$

With the Levi-Civita connection at hand, we can write down the Riemann curvature tensor $R^\alpha_{\beta\lambda\tau\sigma}$, which measures the deviation of a vector concerning the original vector after it travels around a closed loop:

$$R^\alpha_{\beta\lambda\sigma} = \partial_\lambda \Gamma^\alpha_{\sigma\beta} - \partial_\sigma \Gamma^\alpha_{\lambda\beta} + \Gamma^\alpha_{\lambda\tau}\Gamma^\tau_{\sigma\beta} - \Gamma^\alpha_{\sigma\tau}\Gamma^\tau_{\lambda\beta}. \tag{1.10}$$

Contracting the first and the third indices of the Riemann curvature tensor, we get Ricci tensor $R_{\beta\sigma}$:

$$R_{\beta\sigma} = R^\alpha_{\beta\alpha\sigma}. \tag{1.11}$$

Roughly speaking, the Ricci tensor measures how a volume in a curved space differs from that in a flat space. Contracting the indices of the Ricci tensor, we get Ricci scalar R:

$$R = R_{\beta\sigma} g^{\beta\sigma}. \tag{1.12}$$

In terms of Ricci tensor, Ricci scalar, and metric, Einstein field equations read

$$R_{\mu\nu} - \frac{1}{2} g_{\mu\nu} R = T_{\mu\nu}, \tag{1.13}$$

where $T_{\mu\nu}$ is the energy–momentum tensor, determined by the distribution of matter. These ten equations express the relationship between the geometric properties of spacetime and the distribution of matter and energy. The geometric term on the left describes the curvature of spacetime, and the matter term on the right describes the distribution of energy and momentum in spacetime. The equations thus determine the curvature of spacetime and the motion of matter. Einstein field equations is a nonlinear system of equations whose solution needs to include the specific energy-momentum distribution and boundary conditions. Einstein field equations are vital in studying gravitational fields, black holes, cosmology, and other fields, providing a basis for understanding the universe's evolution and the nature of gravity.

1.3 Field theories and the Standard Model

1.3.1 Quantum field theory

In theoretical physics, quantum field theory is a language used to describe the interaction of elementary particles. It is a self-consistent set of concepts and tools that combines quantum mechanics with classical field theory and is compatible with special relativity. Quantum field theory has had very mature contents and achievements, but the development process is very tortuous.

Quantum mechanics dates back to Max Planck's work on black-body radiation in 1900. Planck regarded the atoms emitting and absorbing radiation in the object as tiny quantum harmonic oscillators and assumed that the energy of these quantum harmonic oscillators was not continuous but discrete values and that the radiation energy absorbed and emitted by individual quantum harmonic oscillators was quantized. Five years later, Einstein's photoelectric effect experiments showed that light comprises discrete clumps of energy called photons, which are quanta of light. This means that electromagnetic radiation is a form of particle. In 1924, Louis de Broglie proposed the wave-particle duality hypothesis, which states that microscopic particles behave as waves and particles under different circumstances. The success of early quantum theory, which consisted of many back-of-the-envelope calculations and gut guesses like these, depended on its ability to explain previously unexplainable experimental results. Between 1925 and 1926, thanks to the valuable contributions of de Broglie, Werner Heisenberg, Max Born, Erwin Schrodinger, Paul Dirac, Wolfgang Pauli, and others, quantum theory was developed into a self-consistent theory called "Quantum Mechanics". Since then, the framework of quantum theory has been laid. In those days, electromagnetic fields were a hot topic. Dirac first coined the term "Quantum Electrodynamics" (QED) in his famous paper "The Quantum Theory of the Emission and Absorption of Radiation". His method successfully explained both the emission and absorption of radiation by atoms. His method could also explain the scattering of photons and resonance fluorescence up to second-order perturbation. However, the calculation of higher-order perturbation diverged. Later, in 1928, Dirac proposed the Dirac equation, which could describe the motion of relativistic electrons.

However, the Dirac equation showed electrons seemed to have a negative energy state. Dirac realized that to explain the negative energy state, he would have to assume that antiparticles exist. Finally, in 1932, Carl David Anderson discovered positrons. However, the development of quantum field theory stalled because of the infinity problem mentioned earlier in the calculation. It wasn't until 20 years later, around 1950, that Julian Schwinger, Feynman, Freeman Dyson, and Shinichiro Tomonaga finally found a more reliable method for removing infinity in quantum electrodynamics [22, 23, 24, 25, 26, 27, 28, 29]. This method is now called *renormalization*. Renormalization regards quantities like coupling, mass, and charge as infinity and splits them as finite parts plus the so-called *counter-terms*. Counter-terms are additional terms introduced into quantum field theory to cancel out divergent contributions from loop diagrams and ensure that physical observables remain finite and well-defined. At the same time, Feynman invented Feynman diagrams and path integral representations, which made the calculation more intuitive. Thus, the framework of quantum field theory gradually becomes complete. However, new difficulties arose. First, there are only a handful of renormalizable theories, which means most still suffer from infinity. Secondly, the perturbation expansion calculation of Feynman diagrams is only suitable for small coupling constants and is no longer suitable for large coupling constants, such as strong interactions. In 1954, Chen-Ning Yang and Robert Mills generalized global gauge invariance to local gauge invariance and thus established non-Abelian gauge field theory. In 1960, Sheldon Glashow used gauge field theory to unify electromagnetic and weak interactions. Abdus Salam and John Clive Ward had the same theory four years later. However, the theory is not renormalizable. Subsequently, Peter Higgs, Robert Brout, and Francois Engler proposed that the massless boson in the gauge field theory could gain mass by breaking the symmetry spontaneously, which became known as the *Higgs mechanism*. In 1967, Steven Weinberg and Salam applied the Higgs mechanism to describe the interaction between leptons, successfully establishing the electroweak theory. Weinberg and Salam's electroweak interaction theory was finally extended to quarks in 1970 by Glashow, John Iliopoulos, and Luciano Maiani. Abdus Salam, Sheldon Glashow, and Steven Weinberg later won the 1979 Nobel Prize for unifying elementary particles' electromagnetic and weak interaction. But this was not taken seriously until 1971 when Gerard 't Hooft proved that non-Abelian gauge field theories could be renormalizable. Quantum field theory is back to life. In 1971, Quantum Chromodynamics was systematically established. Two years later, David Gross, Franck Wilczek, and Hugh Politzer proved that non-Abelian gauge field theory is asymptotically free, meaning the strong coupling becomes small when the energy scale increases and vice versa. This series of profound results has brought quantum field theory back to the center of particle physics. Electroweak interaction theory and Quantum Chromodynamics form today's *Standard Model* of elementary particle physics, which describes all fundamental interactions except gravity.

1.3.2 The basics of the Standard Model

The Standard Model of particle physics provides the theoretical framework that describes three of the four fundamental forces except gravity in the universe: electromagnetic, weak, and strong forces, as well as the elementary particles that make up matter and mediate these forces.

Force	Strength	Theory	Mediator	Range
Strong	1	Quantum chromodynamics	gluons	10^{-15}
Electromagnetic	10^{-2}	Quantum electrodynamics	photons	∞
Weak	10^{-5}	Electroweak theory	W and Z bosons	10^{-18}

Elementary particles generally fall into two main categories: fermions and bosons.

Fermions serve as the foundational elements of matter and are comprised of quarks and leptons. Quarks come in six flavors—up, down, charm, strange, top, and bottom, and they usually form neutrons and protons in groups of three, which make up the nucleus of atoms. Leptons constitute another subcategory of matter particles, among which the electron is the most commonly recognized. The lepton family also includes the muon, tau, and corresponding neutrinos.

Bosons are force carriers that mediate the fundamental interactions among particles. The photon mediates the electromagnetic force, the W and Z bosons are responsible for the weak nuclear force, and the gluon mediates the strong nuclear force. The Higgs boson, discovered in 2012, is associated with the Higgs field and generates mass for other particles. The

Standard Model has remarkably succeeded in predicting and explaining various phenomena and is confirmed through numerous experiments, but it is imperfect. It cannot explain several phenomena such as gravity, dark matter/dark energy, neutrino masse, etc.

1.3.3 Gauge theory

Gauge theory describes the particle interactions of the SM. The interaction between gauge bosons and fermions can be derived from local gauge invariance. We start with the simplest $U(1)$ or electromagnetic gauge theory. Consider a Dirac Lagrangian that includes fermions only:

$$\mathcal{L} = i\bar{\psi}\gamma^\mu \partial_\mu \psi - m\bar{\psi}\psi, \tag{1.14}$$

where ψ are spinors representing fermions, and γ^μ's are called *Dirac matrices*. In terms of Pauli matrices $\vec{\sigma} = (\sigma^1, \sigma^2, \sigma^3)$ and 2×2 identity matrix I_2, Dirac matrices are given by

$$\gamma^0 = \begin{pmatrix} I_2 & 0 \\ 0 & -I_2 \end{pmatrix}, \gamma^1 = \begin{pmatrix} 0 & \sigma^1 \\ -\sigma^1 & 0 \end{pmatrix}, \gamma^2 = \begin{pmatrix} 0 & \sigma^2 \\ -\sigma^2 & 0 \end{pmatrix}, \gamma^3 = \begin{pmatrix} 0 & \sigma^3 \\ -\sigma^3 & 0 \end{pmatrix}, \tag{1.15}$$

and they satisfy anticommutation relation:

$$\{\gamma^\mu, \gamma^\nu\} = 2g^{\mu\nu}, \quad g^{\mu\nu} = \text{diag}\{+1, -1, -1, -1\}. \tag{1.16}$$

Eq.1.14 is invariant under *global* phase transformation (also called $U(1)$ transformation)

$$\psi \to e^{i\theta}\psi. \tag{1.17}$$

Global means θ is independent of spacetime coordinates. Now we set θ as a function of spacetime, i.e., $\theta = \theta(x)$. The Lagrangian is not invariant due to the existence of ∂_μ operator:

$$\partial_\mu(e^{i\theta}\psi) = i\partial_\mu\theta e^{i\theta}\psi + e^{i\theta}\partial_\mu\psi, \tag{1.18}$$

and it is shifted by a term $-\partial_\mu\theta\bar{\psi}\gamma^\mu\psi$:

$$\mathcal{L} \to \mathcal{L} - \partial_\mu\theta\bar{\psi}\gamma^\mu\psi. \tag{1.19}$$

There's nothing extraordinary about this math. But now, we require the whole Lagrangian to be invariant under this local transformation. We must modify it so that the additional term can be canceled. In physics, we usually think about the most straightforward and handy method. We now add an interacting term

$$A_\mu \bar{\psi}\gamma^\mu\psi \tag{1.20}$$

to the Lagrangian, where A_μ is the electromagnetic potential that transforms as

$$A_\mu \to A_\mu - \partial_\mu\theta. \tag{1.21}$$

This is called gauge transformation and cancels the extra term $-\partial_\mu\theta\bar{\psi}\gamma^\mu\psi$. From Maxwell's equations, we know the physics is unchanged when A_μ transforms in this way. That is to say, the Lagrangian now is locally gauge invariant. In the reality, we write $\theta(x)$ as $-Q\lambda(x)$, where Q is a constant depends on the fermion ψ. Thus the local gauge transformation and the rule that A_μ follows read

$$\begin{aligned} &\psi \to e^{-iQ\lambda(x)}\psi \\ &A_\mu \to A_\mu + \partial_\mu\lambda(x). \end{aligned} \tag{1.22}$$

We also need to add the kinetic term for A_μ:

$$-\frac{1}{16\pi}F^{\mu\nu}F_{\mu\nu}, \tag{1.23}$$

where $F^{\mu\nu} = \partial_\mu A_\nu - \partial_\nu A_\mu$. In conclusion, we start with Dirac Lagrangian and require it to be invariant under local phase transformation. Then we introduce A_μ and its kinetic term. The complete Lagrangian is now

$$\mathcal{L} = -\frac{1}{16\pi}F^{\mu\nu}F_{\mu\nu} + i\bar{\psi}\gamma^\mu\partial_\mu\psi - m\bar{\psi}\psi - Q\bar{\psi}\gamma^\mu\psi A_\mu \tag{1.24}$$

and is invariant under local gauge transformation Eq.1.22. We usually combine the gauge potential A_μ and derivative operator as the so-called covariant derivative $\mathcal{D}_\mu$

$$\mathcal{D}_\mu = \partial_\mu + iQA_\mu. \tag{1.25}$$

Then we have

$$i\bar{\psi}\gamma^\mu\partial_\mu\psi - Q\bar{\psi}\gamma^\mu\psi A_\mu = i\bar{\psi}\gamma^\mu\mathcal{D}_\mu\psi. \tag{1.26}$$

Therefore the local gauge invariance is equivalent to $\mathcal{D}_\mu$ commuting with local phase transformation:

$$\mathcal{D}_\mu(e^{-iQ\lambda(x)}\psi) = e^{-iQ\lambda(x)}\mathcal{D}_\mu\psi. \tag{1.27}$$

The key point is that the electromagnetic interacting term $A_\mu\bar{\psi}\gamma^\mu\psi$ enters by considering local gauge invariance. It is not hard to write down a non-Abelian gauge theory. Consider a Dirac theory with N massless fermions ψ_1, $\psi_2 ... \psi_N$:

$$\begin{aligned}\mathcal{L} &= \sum_{i=1}^{n} i\bar{\psi}_i\gamma^\mu\partial_\mu\psi_i \\ &= i\bar{\psi}\gamma^\mu\partial_\mu\psi,\end{aligned} \tag{1.28}$$

where we have defined $\psi = (\psi_1, \psi_2, ...\psi_N)^T$. We require $\mathcal{L}$ to be invariant under local transformation

$$\psi \to U(x)\psi, \tag{1.29}$$

where $U(x)$ is a $N \times N$ matrix in group $SU(N)$. $U(x)$ can be written as

$$U(x) = e^{-ig\theta_a(x)T^a}, \tag{1.30}$$

where g is the coupling constant and $\{T^a\}$ is the basis of Lie algebra of $SU(N)$ and satisfies the commutation relation

$$[T^a, T^b] = if_{abc}T^c. \tag{1.31}$$

We introduce gauge field $A_\mu = A_\mu^a T^a$ with N components A_μ^a and write the covariant derivative operator

$$\mathcal{D}_\mu = \partial_\mu + igA_\mu^a T^a. \tag{1.32}$$

The covariant derivative operator should be commuting with local transformation $\psi \to e^{-ig\theta_a(x)T^a}\psi$:

$$\mathcal{D}_\mu(e^{-ig\theta_a(x)T^a}\psi) = e^{-ig\theta_a(x)T^a}\mathcal{D}_\mu\psi, \tag{1.33}$$

which gives the transformation rule for A_μ:

$$A_\mu \to e^{-ig\theta_a(x)T^a}A_\mu e^{ig\theta_a(x)T^a} + \frac{i}{g}(\partial_\mu e^{-ig\theta_a(x)T^a})e^{ig\theta_a(x)T^a}. \tag{1.34}$$

In this way, non-Abelian gauge theory is established, also known as Yang-Mills theory:

$$\begin{aligned}\mathcal{L} &= i\bar{\psi}(\partial_\mu + igA^a_\mu T^a)\psi - \frac{1}{16\pi}F^a_{\mu\nu}F^{a\mu\nu} - g\bar{\psi}\gamma^\mu T^a\psi A^a_\mu \\ F^a_{\mu\nu} &= \partial_\mu A_\nu - \partial_\nu A_\mu + gf^{abc}A^b_\mu A^c_\nu.\end{aligned} \tag{1.35}$$

When $N = 3$, the theory is the well-known Quantum chromodynamics (QCD), which describes the strong nuclear force that binds quarks together to form hadrons, like neutrons, and so forth. Yang-Mills theory also provides the framework for the electroweak theory, which unifies electromagnetic and weak forces. Experimental observations have extensively verified the predictions of Yang-Mills theory, including the discovery of the W and Z in 1983 and the observation of the Higgs boson in 2012. In summary, gauge theory is a pillar of modern theoretical physics and is central to understanding the universe's building blocks.

1.3.4 Glashow–Weinberg–Salam model

Electromagnetic and weak forces are unified at high energy scales, known as the Glashow-Weinberg-Salam model [**30**, **31**]. At this moment, the electroweak possesses a $SU(2)_w \times U(1)_Y$ symmetry, where $SU(2)_w$ is associated with weak isospin, and $U(1)_Y$ is associated with hypercharge. At a low energy scale, $SU(2)_w \times U(1)_Y$ is broken by the non-vanishing vacuum expectation value (vev) of Higgs doublet H of hypercharge $1/2$. This symmetry breaking gives mass to the W and Z bosons, which mediate the weak force, while the photon, which mediates the electromagnetic force, remains massless. This mechanism by which particles aquire mass from symmetry breaking is known as the *Higgs mechanism*. The Lagrangian of Glashow–Weinberg–Salam model is given by

$$\mathcal{L} = -\frac{1}{4}W^a_{\mu\nu}W^{a\mu\nu} - \frac{1}{4}B_{\mu\nu}B^{\mu\nu} + (D_\mu H)^\dagger D^\mu H + m^2 H^\dagger H - \lambda(H^\dagger H)^2 + \mathcal{L}_{fermions}, \tag{1.36}$$

where $W^a_{\mu\nu}$ is the $SU(2)_w$ gauge boson, and $B_{\mu\nu}$ is the $U(1)_Y$ gauge boson. The covariant derivative of H is given by

$$D_\mu H = \partial_\mu H - igW^a\tau^a H - \frac{1}{2}ig' B_\mu H, \tag{1.37}$$

where g and g' are couplings, and τ^a's are $SU(2)$ generators. When H gets a non-vanishing vev $v/\sqrt{2}$, we can expand H as

$$H = \begin{pmatrix} 0 \\ \frac{v}{\sqrt{2}} + \frac{h}{\sqrt{2}} \end{pmatrix}. \tag{1.38}$$

Substituting 1.38 into 1.36, we have

$$\begin{aligned} \mathcal{L} = &-\frac{1}{4}F_{\mu\nu}F^{\mu\nu} - \frac{1}{4}Z_{\mu\nu}Z^{\mu\nu} + \frac{1}{2}m_Z^2 Z_\mu Z^\mu \\ &-\frac{1}{2}(\partial_\mu W_\nu^+ - \partial_\nu W_\mu^+)(\partial^\mu W^{\nu-} - \partial^\nu W^{\mu-}) + m_W^2 W^{\mu+}W_\mu^- + \text{other terms}, \end{aligned} \tag{1.39}$$

where we have defined

$$\begin{aligned} Z_\mu &= \cos\theta_w W_\mu^3 - \sin\theta_w B_\mu \\ A_\mu &= \sin\theta_w W_\mu^3 + \cos\theta_w B_\mu \\ \theta_w &= \arctan\frac{g'}{g} \\ W_\mu^\pm &= \frac{1}{\sqrt{2}}(W_\mu^1 \mp W_\mu^2). \end{aligned} \tag{1.40}$$

We also find that W and Z bosons are massive, and their masses m_w and m_Z are given by

$$m_W = \frac{gv}{2}, \quad m_Z = \frac{m_W}{\cos\theta_w}. \tag{1.41}$$

The W and Z bosons were discovered in 1983 at CERN. Their discovery was a significant milestone in particle physics, confirming the predictions of the Standard Model.

1.3.5 Fermions in electroweak interaction

Gell-Mann–Nishijima formula

In the weak interaction $SU(2)$ gauge bosons only couple to left-handed fermions, which means the weak interaction is chiral. The left-handed leptons (e_L, μ_L, τ_L and corresponding neutrinos $\nu_{eL}, \nu_{\mu L}, \nu_{\tau L}$) are paired into three generations L^1, L^2 and L^3

$$L^i = \begin{pmatrix} \nu_{eL} \\ e_L \end{pmatrix}, \begin{pmatrix} \nu_{\mu L} \\ \mu_L \end{pmatrix}, \begin{pmatrix} \nu_{\tau L} \\ \tau_L \end{pmatrix}, \tag{1.42}$$

and a similar grouping happens to left-handed quarks

$$Q^i = \begin{pmatrix} u_L \\ d_L \end{pmatrix}, \begin{pmatrix} c_L \\ s_L \end{pmatrix}, \begin{pmatrix} t_L \\ b_L \end{pmatrix}. \tag{1.43}$$

The right-handed fermions are not paired into doublets for weak interactions as left-handed fermions are. Instead, they are treated as singlets under the $SU(2)$ gauge symmetry. The right-handed fermions are labeled as follows:

$$\begin{aligned} e_R^i &= \{e_R, \mu_R, \tau_R\}, \quad \nu_R^i = \{\nu_{eL}, \nu_{\mu L}, \nu_{\tau L}\} \\ u_R^i &= \{u_R, c_R, t_R\}, \quad d_R^i = \{d_R, s_R, b_R\}. \end{aligned} \tag{1.44}$$

The weak interaction between fermions and bosons is

$$\begin{aligned} \mathcal{L}_{fermions} =& i\bar{L}^i\gamma^\mu(\partial_\mu - igW_\mu^a\tau^a - ig'Y_LB_\mu)L^i \\ &+ i\bar{Q}^i\gamma^\mu(\partial_\mu - igW_\mu^a\tau^a - ig'Y_QB_\mu)Q^i \\ &+ i\bar{e}_R^i\gamma^\mu(\partial_\mu - ig'Y_eB_\mu)e_R^i + i\bar{\nu}_R^i\gamma^\mu(\partial_\mu - ig'Y_\nu B_\mu)\nu_R^i \\ &+ i\bar{u}_R^i\gamma^\mu(\partial_\mu - ig'Y_uB_\mu)u_R^i + i\bar{d}_R^i\gamma^\mu(\partial_\mu - ig'Y_dB_\mu)d_R^i, \end{aligned} \tag{1.45}$$

where Y's are hypercharges. We want to apply 1.40 to rewrite the interaction. Focusing on W_μ^3 and B_μ, we have

$$-igW_\mu^3\tau^3 - ig'B_\mu Y = -ie(T^3 + Y)A_\mu - ie(\cot\theta_w T^3 - \tan\theta_w Y)Z_\mu, \tag{1.46}$$

where $e = g\sin\theta_w$ is the electromagnetic coupling strength and $T^3 = \tau^3 = \text{diag}\{1/2, -1/2\}$ is the weak isospin operator. Therefore, $T^3 + Y$ is exactly the electric charge Q. This relation is called *Gell-Mann–Nishijima formula* [**32**, **33**, **34**]:

$$Q = T^3 + Y, \tag{1.47}$$

which tells us that a fermion's electric charge is the sum of its weak isospin and hypercharge. For example, the electron has weak isospin $-1/2$ and hypercharge $-1/2$, so its electric charge is $-1/2 - 1/2 = -1$.

Quark masses and the CKM matrix

Similar to W and Z bosons, fermions acquire mass from vev of Higgs doublets H. For quarks, the mass term reads

$$\mathcal{L}_{quark-mass} = -Y^d_{ij}\bar{Q}^i H d^j_R - Y^u_{ij}\bar{Q}^i(i\sigma_2 H^*)u^j_R + h.c. \tag{1.48}$$

Y^d_{ij} and Y^u_{ij} are called *Yukawa matrices*, which mix different left-handed and right-handed quarks. After H gets vev $v/\sqrt{2}$, the mass term becomes

$$\mathcal{L}_{quark-mass} = -\frac{v}{\sqrt{2}}\bar{d}^i_L Y^d_{ij} d^j_R - \frac{v}{\sqrt{2}}\bar{u}^i_L Y^u_{ij} u^j_R + h.c., \tag{1.49}$$

where different quarks are mixing. We can manipulate Yukawa matrices to get diagonal mass matrices. First, we take the square root of $Y_d Y_d^\dagger$ and $Y_u Y_u^\dagger$:

$$Y_d Y_d^\dagger = U_d M_d^2 U_d^\dagger, \;\; Y_u Y_u^\dagger = U_u M_u^2 U_u^\dagger, \tag{1.50}$$

where U_d and U_u are unitary matrices, and M_d and M_u are diagonal matrices. In the next, we can write Y_d and Y_u as

$$Y_d = U_d M_d K_d^\dagger, \;\; Y_u = U_u M_u K_u^\dagger \tag{1.51}$$

for some unitary matrices K_d and K_u. After applying transformation $d_R \to K_d d_R$, $u_R \to K_u u_R$, $d_L \to U_d d_L$ and $u_L \to U_u u_L$, we can get diagonal matrices. The interesting thing is that when diagonalizing the mass term, the interaction between quarks and $W^\pm$ is also changed, while Z_μ and A_μ part is invariant:

$$\mathcal{L}_{quark-W} = \frac{e}{\sqrt{2}\sin\theta_w}\left(W^+_\mu \bar{u}^i_L \gamma^\mu V^{ij} d^j_L + W^-_\mu \bar{d}^i_L \gamma^\mu V^{\dagger ij} u^j_L\right), \tag{1.52}$$

from which we find different quarks are mixing via a matrix $V = U_u^\dagger U_d$. This matrix V is known as *Cabibbo–Kobayashi–Maskawa (CKM) matrix* [**35, 36**]. The CKM matrix uniquely provides quark flavor change transitions in the Standard Model that cannot occur in strong or electromagnetic interactions.

Neutrino masses and PMNS matrix

Neutrinos are one of the more interesting particles in particle physics, mainly because of their chirality, mass term, and flavor change (oscillation). So far, all observed neutrinos are left-handed, and there is no evidence of right-handed neutrinos. We still assume the existence of right-handed neutrinos. The general mass term of leptons is

$$\mathcal{L}_{lepton-mass} = -Y^e_{ij}\bar{L}^i He^j_R - Y^\nu_{ij}\bar{L}^i(i\sigma_2 H^*)\nu^j_R - iM_{ij}(\nu^i_R)^c\nu^j_R + h.c. \tag{1.53}$$

What we're interested in is the neutrino part. In terms of Dirac spinors, the mass term for a neutrino can be written as

$$\mathcal{L}_{neutrino-mass} = -m\bar{\psi}_L\psi_R - \frac{M}{2}\bar{\psi}_R\psi_R, \tag{1.54}$$

where M is called *Majorana mass*, and m is called *Dirac mass*. Diagonalizing the mass matrix, we get the physical neutrino masses:

$$m^\pm_\nu = \sqrt{m^2 + \frac{M^2}{4}} \pm \frac{M}{2}. \tag{1.55}$$

When $M \gg m$, $m^+_\nu \approx M$ and $m^-_\nu \approx m^2/M$. We find when one mass increases, the other mass gets smaller, and vice versa. This is called *see-saw mechanism*.

Next, we face a situation similar to the one we discussed earlier with quark mass: diagonalizing the neutrino mass term affects the neutrino's interaction term with the W bosons. Suppose we diagonalize the neutrinos' mass via a unitary matrix U, i.e.,

$$\begin{pmatrix} \nu_{eL} \\ \nu_{\mu L} \\ \nu_{\tau L} \end{pmatrix} = U \begin{pmatrix} \nu_{1L} \\ \nu_{2L} \\ \nu_{3L} \end{pmatrix}, \tag{1.56}$$

where ν_{1L}, ν_{2L}, and ν_{3L} are called mass basis. The transformed neutrino-W interaction is

$$\mathcal{L}_{\nu-W} = -\frac{g}{\sqrt{2}}(\bar{e}_{iL}U^{ij}W_\mu\gamma^\mu\nu_{jL}) + h.c. \tag{1.57}$$

The matrix U is called *Pontecorvo–Maki–Nakagawa–Sakata (PMNS) matrix* [**37, 38**], an analog of the CKM matrix. The PMNS matrix provides an extraordinary and exciting mechanism: neutrino oscillation [**39, 40**], meaning that different types of neutrinos can be converted into each other. A neutrino of a given flavor α at $t = 0$ is a superposition of different mass eigenstates, with the probability $|U^{\alpha j}|^2$:

$$|\alpha, t=0\rangle = \sum_j U^{\alpha,j} |j\rangle . \tag{1.58}$$

As it travels, its evolution is described by quantum mechanics:

$$\begin{aligned} |\alpha, t\rangle &= \sum_j U^{\alpha,j} e^{-iE_j t} |j\rangle \\ &= \sum_j U^{\alpha,j} e^{-iE_j t} \sum_\beta U^*_{j,\beta} |\beta\rangle \\ &= \sum_\beta \sum_j U^{\alpha,j} U^{*j,\beta} e^{-iE_j t} |\beta\rangle , \end{aligned} \tag{1.59}$$

from which we can read the transition probability of $\alpha \to \beta$ after time t:

$$P(\alpha \to \beta) = |\sum_j U^{\alpha,j} U^{*j,\beta} e^{-iE_j t}|^2. \tag{1.60}$$

The discovery of neutrino oscillations solved the solar neutrino problem and provided crucial insights into the sun's and other stars' inner workings. Studying neutrino oscillations also helps in probing the fundamental properties of neutrinos, such as their mass hierarchy and the possibility of CP-violation in the lepton sector, which could explain the matter-antimatter asymmetry in the universe.

CHAPTER 2

Anomalies in Quantum Field Theory

A transformation that leaves the physical system/state unchanged is called a *symmetry*. A classical physical system may have various symmetries. For instance, rotation is a symmetry for an object in a central force potential; Spacetime symmetries imply that the form of the laws of physics has nothing to do with how we set the coordinate frame. But when it comes to the quantum level, some of the symmetries held at the classical level might be violated. This phenomenon is called *anomaly*. This chapter will discuss anomalies in quantum field theory, starting with the famous decay $\pi_0 \to \gamma\gamma$. Eventually, we will see that the so-called *chiral symmetry* is an anomaly.

2.1 Triangle diagrams and $\pi_0 \to \gamma\gamma$

There has been much controversy over $\pi_0 \to \gamma\gamma$, mainly over the calculation method. Before quantum field theory was mature, calculations were confusing until Adler-Bell-Jackiw anomaly was discovered in 1969 [41, 42].

To study the $\pi_0 \to \gamma\gamma$, we start with a simple model [43]: QED Lagrangian with a pseudoscalar π. The Lagrangian is given by

$$\mathcal{L} = -\frac{1}{4}F_{\mu\nu}F^{\mu\nu} - \frac{1}{2}\pi(\partial^2 + m_\pi^2)\pi + \bar{\psi}(i\partial\!\!\!/ - eA\!\!\!/ - m)\psi + i\lambda\pi\bar{\psi}\gamma^5\psi. \tag{2.1}$$

Then, the leading contribution of decay amplitude $\mathcal{M}$ is given by

$$i\mathcal{M} \sim \langle q_1, q_2 |\, i\lambda\pi\bar{\psi}\gamma^5\psi\bar{\psi}eA\!\!\!/\psi\bar{\psi}eA\!\!\!/\psi \,| p \rangle \tag{2.2}$$

There are two Feynman diagrams contributing to $\mathcal{M}$:

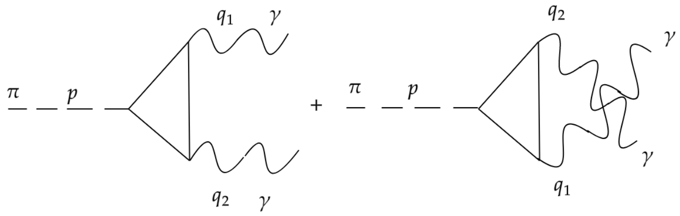

FIGURE 2.1: 1-loop Feynman diagrams for $\pi_0 \to \gamma\gamma$: two non-equivalent contractions

Through a long calculation, we get $\mathcal{M}$ and the decay width:

$$\mathcal{M} = \lambda \frac{e^2}{4\pi^2 m} \epsilon^{\mu\nu\alpha\beta} \epsilon_\mu^{1*} \epsilon_\nu^{2*} q_{1\alpha} q_{2\beta}, \quad \Gamma(\pi \to \gamma\gamma) = \frac{\lambda^2}{64\pi^3} \left(\frac{e^2}{4\pi}\right)^2 \frac{m_\pi^3}{m^2}. \tag{2.3}$$

The real π_0 decay is given by $\lambda = m_N/f_\pi$ and $m = m_N$, where f_π is decay constant and m_N is nucleon mass. Substituting fine structure constant $\alpha_e = 1/137$, pion decay constant $F_\pi = 92$MeV, and pion mass $m_\pi = 139.5$MeV we get:

$$\Gamma(\pi_0 \to \gamma\gamma) = \frac{\alpha_e^2}{64\pi^3} \frac{m_\pi^3}{F_\pi^2} = 7.8eV, \tag{2.4}$$

which is consistent with the experimental value $7.73 \pm 0.16eV$.

The connection between $\pi_0 \to \gamma\gamma$ and chiral anomaly can be seen as follows. The QED Lagrangian

$$\mathcal{L}_{QED} = \bar{\psi}(i\partial\!\!\!/ - eA\!\!\!/ - m)\psi \tag{2.5}$$

is invariant under global *chiral (axial) transformation* $U(1)_A$ in the massless limit $m \to 0$:

$$\psi \to e^{i\alpha\gamma^5}\psi. \tag{2.6}$$

The corresponding current is

$$J_\mu^5 = \bar{\psi}\gamma^\mu\gamma^5\psi, \tag{2.7}$$

which is called *axial* current and its divergence is given by the equations of motion:

$$\partial^\mu J^5_\mu = 2im\bar{\psi}\gamma^5\psi. \tag{2.8}$$

Substituting $\bar{\psi}\gamma^5\psi$ by $\partial^\mu J^5_\mu/2im$ in Eq.2.2 and using Eq.2.3, we obtain the expectation value of $\partial^\mu J^5_\mu$ in the QED background:

$$_{QED}\langle 0|\, \partial^\mu J^5_\mu \,|0\rangle_{QED} = -\frac{e^2}{16\pi^2}\epsilon^{\mu\nu\alpha\beta}F_{\mu\nu}F_{\alpha\beta}. \tag{2.9}$$

Eq.2.9 is called Adler-Bell-Jackiw (ABJ) anomaly [**41, 42**]. The right-hand side of Eq.2.9 is independent of fermion's mass m, meaning that in the massless limit $m = 0$, J^5_μ is conserved at the classical level but is violated at the quantum level. A more intuitive derivation of $\partial^\mu j^5_\mu$ is to use path integral.

2.2 The Path integral

The path integral is an alternative formulation of quantum mechanics developed by Richard Feynman in the 1940s. Instead of tackling the wave functions and the associated Schrödinger equation, the path integral formulation considers all possible paths a particle could take between two points in space-time. Each path represents a possible state of the system, and the path integral assigns each path an amplitude. The total amplitude is obtained by summing over all such amplitudes. The same thought works in quantum field theory. We will briefly review path integral in this section and use it to derive chiral anomaly.

2.2.1 General formalism

Let us consider a one-dimensional quantum system whose Hamiltonian is given by

$$\hat{H} = \frac{\hat{p}^2}{2m} + V(x). \tag{2.10}$$

We want to calculate the amplitude of a particle initially localized at x_I at time t_I and finally localized at x_F at time t_F: $\langle t_F, x_F | t_I, x_I\rangle$. In classical mechanics, particles only move along trajectories determined by their initial states, whereas in quantum mechanics, the movement of particles is random. We have to include all possibilities. We slice the time $t_F - t_I$ into small intervals $t_0 = t_I < t_1 ... < t_{N+1} = t_F$, $t_{j+1} - t_j = \delta t$. Then, the amplitude can be written as

$$\langle t_F, x_F | t_I, x_I \rangle = \int dx_1 dx_2 ... dx_N \langle x_F, t_F | e^{-i\hat{H}\delta t} | t_N, x_N \rangle \langle x_N, t_N | e^{-i\hat{H}\delta t} | t_{N-1}, x_{N-1} \rangle$$
$$... \times \langle x_2, t_2 | e^{-i\hat{H}\delta t} | t_1, x_1 \rangle \langle x_1, t_1 | e^{-i\hat{H}\delta t} | t_I, x_I \rangle . \tag{2.11}$$

Inserting the identity operator $I = \int dp/2\pi |p\rangle \langle p|$ at each left ket $\langle t_j, x_j|$ and using Gaussian integrals gives

$$\langle t_F, x_F | t_I, x_I \rangle \propto \int dx_1 dx_2 ... dx_N e^{iL(x_1, \dot{x_1})\delta t} e^{iL(x_2, \dot{x_2})\delta t} ... e^{iL(x_N, \dot{x_N})\delta t}, \tag{2.12}$$

where $L(x_i, \dot{x}_i)$ is the Lagrangian $\frac{1}{2} m \dot{x_i}^2 - V(x_i)$. As δt approaches 0, $\int dx_1 dx_2 ... dx_N$ includes all the points of a path, and therefore all possible paths are summed. The functional integral should replace the usual integral:

$$\int dx_1 dx_2 ... dx_N \to \int_{x(t_F)=x_F}^{x(t_I)=x_I} \mathcal{D}x(t), \tag{2.13}$$

where the symbol $\int \mathcal{D}x(t)$ means integrating over all paths. The final result of the amplitude is

$$\langle t_F, x_F | t_I, x_I \rangle = N \int_{x(t_F)=x_F}^{x(t_I)=x_I} \mathcal{D}x(t) e^{i \int_{t_I}^{t_F} L(x, \dot{x}) dt}, \tag{2.14}$$

where N is some normalization constant.

The path integral for quantum field theory follows the same philosophy: we must add all field configurations. In the above example from quantum mechanics, a configuration corresponds to a path the particle moves along. We will not repeat the long derivation but directly present the result for quantum field theory. For a scalar field $\Phi(t, \vec{x})$, the vacuum-to-vacuum amplitude is:

$$\langle 0; t_F | 0; t_I \rangle = N \int D\Phi(t, \vec{x}) e^{iS[\Phi]}, \tag{2.15}$$

where the quantity S (called the "action") is an integral of the Lagrangian density:

$$S[\Phi] = \int d^4 x \mathcal{L}[\Phi]. \tag{2.16}$$

We are interested in the vacuum expectation values of the product of single or more operators:

$$\begin{aligned}\langle 0| T\{\hat{\mathcal{O}}_1\hat{\mathcal{O}}_2..\hat{\mathcal{O}}_n\} |0\rangle =&\frac{N\int D\Phi(t,\vec{x})\mathcal{O}_1..\mathcal{O}_n e^{iS[\Phi]}}{N\int D\Phi(t,\vec{x})e^{iS[\Phi]}}\\ =&\frac{\int D\Phi(t,\vec{x})\mathcal{O}_1..\mathcal{O}_n e^{iS[\Phi]}}{\int D\Phi(t,\vec{x})e^{iS[\Phi]}},\end{aligned} \tag{2.17}$$

where the operator T is the time-ordering operator and we have normalized the vacuum $\langle 0|0\rangle = 1$.

2.2.2 Fermionic path integral

Fermions obey Fermi-Dirac statistics and the Pauli exclusion principle, therefore the path integral for them is subtly different from the case of bosons which obey Bose-Einstein statistics.

We shall start with introducing **Grassmann algebra**. A Grassmann algebra is a vector space $\mathcal{G}$ over $\mathbb{C}$ taking $\{\theta_i\}$ as a basis, and these basis vectors are anticommutative with each other under multiplication: $\theta_i\theta_j = -\theta_j\theta_i$. The integrations of Grassmann numbers are defined as follows:

$$\int d\theta_i\theta_j = \delta_{i,j}. \tag{2.18}$$

Usually, we have

$$\int d\theta_n d\theta_{n-1}...d\theta_1\theta_{i_1}\theta_{i_2}...\theta_{i_n} = \epsilon_{i_1 i_2 ... i_n}, \tag{2.19}$$

where $\epsilon_{i_1 i_2 ... i_n}$ is the Levi-Civita symbol. In quantum field theory, we need to deal with an integral of an exponential of the quadratic form of two independent Grassmann algebras $\{\theta_i\}$ and $\{\bar{\theta}_j\}$, a handy formula is:

$$\int d\bar{\theta}_1 d\bar{\theta}_2...d\bar{\theta}_n d\theta_1 d\theta_2...d\theta_n e^{-\bar{\theta}_i M_{ij}\theta_j} = \det M. \tag{2.20}$$

This is quite different from the Gaussian integral:

$$\int dx_1 dx_2...dx_n e^{-\frac{1}{2}x_i M_{ij} x_j} = \sqrt{\frac{(2\pi)^n}{\det M}}. \tag{2.21}$$

Under the continuum limit, the Grassmann field $\Psi = \Psi(x)$ is labeled by continuous variable x, just like θ labeled by integers. Then the fermionic path integral goes through all configurations $\Psi(x)$ and $\bar{\Psi}(x)$:

$$Z = \int D\bar{\Psi}D\Psi e^{i\int d^4x\mathcal{L}[\Psi,\bar{\Psi}]} \tag{2.22}$$

A formula analogous to Eq.2.20 is

$$\int D\bar{\Psi}D\Psi e^{-\int d^4xd^4y\bar{\Psi}(x)\hat{K}_{x,y}\Psi(y)} = \det \hat{K}, \tag{2.23}$$

where $\hat{K}$ usually is an operator, and $\det \hat{K}$ is the product of its all eigenvalues. An unusual feature of Grassmann's field is that the Jacobian determinant's power will differ from the usual integrals when the integral variables are changed. Specifically, we have:

$$D\bar{\Psi}'D\Psi' = \det F^{-1} \det F^{\dagger -1} D\Psi D\bar{\Psi}, \tag{2.24}$$

where

$$\Psi' = F[\Psi, \bar{\Psi}] \quad \bar{\Psi}' = F^{\dagger}[\Psi, \bar{\Psi}]. \tag{2.25}$$

2.3 Fujikawa method

Fujikawa method was proposed by Kazuo Fujikawa [44, 45, 46, 47] in 1970s. He introduced a systematic way to compute chiral anomalies in quantum field theory. The core idea is that the path integral should be *invariant* under renaming integral variables. Specifically, we have:

$$Z = \int D\bar{\Psi}'D\Psi' e^{i\int \mathcal{L}[A,\bar{\Psi}',\Psi']} = \int D\bar{\Psi}D\Psi e^{i\int \mathcal{L}[A,\bar{\Psi},\Psi]}, \tag{2.26}$$

where $\Psi' = F[\Psi, \bar{\Psi}]$, $\bar{\Psi}' = F^{\dagger}[\Psi, \bar{\Psi}]$. In the next, we take QED Lagrangian with a massless fermion as an example:

$$\mathcal{L}[A, \bar{\Psi}, \Psi] = -\frac{1}{4}F_{\mu\nu}F^{\mu\nu} + \bar{\Psi}(i\partial\!\!\!/ - eA\!\!\!/)\Psi. \tag{2.27}$$

Consider the *local* chiral transformation on fermionic fields:

$$\begin{aligned}\Psi'(x) &= e^{i\alpha(x)\gamma^5}\Psi(x) = \int d^4y J_{x,y}\Psi(y)\\ \bar{\Psi}'(x) &= \bar{\Psi}e^{i\alpha(x)\gamma^5} = \int d^4y J_{x,y}\bar{\Psi}'(y),\end{aligned} \tag{2.28}$$

which is treated as a transformation of the vectors carrying continuous index x, and the corresponding matrix J with two continuous indices x, y is given by:

$$J_{x,y} = \delta(x-y)e^{i\alpha(x)\gamma^5}. \tag{2.29}$$

The new Lagrangian is related to the old one by:

$$\mathcal{L}[A, \bar{\Psi}', \Psi'] = \mathcal{L}[A, \bar{\Psi}, \Psi] + \alpha(x)\partial^\mu J^5_\mu, \tag{2.30}$$

where J^5_μ is the axial current Eq.2.7:

$$J^{5\mu} = \bar{\Psi}\gamma^\mu\gamma^5\Psi. \tag{2.31}$$

Because this is a fermionic path integral, according to Eq.2.24, we have

$$D\bar{\Psi}'D\Psi' = (\det J)^{-2}D\bar{\Psi}D\Psi. \tag{2.32}$$

We now compute the determinant by applying the identity $\log\det J = \mathrm{Tr}\log J$. Also, notice that powering the matrix J is equivalent to powering its exponent factor:

$$\begin{aligned}J^2_{x,y} &= \int dz J_{x,z}J_{z,y}\\ &= \delta(x-y)e^{2i\alpha(x)\gamma^5}, \quad \text{and so forth.}\end{aligned} \tag{2.33}$$

Therefore we conclude

$$\log J_{x,y} = \delta(x-y)\cdot i\alpha(x)\gamma^5. \tag{2.34}$$

Using $\log\det J = \mathrm{Tr}\log J$, the determinant can be written as

$$(\det J)^{-2} = \exp\Big[-2i\int d^4x\alpha(x)\mathrm{Tr}\delta(x-x)\gamma^5\Big]. \tag{2.35}$$

Substituting Eq.2.35 and Eq.2.30 into Eq.2.26, we have

$$\begin{aligned}
&\int D\bar{\Psi} D\Psi \exp\left[i\int d^4x\Big(\mathcal{L}[A,\Psi,\bar{\Psi}]+\alpha(x)\partial^\mu J^5_\mu\Big)-2i\int d^4x\alpha(x)\mathrm{Tr}\delta(x-x)\gamma^5\right]\\
&=\int D\bar{\Psi} D\Psi \exp\left[i\int d^4x\mathcal{L}[A,\Psi,\bar{\Psi}]\right].
\end{aligned}\tag{2.36}$$

Due to the presence of $\delta(0)$, we must regulate δ-function. We introduce a regulator M in momentum space and set it to be ∞ at the end of the calculation:

$$\begin{aligned}
\delta(x-y)&=\int\frac{d^4k}{(2\pi)^4}e^{(i\not{D})^2/M^2}\circ e^{-ik(x-y)}\\
&=\int\frac{d^4k}{(2\pi)^4}e^{-ik(x-y)}e^{(i\not{D}+\not{k})^2/M^2},
\end{aligned}\tag{2.37}$$

where $D_\mu=\partial_\mu-ieA_\mu$ is the covariant derivative and $\not{D}=\gamma^\mu D_\mu$, and $\circ$ operator here implies the composition, instead of product. Expanding the square, we have

$$\begin{aligned}
(i\not{D}+\not{k})^2&=k^2+2ik^\mu D_\mu-\gamma^\mu\gamma^\nu D_\mu D_\nu\\
&=k^2+2ik^\mu D_\mu-D^2+\frac{ie}{4}[\gamma^\mu,\gamma^\nu]F_{\mu\nu}.
\end{aligned}\tag{2.38}$$

Putting Eq.2.38 into Eq.2.37 and setting $k^\mu=Mq^\mu$, the regularization now reads

$$\delta(x-y)=M^4\int\frac{d^4q}{(2\pi)^4}e^{-iMq(x-y)}e^{q^2+2ik^\mu D_\mu/M-D^2/M^2+ie[\gamma^\mu,\gamma^\nu]F_{\mu\nu}/4M^2}\tag{2.39}$$

.

The $\mathrm{Tr}\delta(x-x)\gamma^5$ at $M\to\infty$ limit is now:

$$\mathrm{Tr}\delta(x-x)\gamma^5=\frac{e^2}{2}\int\frac{d^4q}{(2\pi)^4}e^{q^2}F_{\mu\nu}F_{\alpha\beta}\mathrm{Tr}\left\{\frac{i}{4}[\gamma^\mu,\gamma^\nu]\frac{i}{4}[\gamma^\alpha,\gamma^\beta]\gamma^5\right\}.\tag{2.40}$$

To calculate the integral, we perform a *Wick rotation* $q_0\to iq_0$, and this gives:

$$\int\frac{d^4q}{(2\pi)^4}e^{q^2}=\frac{i}{16\pi^2}.\tag{2.41}$$

The trace of gamma matrices is given by:

$$F_{\mu\nu}F_{\alpha\beta}\mathrm{Tr}\left\{\frac{i}{4}[\gamma^\mu,\gamma^\nu]\frac{i}{4}[\gamma^\alpha,\gamma^\beta]\gamma^5\right\}=i\epsilon^{\mu\nu\alpha\beta}F_{\mu\nu}F_{\alpha\beta}.\tag{2.42}$$

The final result of regularization is then:

$$\mathrm{Tr}\delta(x-x)\gamma^5 = -\frac{e^2}{32\pi^2}\epsilon^{\mu\nu\alpha\beta}F_{\mu\nu}F_{\alpha\beta}. \tag{2.43}$$

For Eq.2.36 to hold, we must have

$$\partial^\mu J^5_\mu = -\frac{e^2}{16\pi^2}\epsilon^{\mu\nu\alpha\beta}F_{\mu\nu}F_{\alpha\beta}. \tag{2.44}$$

It is straightforward to generalize the above to non-Abelian gauge theory:

$$\partial^\mu J^5_\mu = -\frac{g^2}{16\pi^2}T(R)\epsilon^{\mu\nu\alpha\beta}F^a_{\mu\nu}F^a_{\alpha\beta}, \tag{2.45}$$

where $T(R)$ is the *index* of the representation R of the gauge group.

The chiral anomaly has been a cornerstone in deepening our understanding of the interplay between symmetries and quantum mechanics, enriching the landscape of quantum field theory, and bridging the gap between theory and experiment. Notably, the chiral anomaly provided explanations for experimental observations inconsistent with the theoretical framework. Furthermore, it has become a fundamental concept in various branches of theoretical physics, inspiring research in condensed matter physics, especially in topological materials.

CHAPTER 3

Instantons

An instanton is a classical solution to equations of motion on a Euclidean spacetime [48]. Instanton can exist in both quantum mechanics and quantum field theory. Quantum mechanical instanton gives the amplitude of penetration of energy barrier: tunneling between different vacua. In quantum field theory, instanton is the solution of the (anti)self-dual solution of the Yang-Mills equation. The so-called winding number, a topological invariant, classifies it. Therefore, the true vacuum is a superposition of topologically inequivalent vacua. This chapter aims to present some basics of the instanton. We start with tunneling in quantum mechanics and BPST solution [1] in quantum field theory. We also briefly review the $U(1)_A$ problem and Eguchi–Hanson gravitational instanton.

3.1 Instanton in quantum mechanics

3.1.1 Double-well potential

Let us consider the motion of a single particle [49], and the action is given by:

$$S = \int dtL, \quad L = \left(\frac{dx}{dt}\right)^2 - V(x), \quad V(x) = \lambda(x^2 - a^2)^2, \tag{3.1}$$

where $V(x)$ is called double-well potential. The system possesses two lowest energy states: $x = -a$ and $x = a$. Classically, the particle can't go from $-a$ to a and vice versa due to the energy barrier. We then would like to calculate the transition amplitude $\langle \pm a| e^{-iHt} |\pm a\rangle$ for large t in quantum mechanics. We shall focus on $\langle a| e^{-iHt} |-a\rangle$, and the rest will follow a similar way. Following the formalism of path integral, the amplitude is given by

$$\langle a| e^{-iHt/\hbar} |-a\rangle = N \int \mathcal{D}x(t) e^{iS/\hbar}, \tag{3.2}$$

where N is a normalization constant. Performing a Wick rotation $T = it$, we have

$$\begin{aligned} iS &= -S_E, \\ S_E &= \int d\tau \left(\frac{dx}{d\tau}\right)^2 + \lambda(x^2 - a^2)^2 = \int d\tau \left(\frac{dx}{d\tau}\right)^2 - (-\lambda(x^2 - a^2)^2). \end{aligned} \tag{3.3}$$

The amplitude $\langle a| e^{-iHt/\hbar} |-a\rangle$ now reads

$$\langle a| e^{-iHt/\hbar} |-a\rangle = \langle a| e^{-HT/\hbar} |-a\rangle = N \int \mathcal{D}x(\tau) e^{-S_E/\hbar}. \tag{3.4}$$

It is straightforward to solve the classical equation of motion $X(\tau)$ subject to boundary condition $X(\pm\infty) = \pm a$:

$$X(\tau) = a \tanh \frac{\omega(\tau - \tau_0)}{2}, \quad \omega^2 = 8\lambda a^2 = V''(0), \tag{3.5}$$

where τ_0 is an integral constant called the *center* of instanton. We can also reverse the boundary condition as $X(\pm\infty) = \mp a$ to get the *anti-instanton* solution:

$$\bar{X}(\tau) = -a \tanh \frac{\omega(\tau - \tau_0)}{2}. \tag{3.6}$$

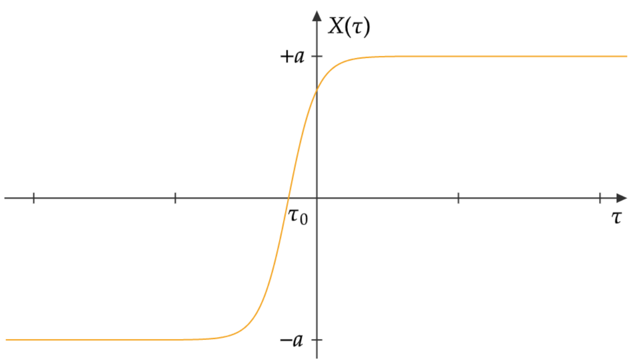

FIGURE 3.1: Instanton solution $X(\tau)$

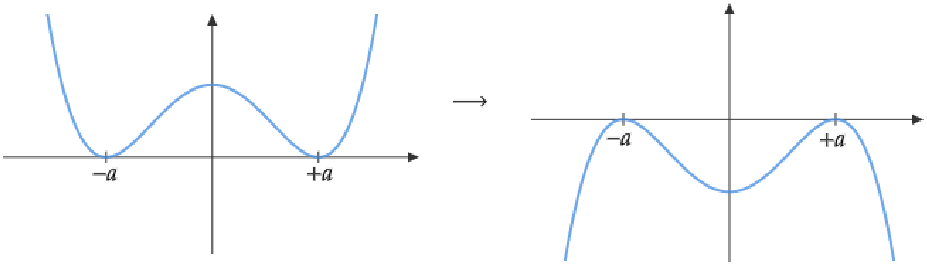

FIGURE 3.2: The potential $\lambda(x^2 - a^2)^2$ gets reversed.

The physical interpretation for instanton/anti-instanton here is intuitive: by Wick rotation, the potential $\lambda(x^2 - a^2)^2$ gets reversed. Therefore the original potential barrier becomes a track connecting $-a$ and a. For large T, Eq.3.5 is not the unique solution describing the motion $-a \to a$. We can also construct other solutions by alternatively arranging n widely separated instanton/anti-instanton along the time axis. For instance, $n = 3$, the particle goes from $-a$ to a via an instanton solution, returns to $-a$ through an anti-instanton solution, and again goes from $-a$ to a via another instanton solution.

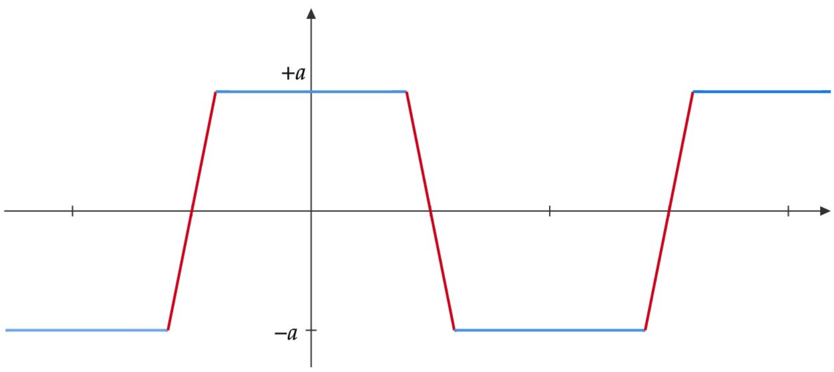

FIGURE 3.3: $n = 3$: a string of two instantons and one anti-instanton. The red segments represent the steeper parts of the instanton/anti-instanton, while the blue segments represent the asymptotic behavior (approaching $\pm a$)

Generally, there will be an odd number of instanton/anti-instantons along the time axis for $-a \to a$. For each odd n, the leading contribution to $\langle a| e^{-HT/\hbar} |-a\rangle$ reads [49]

$$\left(\frac{\omega}{\pi\hbar}\right)^{1/2} e^{-\omega T/2} \frac{(\kappa e^{-S_0/\hbar} T)^n}{n!}, \tag{3.7}$$

where $S_0 = S_E[X(\tau)]$ and κ is some constant which indicates one instanton effect. Thus, the total amplitude is

$$\begin{aligned}\langle a| e^{-HT/\hbar} |-a\rangle &= \sum_{n=1,3,5..} \left(\frac{\omega}{\pi\hbar}\right)^{1/2} e^{-\omega T/2} \frac{(\kappa e^{-S_0/\hbar} T)^n}{n!} \\ &= \left(\frac{\omega}{\pi\hbar}\right)^{1/2} e^{-\omega T/2} \sinh\left(\kappa e^{-S_0/\hbar} T\right).\end{aligned} \tag{3.8}$$

Similarly,

$$\langle -a| e^{-HT/\hbar} |-a\rangle = \left(\frac{\omega}{\pi\hbar}\right)^{1/2} e^{-\omega T/2} \cosh\left(\kappa e^{-S_0/\hbar} T\right). \tag{3.9}$$

To get the ground state energy, we can insert identity $I = \sum_n |n\rangle \langle n|$ of energy eigenstates $|n\rangle$ into $\langle a| e^{-HT/\hbar} |-a\rangle$:

$$\langle \pm a| e^{-HT/\hbar} |-a\rangle = \sum_n e^{-E_n T/\hbar} \langle \pm a|n\rangle \langle n|-a\rangle \,. \tag{3.10}$$

Comparing to Eq.3.8 and Eq.3.9, we can define:

$$E^0_{\pm} = \frac{1}{2}\hbar\omega \pm \hbar\kappa e^{-S_0/\hbar}, \tag{3.11}$$

where E_+ corresponds to the energy of reflection-odd vacuum state $|+\rangle = (|+a\rangle - |-a\rangle)/\sqrt{2}$, and E_- corresponds to the energy of reflection-even vacuum state $|-\rangle = (|+a\rangle + |-a\rangle)/\sqrt{2}$.

The above calculation shows that instantons enable the particle to penetrate the potential energy barrier at the quantum level, allowing some motion that cannot be seen at the classical level. Moreover, the ground state energy also gets a correction proportion to κ, which indicates the instanton effect.

3.1.2 Collective coordinates

In the previous discussion, we see there is an integration constant τ_0 in Eq.3.5:

$$X(\tau) = a \tanh \frac{\omega(\tau - \tau_0)}{2}. \tag{3.12}$$

Changing τ_0 leaves total action S_E invariant, but it does affect the shape of $X(\tau)$. This integration constant τ_0 is called *collective coordinate*. The path integral can be changed to an ordinary integral of collective coordinate. To do this, we first expand the $x(\tau)$ as $X(\tau, \tau_0) + \delta x(\tau)$:

$$S_E[X(\tau) + \delta x(\tau)] = S_0 + \int d\tau' \delta x(\tau') \Big[-\frac{1}{2}\frac{d^2}{d\tau'^2} + V''[X(\tau')] \Big] \delta x(\tau'). \tag{3.13}$$

The linear order of $\delta x(\tau)$ vanishes due to the equation of motion. The functional measure now reads

$$\int \mathcal{D}x(\tau) = \int \mathcal{D}\delta x(\tau). \tag{3.14}$$

Choosing a set of orthonormal eigenfunctions $\{x_i(\tau')\}$ as basis for operator $-\frac{1}{2}d^2/d\tau'^2 + V''[X(\tau')]$ and expanding $x(\tau')$ as:

$$\begin{aligned} x(\tau') &= X(\tau, \tau_0) + \delta x(\tau) \\ &= X(\tau, \tau_0) + \sum_i c_i x_i(\tau) \end{aligned} \tag{3.15}$$

then $\int \mathcal{D}\delta x(\tau)$ can be further written as

$$\int \mathcal{D}\delta x(\tau) = \int \prod dc_i. \tag{3.16}$$

The whole path integral is evaluated as

$$\begin{aligned} Z &\propto e^{-S_0} \int \prod dc_i \exp\Big\{ -\frac{1}{2}\lambda_i c_i^2 \Big\} \\ &= e^{-S_0} \prod_i \lambda_i^{-1/2}. \end{aligned} \tag{3.17}$$

But changing τ_0 leaves S_E invariant:

$$\begin{aligned} & S_E[X(\tau, \tau_0 + \Delta\tau_0)] = S_E[X(\tau, \tau_0)] \\ \Longrightarrow \ & S_E[X(\tau, \tau_0)] = S_E[X(\tau, \tau_0) + \partial_{\tau_0} X \cdot \Delta\tau_0]. \end{aligned} \tag{3.18}$$

Therefore $S_0^{-1/2}\partial_{\tau_0} X(\tau, \tau_0)$ is a zero mode of $-\frac{1}{2}d^2/d\tau'^2 + V''[X(\tau')]$, which implies $\prod_i \lambda_i^{-1/2}$ is badly defined. To fix this, let us set the first eigenfunction $x_1(\tau)$ to be $S_0^{-1/2}\partial_{\tau_0} X(\tau, \tau_0)$ and $\lambda_1 = 0$. We must change integral $\int dc_1$ to $\int d\tau_0$. If one changes c_1 by dc_1, then the increment of $x(\tau)$ is

$$dx(\tau) = x_1(\tau) dc_1. \tag{3.19}$$

On the other hand, a shift $d\tau_0$ of τ_0 gives

$$dx(\tau) = \frac{dX(\tau,\tau_0)}{d\tau_0}d\tau_0 = \sqrt{S_0}x_1(\tau)d\tau_0. \tag{3.20}$$

Equating two $dx(\tau)$'s we have

$$dc_1 = \sqrt{S_0}d\tau_0, \;\; \tau_0 \in (-T/2, T/2). \tag{3.21}$$

In summary, when calculating path integral involving instantons, one can convert functional integral to ordinary integral of collective coordinates and compute the Jacobian. This is true not only for quantum mechanics but also for quantum field theory.

3.2 Yang-Mills instanton

3.2.1 BPST solution

We have seen that the presence of an instanton allows a particle to penetrate a potential barrier. The next question we would like to ask is, are there similar phenomena in field theory?

Consider $SU(2)$ Yang-Mills theory in Euclidean spacetime $(+,+,+,+)$. The ground state has vanishing field strength tensor $F_{\mu\nu} = 0$. The corresponding gauge potential A_μ is therefore a pure gauge:

$$A_\mu = \frac{i}{g}U\partial_\mu U^\dagger, \;\; U \in SU(2). \tag{3.22}$$

We restrict ourselves to temporal gauge $A_0 = 0$, which implies U is independent of time, so $U = U(\vec{x})$. We also require $U(\vec{x})$ to be defined at $|\vec{x}| = \infty$, independent of direction. This means $U(\vec{x})$ is defined on $\mathbb{R}^3 \cup \infty$, which is a topological space homeomorphic to S^3[1]. On the other hand, the gauge group $SU(2)$ is homeomorphic to S^3 as well. This can be seen from the explicit construction:

$$a_0 I + \vec{a}\cdot i\vec{\sigma} \in SU(2), \;\; a_0^2 + |\vec{a}|^2 = 1, \tag{3.23}$$

[1]Topologically, this is called one-point compactification

where $\vec{\sigma}$ are Pauli matrices. Therefore $U(\vec{x})$ is a map from S^3 to itself. Consider two such pure gauge configurations:

$$A_\mu = \frac{i}{g} U_A \partial_\mu U_A^\dagger, \quad B_\mu = \frac{i}{g} U_B \partial_\mu U_B^\dagger. \tag{3.24}$$

Both A_μ and B_μ give vanishing field strength. If U_A can be deformed to U_B smoothly[2], then A_μ and B_μ are equivalent, and there is single quantum vacuum state. The real thing is, such $U(\vec{x})$ is a map from S^3 to itself that can be classified by a topological invariant called *winding number*, usually denoted as ν, a mathematical concept used to quantify how many times a closed path encircles a point. In quantum field theory, the winding number determines how often a field wraps around a specific space, e.g., S^3. It has been shown that ν is given by:

$$\nu = -\frac{1}{24\pi^2} \int_{S^3} d^3x \epsilon^{ijk} \mathrm{Tr}(U \partial_i U^\dagger U \partial_j U^\dagger U \partial_k U^\dagger). \tag{3.25}$$

The winding number has some important properties:

- ν is always an integer. If U_1 has winding ν_1 and U_2 has winding number ν_2, then $U_1 U_2$ has winding number $\nu_1 + \nu_2$, i.e., $\nu(U_1 U_2) = \nu(U_1) + \nu(U_2)$.
- Two U's give the same ν if and only if they are homotopic (one can be smoothly deformed to the other).
- The integral is coordinate-free. One can simple replace d^3x and ∂_x with d^3y and ∂_y when working in new coordinate frame $\vec{y}$.

So we conclude that the $SU(2)$ pure Yang-Mills theory has infinitely many vacuum states $|n\rangle$ classified by winding number n. Energy barriers separate these vacua because the tunneling between two distinct vacuum states(of different winding numbers) is not smooth and hence must experience a moment when A_μ is not a pure gauge, giving non-vanishing field strength tensor $F_{\mu\nu}$.

To find a classical solution to the Yang-Mills equation, we can view Euclidean spacetime $\mathbb{R}^4$ as a cylinder with sufficiently large radius R and height T. At $t = \pm T/2$, A_μ is pure gauge $iU_\pm \partial_\mu U_\pm^\dagger / g$ with winding number $\nu_\pm$ and is vanishing at $|\vec{x}| = \infty$ for any time

[2]Topologically, U_A is homotopic to U_B

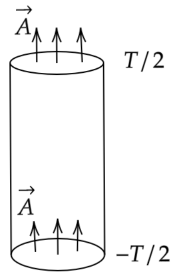

FIGURE 3.4: A visualization of A: we have chosen $A_0 = 0$ so A is perpendicular to time axis. A is always vanishing at the space boundary at any time.

t. Since the surface of a cylinder is homeomorphic to S^3 as well, we therefore have a map $U : S^3 \to SU(2)$ at $r = \sqrt{t^2 + |\vec{x}|^2} = \infty$. The corresponding winding number ν is clearly $\nu_+ - \nu_-$ and can be conventionally written in terms of spherical coordinates $(t, \vec{x}) = (r \sin\chi \sin\psi \cos\phi, r \sin\chi \sin\psi \sin\phi, r \sin\chi \cos\psi, r \cos\chi)$:

$$\nu = -\frac{1}{24\pi^2} \int_0^\pi d\chi \int_0^\pi d\psi \int_0^{2\pi} d\phi \epsilon^{\alpha\beta\gamma} \mathrm{Tr}(U\partial_\alpha U^\dagger U \partial_\beta U^\dagger U \partial_\gamma U^\dagger), \tag{3.26}$$

where $\alpha,\ \beta,\ \gamma$ run over angles, and U is independent of r. It is also useful to define the *Chern-Simons current*:

$$J^\mu = 2\epsilon^{\mu\nu\alpha\beta} \mathrm{Tr}(A_\nu F_{\alpha\beta} + \frac{2}{3} ig A_\nu A_\alpha A_\beta). \tag{3.27}$$

A simple calculation shows:

$$\begin{aligned} \nu &= \frac{g^2}{32\pi^2} \int d^4x \partial_\mu J^\mu \\ &= \frac{g^2}{16\pi^2} \int d^4x \mathrm{Tr}(*F_{\mu\nu} F^{\mu\nu}), \end{aligned} \tag{3.28}$$

where $*F_{\mu\nu} = \frac{1}{2}\epsilon_{\mu\nu\alpha\beta} F^{\alpha\beta}$ is the *dual* field strength tensor. The boundary condition for A_μ is

$$\lim_{r\to\infty} A_\mu(t, \vec{x}) = \frac{i}{g} U(x/r) \partial_\mu U^\dagger(x/r). \tag{3.29}$$

Since Yang-Mills theory is gauge-invariant, we can gauge A_μ with any $g_k \in SU(2)$ of winding number k. This will shift $\nu_\pm$ by k, but the total winding number ν is unchanged. To derive the Yang-Mills equation, we shall minimize Euclidean action

$$S_E = \frac{1}{2} \int d^4x \mathrm{Tr}(F_{\mu\nu} F^{\mu\nu}) \tag{3.30}$$

with the given winding number ν. The key point is the following equality:

$$\text{Tr}(*F_{\mu\nu} \pm F_{\mu\nu})^2 = 2\text{Tr}(F_{\mu\nu}F^{\mu\nu}) \pm 2\text{Tr}(*F_{\mu\nu}F^{\mu\nu}), \tag{3.31}$$

from which we have

$$S_E \geq \frac{1}{2}\left| \int d^4x \text{Tr}(*F_{\mu\nu}F^{\mu\nu}) \right| = \frac{8\pi^2}{g^2}|\nu|. \tag{3.32}$$

We can see that the equation holds if and only if

$$*F_{\mu\nu} = \pm F_{\mu\nu}, \tag{3.33}$$

i.e., $F_{\mu\nu}$ is (anti)self-dual, and corresponding A_μ is (anti) instanton. Using Eq.3.29, we can make the ansatz

$$A_\mu(t, \vec{x}) = \frac{i}{g} f(r) U(x/r) \partial_\mu U^\dagger(x/r), \tag{3.34}$$

where $f(\infty) = 1$ and $f(0) = 0$. We consider $\nu = 1$ instanton solution $F_{\mu\nu} = *F_{\mu\nu}$, and U is precisely constructed from Eq.3.23:

$$U(x/r) = \frac{t + \vec{x} \cdot i\vec{\sigma}}{r}. \tag{3.35}$$

Solving the self-dual equation, we get

$$A_\mu = \frac{i}{g}\frac{r^2}{r^2 + a^2} U(x/r) \partial_\mu U^\dagger(x/r), \tag{3.36}$$

where a is a constant of integration, known as the *size* of instanton. The solution Eq.3.36 is called *BPST* solution [1]. It mediates the tunneling between a vacuum of winding number ν_- at $t = -T/2$ and another vacuum of winding number $\nu_+ = \nu_- + 1$ at $t = T/2$. This once again confirms the property of instanton: it allows the system to penetrate barriers, tunneling between inequivalent vacua.

3.2.2 θ-vacuum and θ-term

Due to the instantons, we see that the true $SU(2)$ Yang-Mills theory vacuum should be a superposition of an infinite set of topologically inequivalent vacuum states $|n\rangle$'s, where n is the instanton number. This is known as θ-vacuum:

$$|\theta\rangle = \sum_n e^{-in\theta} |n\rangle . \tag{3.37}$$

To understand more about the θ vacuum, we calculate the amplitude $|\theta\rangle \to |\theta'\rangle$:

$$\begin{aligned}
\langle\theta'| e^{-HT} |\theta\rangle &= \sum_{\nu_+,\nu_-} \langle\nu_+| e^{-HT} e^{i\nu_+\theta' - i\nu_-\theta} |\nu_-\rangle \\
&= \sum_{\nu_+,\nu_-} \langle\nu_+| e^{-HT} e^{i\nu_-\theta' + i\nu\theta' - i\nu_-\theta} |\nu_-\rangle \\
&= \delta(\theta - \theta') \sum_\nu \langle\nu_+| e^{-HT} e^{i\nu\theta} |\nu_-\rangle \\
&= \delta(\theta - \theta') \sum_\nu \int \mathcal{D}A_{[\nu]} e^{-S_E + i\nu\theta},
\end{aligned} \tag{3.38}$$

where $A_{[\nu]}$ represents a gauge potential of winding number ν. To complete the summation, we can see that the $\sum_\nu \int \mathcal{D}A_{[\nu]}$ sums over all possible configurations of A, and we can replace it with $\int \mathcal{D}A$. Using Eq.3.28, we have

$$\sum_\nu \int \mathcal{D}A_{[\nu]} e^{-S_E + i\nu\theta} = \int \mathcal{D}A \exp\left\{ \int d^4x \left[-\frac{1}{2}\mathrm{Tr}(F_{\mu\nu}F^{\mu\nu}) + \frac{ig^2\theta}{16\pi^2}\mathrm{Tr}(*F_{\mu\nu}F^{\mu\nu}) \right] \right\}. \tag{3.39}$$

We can see an additional interacting term $\mathrm{Tr}(*FF)$, and the coupling constant is proportional to θ. We can go back to Minkowski spacetime to get the path integral of Yang-Mills theory:

$$\begin{aligned}
Z(A) &= \int \mathcal{D}A e^{i\int d^4x(\mathcal{L}_{YM} + \mathcal{L}_\theta)} \\
&= \int \mathcal{D}A \exp\left\{ \int d^4x \left[-\frac{i}{2}\mathrm{Tr}(F_{\mu\nu}F^{\mu\nu}) - \frac{ig^2\theta}{16\pi^2}\mathrm{Tr}(*F_{\mu\nu}F^{\mu\nu}) \right] \right\},
\end{aligned} \tag{3.40}$$

where

$$\mathcal{L}_{YM} = -\frac{1}{2}\mathrm{Tr}(F_{\mu\nu}F^{\mu\nu}), \quad \mathcal{L}_\theta = -\frac{g^2\theta}{16\pi^2}\mathrm{Tr}(*F_{\mu\nu}F^{\mu\nu}). \tag{3.41}$$

The $\mathcal{L}_\theta$ is known as θ-term, and it didn't appear in Yang-Mills theory until we consider the nontrivial topology of the vacuum. θ-term is a total divergence by Eq.3.28 and therefore doesn't affect the equation of motion or the Feynman rules. However, this term is gauge-invariant and violates CP symmetry, leading to the well-known strong CP problem.

3.3 $U(1)_A$ problem

For a long time, chiral symmetry has been considered spontaneously broken. According to Goldstone's theorem, there must be a very light boson. However, it was not observed in the experiment. This is the $U(1)_A$ problem [50]. We will review the basic chiral symmetry breaking and present 't Hooft's instanton solution to $U(1)_A$ problem.

3.3.1 Chiral symmetry breaking and the missing Goldstone boson

Let us consider a simple QCD model with only up and down quarks:

$$\mathcal{L} = -\frac{1}{4}G^a_{\mu\nu}G^{a\mu\nu} + i\bar{u}\not{D}u + i\bar{d}\not{D}d, \tag{3.42}$$

where we have ignored quarks' mass since it is small compared to $\Lambda_{QCD} \sim 300MeV$. To demonstrate the symmetry better, we can also write the Lagrangian in terms of left- and right-handed spinors $u_{L/R} = \frac{1}{2}(1 \mp \gamma^5)u$ and $d_{L/R} = \frac{1}{2}(1 \mp \gamma^5)d$:

$$\mathcal{L} = -\frac{1}{4}G^a_{\mu\nu}G^{a\mu\nu} + i\bar{u}_L\not{D}u_L + i\bar{u}_R\not{D}u_R + i\bar{d}_L\not{D}d_L + i\bar{d}_R\not{D}d_R. \tag{3.43}$$

We see that the Lagrangian is invariant under chiral symmetry $U(2)_L \times U(2)_R = SU(2)_V \times SU(2)_A \times U(1)_V \times U(1)_A$. In terms of flavour doublet $q^i_{L/R} = (u_{L/R}, d_{L/R})^T$, these four symmetries are written as:

$$\begin{aligned} &SU(2)_V: \;\; q_L \to gq_L, \;\; q_R \to gq_R \\ &SU(2)_A: \;\; q_L \to gq_L, \;\; q_R \to g^\dagger q_R \\ &U(1)_V: \;\; q_L \to e^{i\theta}q_L, \;\; q_R \to e^{i\theta}q_R \\ &U(1)_A: \;\; q_L \to e^{i\theta}q_L, \;\; q_R \to e^{-i\theta}q_R, \end{aligned} \tag{3.44}$$

where $g \in SU(2)$ and $\theta \in \mathbb{R}$. At low temperatures (roughly below Λ_{QCD}), the bilinear quark operator $q^i_L\bar{q}^j_R$ acquires a non-vanishing expectation value:

$$< \bar{q}^i_L q^j_R >= -V^3\delta^i_j, \;\; V \sim \Lambda_{QCD}. \tag{3.45}$$

This phenomenon is known as *quark condensate*. We see that the vacuum only respects symmetry $SU(2)_V \times U(1)_V$, and $SU(2)_A \times U(1)_A$ is *spontaneous broken*. According to Goldstone theorem, there will be four massless bosons[3]. The first three bosons are *pions* $\vec{\pi} = (\pi^{\pm}, \pi^0)$, and the fourth has never been observed in the laboratory. This is called $U(1)_A$ *problem* [50]. In fact, there is a candidate particle: η', but its mass ($950MeV$) is much heavier than theoretic bound $\sqrt{3}m_\pi \approx 240MeV$. An alternative form of the $U(1)_A$ problem is: *Why is η' so heavy*?

3.3.2 Instanton solution

The resolution is pretty simple: from Chapter 2, we know that $U(1)_A$ is an anomaly; therefore, we shouldn't expect any Goldstone boson. Gerard 't Hooft presented a toy model [51] to visualize how instanton solves this issue. As shown in [52], the instanton induces an effective quark determinant interaction:

$$\mathcal{L}_{eff} = \kappa e^{i\theta} \det \bar{q}_R q_L + h.c, \tag{3.46}$$

where κ is a constant and $\det$ is taken on flavour indices. This interaction violates $U(1)_A$. To model the instanton solution, we define a meson field ϕ that transforms under $U(2)_L \times U(2)_R$:

$$\phi_{ij} = \bar{q}^i_R q^j_L. \tag{3.47}$$

We also have an Lagrangian invariant under $U(2)_L \times U(2)_R$:

$$\mathcal{L}_0 = -\text{Tr}\partial_\mu\phi\partial_\mu\phi^\dagger - V(\phi) \tag{3.48}$$

Because ϕ is a 2×2 complex field, we can expand it as eight physical particle states $\sigma, \eta, \vec{\alpha}, \vec{\pi}$:

$$\phi = \frac{1}{2}(\sigma + i\eta) + \frac{1}{2}(\vec{\alpha} + i\vec{\pi}) \cdot \vec{\tau}, \tag{3.49}$$

where $\vec{\tau}$ are Pauli matrices. Since the symmetry breaks down to $SU(2)_V \times U(1)_V$, we must have

$$\langle\sigma\rangle = f \neq 0, \;\; \langle\eta\rangle = \langle\vec{\alpha}\rangle = \langle\vec{\pi}\rangle = 0. \tag{3.50}$$

[3] In reality, chiral symmetry is explicitly broken by the mass of quarks. Hence the bosons are not massless.

The four massless Goldstone bosons are η and $\vec{\pi}$. However, due to the instanton effect, $\mathcal{L}_0$ gets modified by interaction Eq.3.46:

$$\begin{aligned}\mathcal{L}_{eff} &= \kappa e^{i\theta} \det \bar{q}_R q_L + h.c \\ &= \kappa e^{i\theta}[(\sigma + i\eta)^2 - (\vec{\alpha} + i\vec{\pi})^2] + h.c.\end{aligned} \tag{3.51}$$

We can use the $U(1)$ symmetry of ϕ to rotate θ via

$$\phi \to e^{i(\pi-\theta)/2}\phi. \tag{3.52}$$

So $\mathcal{L}_{eff}$ becomes

$$\mathcal{L}_{eff} = -2\kappa(\sigma^2 + \vec{\pi}^2 - \eta^2 - \vec{\alpha}^2). \tag{3.53}$$

We see that η's mass is lifted by instanton effect κ, while pions are still massless. The key ingredients of the Instanton solution are:

- The axial $U(1)_A$symmetry is explicitly broken by effective interaction $\mathcal{L}_{eff}$ which is induced by instanton.
- For $\mathcal{L}_0$, the symmetry is spontaneously broken, but one of the resulting Goldstone bosons acquires mass from the instanton effect.

3.4 Gravitational instanton

Gravitational instanton [53, 54, 2] is a solution to the vacuum Einstein field equations with finite action on Riemannian manifold, giving (anti)self-dual curvature tensor. They are analogs in Yang-Mills theory's quantum theories of gravity of instantons. This chapter discusses an (anti)self-dual solution to Euclidean gravity and Yang-Mills instanton in this background.

3.4.1 Eguchi–Hanson solution

Let (t, x, y, z) be a coordinate system on a Riemannian manifold. Changing to spherical coordinates (r, θ, ϕ, ψ), we have

$$x + iy = r\cos\frac{\theta}{2}\exp\left\{\frac{i}{2}(\psi+\phi)\right\}, \quad z + it = r\cos\frac{\theta}{2}\exp\left\{\frac{i}{2}(\psi-\phi)\right\}, \tag{3.54}$$

where $r^2 = t^2 + x^2 + y^2 + z^2$ and the range of angles θ, ϕ, ψ are

$$0 \le \theta \le \pi, \quad o \le \phi \le 2\pi, \quad 0 \le \psi \le 4\pi. \tag{3.55}$$

It is useful to introduce three useful 1-forms:

$$\begin{aligned} \sigma_x &= \frac{1}{2}(\sin\psi d\theta - \sin\theta\cos\psi d\phi) \\ \sigma_y &= \frac{1}{2}(-\cos\psi d\theta - \sin\theta\sin\psi d\phi) \\ \sigma_z &= \frac{1}{2}(d\psi + \cos\theta d\phi). \end{aligned} \tag{3.56}$$

These 1-forms satisfy identities

$$d\sigma_x = 2\sigma_y \wedge \sigma_z, \quad \text{and so forth.} \tag{3.57}$$

Consider the structure equations for connection 1-form $\omega^a{}_b$:

$$de^a + \omega^a{}_b \wedge e^b = 0, \tag{3.58}$$

where e^a is the tetrad under which the metric is locally flat, i.e., the component is δ_{ab}. Differentiating Eq.3.58, we get the first Bianchi identity

$$R^a{}_b \wedge e^b = 0 \Longleftrightarrow \epsilon_{ebcd}R^a{}_{bcd} = 0, \tag{3.59}$$

where $R = d\omega + \omega\wedge\omega$ is the Riemann tensor. Define the "dual' of R:

$$\tilde{R}^a{}_b = \frac{1}{2}\epsilon_{abcd}R^c{}_d, \tag{3.60}$$

then the vacuum Einstein equation $R^{ac}{}_{bc} = 0$ can be conventionally written as

$$\tilde{R}^a{}_b \wedge e^b = 0. \tag{3.61}$$

Combining with Eq.3.59, we see that if the Riemann tensor R is (anti) self-dual:

$$R^a{}_b = \pm \tilde{R}^a{}_b, \tag{3.62}$$

then the vacuum Einstein equation is solved. Further, it can be shown that the corresponding connection 1-form ω is (anti) self-dual as well by choosing the appropriate gauge, i.e.,

$$\omega^a{}_b = \pm \frac{1}{2}\epsilon_{abcd}\omega^c{}_d. \tag{3.63}$$

We now make an axially symmetric ansatz for the metric:

$$ds^2 = f^2(r)dr^2 + r^2(\sigma_x^2 + \sigma_y^2 + g^2(r)\sigma_z^2), \tag{3.64}$$

where the boundary conditions for the unknown function $f(r)$ and $g(r)$ are

$$f(+\infty) = 1, \quad g(+\infty) = 1. \tag{3.65}$$

That is to say, at $r = \infty$, the metric is flat. It is not difficult to get corresponding tetrad e^a's

$$e = (f(r)dr, \; r\sigma_x, \; r\sigma_y, \; g(r)\sigma_z), \tag{3.66}$$

and the connection ω is

$$\begin{aligned} &\omega^0{}_1 = \frac{1}{rf(r)}e^1, \quad \omega^2{}_0 = \frac{1}{rf(r)}e^2, \quad \omega^3{}_0 = \left(\frac{1}{rf(r)} + \frac{g'(r)}{f(r)g(r)}\right)e^3 \\ &\omega^2{}_3 = \frac{g(r)}{r}e^1, \quad \omega^3{}_1 = \frac{g(r)}{r}e^2, \quad \omega^1{}_2 = \frac{2-g^2(r)}{rg(r)}e^3. \end{aligned} \tag{3.67}$$

Imposing anti self-dual condition, we get differential equations for $f(r)$ and $g(r)$:

$$f(r)g(r) = 1, \quad g(r) + rg'(r) = f(r)(2 - g^2(r)). \tag{3.68}$$

This system is solvable, and the result is

$$f^2(r) = \frac{1}{1-\frac{a^4}{r^4}}, \quad g^2(r) = 1 - \frac{a^4}{r^4}, \tag{3.69}$$

where a is a constant. Therefore the metric is

$$ds^2 = \frac{1}{1-\frac{a^4}{r^4}}dr^2 + r^2(\sigma_x^2 + \sigma_y^2) + r^2(1 - \frac{a^4}{r^4})\sigma_z^2, \tag{3.70}$$

which is known as *Eguchi-Hanson* metric [55, 56, 57].

We now analyze the singularity $r = a$. By defining

$$u^2 = r^2\left(1 - \frac{a^4}{r^4}\right), \tag{3.71}$$

the metric Eq.3.70 can be written as

$$ds^2 = \frac{1}{(1 + \frac{a^4}{r^4})^2} du^2 + u^2\sigma_z^2 + r^2(\sigma_x^2 + \sigma_y^2). \tag{3.72}$$

Near $r = a$ ($u = 0$), the metric is

$$ds^2 \approx \frac{1}{4}du^2 + \frac{1}{4}u^2(d\psi + \cos\theta d\phi)^2 + \frac{a^2}{4}(d\theta^2 + \sin^2\theta d\phi^2). \tag{3.73}$$

We find that for fixed $\theta,\ \phi$ the metric reduces to the flat one on $\mathbb{R}^2$ provided we half the range of ψ:

$$0 < \psi < 4\pi \to 0 < \psi < 2\pi. \tag{3.74}$$

By doing so, $u = 0$ is a removable singularity caused by a bad choice of coordinates frame, and the topology near there is then $\mathbb{R}^2 \times S^2$. However, the boundary now is not S^3, although the metric there is flat as r becomes large. Instead, the boundary is $S^3/\mathbb{Z}_2 = \mathbb{R}P^3$, locally homeomorphic to Euclidean space. Such a manifold is called *asymptotically locally Euclidean* [58].

3.4.2 Gauge fields in Gravitational instanton background

Consider the Einstein–Yang-Mills theory, which involves gravity and gauge field on the Riemann manifold:

$$S = -\frac{1}{16\pi}\int_M d^4x\sqrt{g}R + \frac{1}{4g_{QCD}^2}\int_M d^4x\sqrt{g}F^a_{\mu\nu}F^{a\mu\nu}. \tag{3.75}$$

The equations of motion read:

$$
\begin{aligned}
&R_{\mu\nu} - \frac{1}{2} g_{\mu\nu} R = T_{\mu\nu}, \\
&T_{\mu\nu} = \frac{8\pi}{g^2_{QCD}} \left[F^a_{\mu\beta} F^{a\beta}_{\nu} - \frac{1}{4} g_{\mu\nu} (F^a_{\lambda\tau} F^{a\lambda\tau}) \right], \\
&D_\mu(\sqrt{g} * F^{a\mu\nu}) = 0,
\end{aligned}
\tag{3.76}
$$

where $R_{\mu\nu}$ is the Ricci tensor, R is the Ricci scalar and $D_\mu = \partial_\mu + A_\mu$ is the covariant derivative operator. The first is the Einstein equation, and the third is the Yang-Mills equation. On the Riemann manifold, energy–momentum tensor $T_{\mu\nu}$ has an important property: its sign gets flipped when replacing F_μ by its dual $*F_{\mu\nu}$. Therefore when the Yang-Mills equation is solved by $F = \pm * F$, we get a vacuum Einstein equation. In other words, the first and the third equations in Eq.3.76 can be satisfied by vacuum solutions simultaneously [59]:

$$
R_{\mu\nu} - \frac{1}{2} g_{\mu\nu} R = 0, \quad F_{\mu\nu} = \pm * F_{\mu\nu}. \tag{3.77}
$$

When the gauge group is Abelian, i.e., $U(1)$ gauge theory, the solution is given by [58, 55, 56]:

$$
A_r = A_\theta = 0, \quad A_\phi = \frac{Qa^2}{r^2} \cos\theta, \quad A_\psi = \frac{Qa^2}{r^2}. \tag{3.78}
$$

Solution Eq.3.78 violates the chiral charge, leading to an extra CP-violation term [60]. This is quite different from the situation in flat spacetime where there does not exist $U(1)$ instanton due to the triviality of $\pi_3(S^1)$.

The interesting thing here is the solution for the non-Abelian gauge theory. We choose Eguchi-Hanson metric Eq.3.70 to satisfy Einstein's equation:

$$
\begin{aligned}
&ds^2 = c_r^2 dr^2 + \sum_{i=1}^{3} c_i^2 (\sigma^i)^2, \\
&c_r = \frac{1}{\sqrt{1 - \frac{a^4}{r^4}}}, \quad c_1 = c_2 = \frac{1}{2} r, \quad c_3 = \frac{1}{2} r \sqrt{1 - \frac{a^4}{r^4}},
\end{aligned}
\tag{3.79}
$$

where we have re-scaled it. We also remove the factor $-1/2$ of 1-forms Eq.3.56:

$$
\begin{aligned}
\sigma^1 &= -\sin\psi d\theta + \cos\psi \sin\theta d\phi, \\
\sigma^2 &= \cos\psi d\theta + \sin\psi \sin\theta d\phi, \\
\sigma^3 &= -d\psi - \cos\theta d\phi.
\end{aligned}
\tag{3.80}
$$

We shall focus on $SU(2)$ gauge theory:

$$
A = A_i \sigma_i, \quad A_i = A_i^a T^a, \tag{3.81}
$$

where A_i's are matrices and $T^a = -i\tau^a/2$ is anti-Hermitian $SU(2)$ generator: $[T^a, T^b] = \epsilon^{abc} T^c$. The corresponding field strength tenor F is then

$$
\begin{aligned}
F &= dA + A \wedge A \\
&= \frac{\partial_r A_i}{c_r c_i} e^0 \wedge e^i - \sum_{j<k} \frac{A_i}{c_j c_k} \epsilon^{ijk} e^j \wedge e^k + \sum_{j<k} [A_j, A_k] e^j \wedge e^k
\end{aligned}
\tag{3.82}
$$

where $e^\mu = \{e^0 = c_r dr,\ e^i = c_i \sigma^i\}$ is the tetrad basis. The self-dual equation $F = *F$ explicitly reads

$$
\begin{aligned}
\frac{\partial_r A_1}{c_r c_1} &= -\frac{A_1}{c_2 c_3} + \frac{1}{c_2 c_3}[A_2, A_3] \\
\frac{\partial_r A_2}{c_r c_2} &= -\frac{A_2}{c_1 c_3} + \frac{1}{c_1 c_3}[A_3, A_1] \\
\frac{\partial_r A_3}{c_r c_3} &= -\frac{A_3}{c_1 c_2} + \frac{1}{c_1 c_2}[A_1, A_2].
\end{aligned}
\tag{3.83}
$$

The solution is then

$$
\begin{aligned}
A_1^1 = A_2^2 &= 2\sqrt{\Delta} \frac{\lambda (r^4 - a^4)^{\sqrt{\Delta}/(2a^2)}}{\lambda^2 (r^2 + a^2)^{\sqrt{\Delta}/a^2} - (r^2 - a^2)^{\sqrt{\Delta}/a^2}} \cdot \frac{1}{\sqrt{r^4 - a^4}} \\
A_3^3 &= \sqrt{\Delta} \frac{\lambda^2 (r^2 + a^2)^{\sqrt{\Delta}/a^2} + (r^2 - a^2)^{\sqrt{\Delta}/a^2}}{\lambda^2 (r^2 + a^2)^{\sqrt{\Delta}/a^2} - (r^2 - a^2)^{\sqrt{\Delta}/a^2}} \cdot \frac{1}{r^2},
\end{aligned}
\tag{3.84}
$$

where λ and Δ are integration constants. Solution Eq.3.84 is equivalent to [**61**, **62**, **63**, **64**, **65**], and we can also recover the solutions in [**59**] and [**66**]. For instance, choosing

$$
\lambda = 1, \quad \sqrt{\Delta} = 2a^2 \tag{3.85}
$$

gives

$$A_1^1 = A_2^2 = \sqrt{1 - \frac{a^4}{r^4}}, \;\; A_3^3 = 1 + \frac{a^4}{r^4}, \tag{3.86}$$

Which is the solution in [59]. Choosing

$$\sqrt{\Delta} = a^2, \;\; t^2 = \frac{\lambda^2 + 1}{\lambda^2 - 1} a^2 \tag{3.87}$$

and keeping λ general gives

$$A_1^1 = A_2^2 = \frac{\sqrt{t^4 - a^4}}{r^2 + t^2}, \;\; A_3^3 = \frac{t^2 r^2 + a^4}{r^2(r^2 + t^2)}, \tag{3.88}$$

which is the solution in [66]. We call this combined solution $(g_{\mu\nu}, A_\mu)$ *colored gravitational Eguchi-Hanson instanton* (CEH), for the reason that $F_{\mu\nu}$ is a non-Abelian gauge field living in gravitational instanton background.

3.5 Appendix:tetrad and Bianchi identities

3.5.1 tetrad in geometry

The concept of a tetrad, also known as a vierbein, is a set of four linearly independent vectors (usually denoted as $e_a, a = 0, 1, 2, 3$) at each point of a four-dimensional spacetime manifold. Under a tetrad, the metric is *locally* flat, meaning it is Minkowski $(-1, +1, +1, +1)$ or Euclidean $(+1, +1, +1, +1)$ within certain open set. A vector T's components under vector basis ∂_μ and tetrad are related by matrix e_a^μ:

$$\begin{aligned} &T = T^\mu \partial_\mu, \;\; T = T^a e_a, \\ &T^\mu = T^a e_a^\mu, \end{aligned} \tag{3.89}$$

where e_a^μ is defined by

$$e_a = e_a^\mu \partial_\mu. \tag{3.90}$$

The physical meaning of tetrad is the "free-falling frame" in which the effects of gravity are not experienced. The physics of free-falling observers see is as if they were in an inertial frame.

3.5.2 Bianchi identities

Recall Riemann curvature tensor is given by

$$R_{ijkl} = \partial_j \omega_{ik}^l - \partial_k \omega_{ij}^l + \omega_{jm}^l \omega_{ik}^m - \omega_{km}^l \omega_{ij}^m \tag{3.91}$$

It is easy to see, for a fixed l, we have the first Bianchi identity:

$$R_{ijkl} + R_{kijl} + R_{jkil} = 0. \tag{3.92}$$

For the second Bianchi identity, we first compute the covariant of the Riemann tensor:

$$\nabla_p R_{ijkl} = \partial_p R_{ijkl} - \Gamma_{pi}^m R_{mjkl} - \Gamma_{pj}^m R_{imkl} - \Gamma_{pk}^m R_{ijml} - \Gamma_{pl}^m R_{ijkm}. \tag{3.93}$$

We then sum cyclically over the indices p, j, k to get the second Bianchi identity:

$$\nabla_p R_{ijkl} + \nabla_j R_{ikpl} + \nabla_k R_{ijpl} = 0 \tag{3.94}$$

CHAPTER 4

The strong CP problem and the axion

Nature has three fundamental discrete symmetries: charge conjugation C that converts particles with their antiparticles and vice versa; parity P that reverses the spatial axes, converting left-handed particles into right-handed ones and vice versa; time reversal T that reverses the direction of time. CPT theorem [67, 68] states that physical laws are invariant under the product of these three transformations. People are interested in some symmetry-breaking effects, especially CP-violating ones. CP violation refers to the product CP being broken, giving unusual differences between particles and antiparticles. The earliest CP-violating phenomenon was the decay of neutral kaons, observed in 1964 [69]: neutral kaon decays into two pions, while its antiparticle decays into two antipions. These two processes had different rates, implying CP violation.

In the electroweak theory, the CKM matrix [35, 36], which mixes different generations of quarks, is a source of CP violation. Its phase is crucial for matter-antimatter asymmetry from the baryogenesis in the early universe.

PMNS matrix [37, 38], is another source of CP violation in the electroweak theory. It describes the mixing between different generations of neutrinos, giving so-called *neutrino oscillations*, and its phase leads to different survival probabilities of neutrinos and antineutrinos. Nevertheless, it is hard to detect CP violation in QCD, which is inconsistent with its mathematical construction, leading to the well-known *strong CP* problem.

4.1 The Strong CP problem

The neutron possesses a non-zero electric dipole moment (nEDM), which measures the separation of positive and negative electric charges. The nEDM violates parity P and time-reversal T symmetry, implying CP is also violated. The current bound of nEDM is $d_n < 3 \times 10^{-26} ecm$ [70, 71, 72, 73, 74, 75, 76], which leads to a rather tiny bound on QCD-θ parameter (see Eq.3.41) [3, 77]:

$$\theta < 10^{-10}. \tag{4.1}$$

This is the *strong CP problem*: why is θ so small?

As a fundamental parameter in QCD, θ is expected to be of order one, but it is hard to detect CP violation in strong interactions in the experiment. Moreover, any physical laws or principles do not constrain it, and even the SM cannot account for this tiny bound.

4.2 Axion

4.2.1 Peccei–Quinn solution

The key point of Peccei–Quinn (PQ) solution [4, 5] to the strong CP problem is to promote θ as a field such that its expectation value is small enough. To achieve this, one has to extend SM with an additional Higgs field such that a new $U(1)$ symmetry called $U(1)_{PQ}$ is spontaneously broken, and the resultant Goldstone boson is called *axion* [78, 79, 80, 81, 82, 83].

The fermion-Higgs Yukawa coupling for two flavors (u, d) reads

$$\mathcal{L}_Y = Y_u \bar{Q}_L H_2 u_R + Y_d \bar{Q}_L H_1 d_R + h.c. \tag{4.2}$$

where $Q_L = (u_L, d_L)$, $H_1 = (\phi_1^+, \phi_1^0)$ is the SM Higgs field and $H_2 = (\phi_2^+, \phi_2^0)$ is the new introduced Higgs field. This modified Yukawa coupling possesses a new charged symmetry

$U(1)_{PQ}$:

$$Q_L \to e^{iX_L} Q_L, \;\; u_R \to e^{-iX_{u_R}}, \;\; d_R \to e^{-iX_{d_R}} d_R, \;\; H_{1,2} \to e^{-iX_{1,2}} H_{1,2}, \tag{4.3}$$

and these PQ charges satisfy

$$X_1 = X_L - X_{d_R}, \;\; X_2 = X_L - X_{u_R}. \tag{4.4}$$

Evidently, $U(1)_{PQ}$ is comprised of $U(1)_A$ and another two $U(1)$'s from Higgs sector. When $\phi^0_{1,2}$ acquire their vacuum expectation value $v_{1,2}/\sqrt{2}$, the spontaneous symmetry breaking occurs. One Goldstone boson is eaten by Z^0 boson, and its orthogonal complement part is the axion field $a = a(x)$. Specifically, we have

$$H_1 = \frac{v_1}{\sqrt{2}} e^{i\frac{av_2}{f_a v_1}} \begin{pmatrix} 0 \\ 1 \end{pmatrix}, \;\; H_2 = \frac{v_2}{\sqrt{2}} e^{i\frac{av_1}{f_a v_2}} \begin{pmatrix} 1 \\ 0 \end{pmatrix}, \tag{4.5}$$

where $f_a = \sqrt{v_1^2 + v_2^2}$ is the symmetry breaking scale. We can continue to rotate a field away from mass term [1]:

$$u \to e^{-i\gamma^5 \frac{av_1}{2f_a v_2}} u, \;\; d \to e^{-i\gamma^5 \frac{av_2}{2f_a v_1}} d. \tag{4.6}$$

This local $U(1)_A$ induces a modification of θ term in Lagrangian:

$$\frac{g^2\theta}{16\pi^2} \mathrm{Tr}(*G_{\mu\nu}G^{\mu\nu}) \to \frac{g^2}{16\pi^2} \left[\theta + \frac{a}{f_a} N\left(x + \frac{1}{x}\right)\right] \mathrm{Tr}(*G_{\mu\nu}G^{\mu\nu}), \tag{4.7}$$

where N is the *anomaly coefficient* and $x = v_1/v_2$. The axion now extends the SM Lagrangian:

$$\mathcal{L} = \mathcal{L}_{SM} + \frac{g^2}{16\pi^2} \left[\theta + \frac{a}{f_a} N\left(x + \frac{1}{x}\right)\right] \mathrm{Tr}(*G_{\mu\nu}G^{\mu\nu}) - \frac{1}{2}\partial_\mu a \partial^\mu a + \mathcal{L}[\partial a, \Psi]. \tag{4.8}$$

This model is called Peccei-Quinn-Weinberg-Wilczek (PQWW) model [**4**, **5**, **78**, **79**]. Integrating out QCD instanton, the coupling between axion and gluons gives rise to the effective potential for the axion:

$$V_{eff} = -K \cos\left(N\frac{a}{f_a} + \theta\right). \tag{4.9}$$

This potential is minimized when

$$N\frac{\langle a \rangle}{f_a} + \theta = 0, \tag{4.10}$$

[1] In the original model, left-handed quarks are not PQ charged.

so that the CP-odd term in QCD is eliminated. This ingenious idea has been ruled out by the experiment [84, 85, 86, 87]. Because f_a is the source of both fermions and W/Z bosons, SM requires a small $f_a \approx 246$GeV, which predicts a detectable signal in the laboratory. Yet nothing has been detected.

4.2.2 Invisible axion models

The flaw of the PQWW model is that the axion field is identified with the phase of the scalar field whose vacuum expectation value f_a is also the source of SM particles. The smallness of f_a implies a relatively large coupling ($\propto 1/f_a$) between the axion and other particles. To avoid this dilemma, it is reasonable to introduce a scalar field Φ (generally called the PQ field) whose vacuum expectation value is much higher than the electroweak scale and carries no electric or weak charge. Large f_a gives a rather weak coupling between axion and other particles, therefore 'invisible'.There are two benchmark invisible axion models: Kim-Shifman-Vainshtein-Zakharov (KSVZ) model and Dine-Fischler-Srednicki-Zhitnisky (DFSZ) model.

The KSVZ model

In the KSVZ model [80, 81], the scalar field Φ couples to a heavy quark Q which is a singlet under electroweak symmetry $SU(2)_L \times U(1)_Y$ and fundamental in color symmetry $SU(3)_c$:

$$\mathcal{L}_{PQ} = -\lambda_Q \bar{Q}_L \Phi Q_R + h.c. \tag{4.11}$$

Only Φ and Q are PQ-charged, while the fermions are not. The $U(1)_{PQ}$ symmetry reads

$$Q_L \to e^{i\alpha/2} Q_L, \quad Q_R \to e^{-i\alpha/2} Q_R, \quad \Phi \to e^{i\alpha}\Phi, \tag{4.12}$$

and the symmetry of potential $V(|\Phi|^2 - f_a^2)$ of Φ is spontaneous broken under $U(1)_{PQ}$. In the KSVZ model, axion does not couple to fermions at tree level, and the unique coupling between axion and SM is $aG\tilde{G}$.

The DFSZ model

The construction of the DFSZ [83, 82] model is a little complicated. We still have two Higgs fields as in the PQWW model, and the PQ field Φ is an SM singlet. They couple to each other via a quartic term:

$$\mathcal{L}_{PQ} = -\lambda \phi_1^T C (\Phi^\dagger)^2 \phi_2 + h.c. \tag{4.13}$$

The fermions are PQ-charged but indirectly couple to Φ via Higgs potential.

CHAPTER 5

Axion phenomenology

This chapter discusses the phenomenology of the axion. We will briefly review the observation methods of axions and the constraints of the coupling coefficients of axions with electrons, photons, and nucleons. We will also discuss dark matter axions and their production. The axion-photon limit picture is from `github.com/cajohare/AxionLimits`.

5.1 Axion detection

We generally use helioscopes to detect solar axions. Typical experiments in solar axion detection include the CERN Axion Solar Telescope (CAST) [88, 89, 90] and the proposed International Axion Observatory (IAXO) [91, 92]. CAST uses a decommissioned Large Hadron Collider (LHC) test magnet to convert solar axions back to photons. IAXO represents the next generation of axion helioscopes. Its design includes a new large-scale magnet, a superconducting, multi-bore, toroidal configuration, producing an intense magnetic field over a large volume. IAXO aims to be more sensitive to the axion-photon coupling than an order of magnitude beyond the CAST bound. It will also be capable of testing the range of values for axion-electron coupling, exploring areas beyond current astrophysical bounds.

In addition to solar axions, research also focuses on dark matter axions. Experiments like the Axion Dark Matter Experiment (ADMX) [93] and the Haloscope at Yale (HAYSTAC) [94] use haloscopes, which comprise a powerful magnet and a microwave cavity to convert dark matter axions into photons for detection. Further developments in dark matter axions detection are seen in the CAST-CAPP [95] and RADES [96], which experiment with new cavity designs to enhance sensitivity to higher axion mass ranges.

Some detections are just done in the laboratory. The OSQAR [97] experiments at CERN explore axion-like particles (ALPs) through a technique known as "Light Shining through Wall" (LSW). In this innovative approach, a laser beam is directed at a barrier that blocks photons but theoretically allows axions to pass through. If axions exist and are produced, they would traverse the barrier and then convert back into detectable photons on the other side, essentially "shining" light through an opaque wall. This conversion is expected to occur in strong magnetic fields, facilitating the photon-axion-photon transformation.

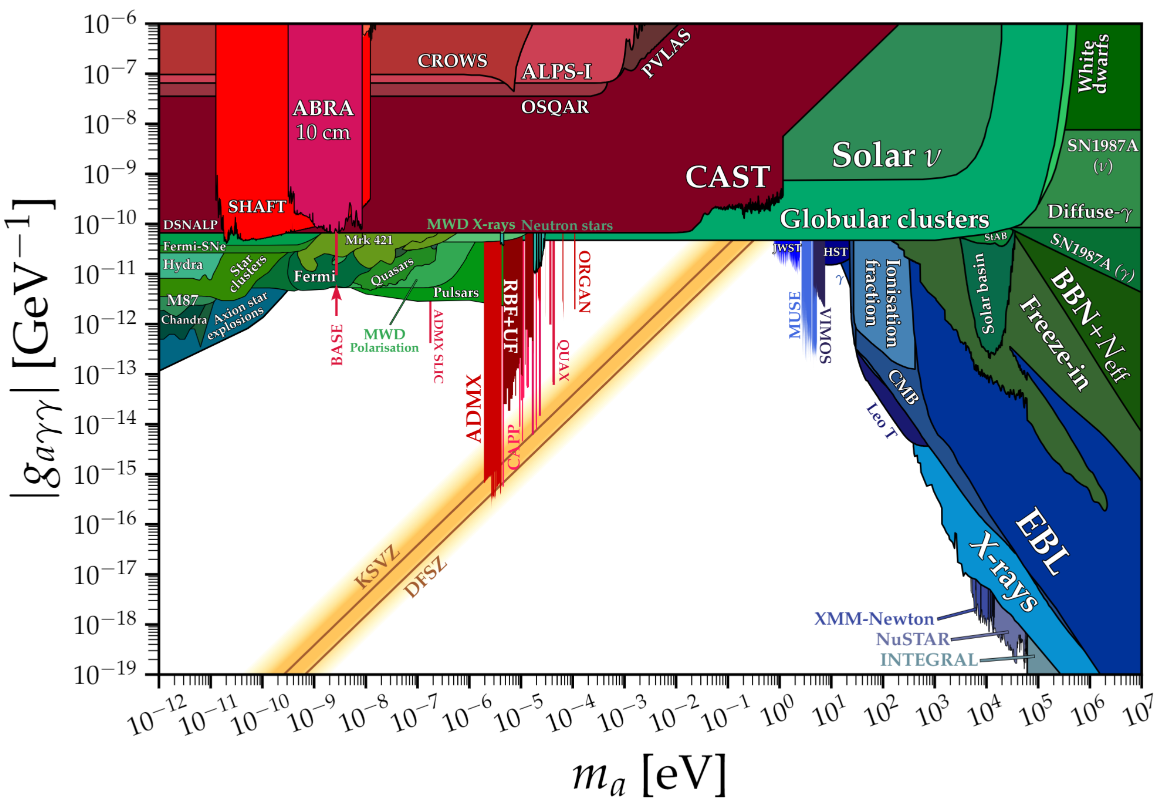

FIGURE 5.1: Current axion-photon limits. Red: purely laboratory experiments. Green: astrophysical detection. Blue: cosmological constraints. The yellow band is the so-called "QCD-band, " which shows KSVZ and DFSZ models.

5.2 Axions in Astrophysics

The axions can be produced in the stars and can escape easily. This process makes the star lose energy and shortens the star's life. We can make use of this mechanism to constrain the axion.

Helium Ignition and white dwarfs

When a star like the Sun exhausts its hydrogen fuel in the core, it doesn't immediately begin to burn helium. Instead, the core (now predominantly helium) contracts and heats up due to gravitational pressure. This contraction of the core triggers hydrogen burning in a surrounding shell, expanding the star's outer layers, cooling them, and giving the star a reddened appearance. This begins the Red Giant Branch (RGB) phase of a star's life. The star does not burn helium at the beginning of this phase. Instead, the increasing pressure and temperature in the core eventually lead to helium ignition. This event, known as the helium flash, occurs at the end of the RGB phase.

If the axion couples to electrons, they would be produced via two processes: $\gamma + e \to e^- + a$ and $e^- + Z \to Z + e^- + a$. The core of a red giant could cool more rapidly if axions carry away the energy, potentially delaying the onset of helium ignition, which makes helium ignition a potential mechanism to constrain axions.

The star sheds its outer layers after the Asymptotic Giant Branch (AGB) phase, creating a planetary nebula. The remaining core then cools and contracts, forming a white dwarf composed primarily of carbon and oxygen. By measuring the cooling rates of white dwarfs, we can test for deviations from the expected rates to constrain axion-electron coupling.
The bound of axion-electron coupling g_{aee} from Helium ignition and white dwarfs cooling reads [98, 99]:

$$g_{aee} < 1.3 \times 10^{-27}. \tag{5.1}$$

Horizontal branch

The Horizontal Branch (HB) is a significant phase in the life cycles of low to intermediate-mass stars, such as the Sun, characterized by the fusion of helium into carbon and oxygen in the core and hydrogen burning in a shell around the core. This phase is characterized by the star having a nearly constant luminosity and surface temperature, and it appears in a horizontal line on the Hertzsprung-Russell diagram, hence the name.

In the core of an HB star, the axions are produced mainly through the *Primakoff effect*:

$$\gamma + Ze \to Ze + a. \tag{5.2}$$

The escape of axions reduces HB lifetime and the number of HB stars. Measuring the HB lifetime gives the constraint on axion-photon coupling $g_{a\gamma\gamma}$ [100]:

$$g_{a\gamma\gamma} < 1.0 \times 10^{-10}\text{GeV}^{-1}. \tag{5.3}$$

Supernova 1987A

During a Type II supernova explosion, when a massive star ends its life, the main energy released is a flux of neutrinos. The potential release of axions can influence the duration of these neutrino bursts emitted. Observations of neutrino bursts from supernovae, such as SN1987A, can, therefore, be used to place constraints on the axion-nucleon coupling g_{aNN}. If the axion-nucleon coupling is small, axions can be produced efficiently and escape the supernova core, leading to rapid energy loss and a shorter neutrino burst due to faster core cooling. On the other hand, if the axion-nucleon coupling is large, axions would interact more with the core's matter, becoming trapped. This trapping would diminish their role in energy transport, reducing the cooling efficiency and potentially not shortening the neutrino burst as expected. The bound of g_{aNN} from Supernova 1987A is [101, 102]

$$3 \times 10^{-10} < g_{aNN} < 3 \times 10^{-7}. \tag{5.4}$$

5.3 Axions as dark matter

An invisible axion is an ideal candidate for dark matter [103, 104, 105, 106, 107, 108, 109] due to its stability and very weak coupling to ordinary matter. Cutting-edge dark matter research focuses on finding mechanisms that generate the correct abundance of cold dark matter. We first review the mechanisms by which they were produced in the early universe.

Misalignment mechanism

The picture of the misalignment mechanism [103, 105, 109] is quite simple: when the temperature is high enough (i.e., early universe), the axion field takes some initial value θ_0 differing from the CP-conserving one. When the temperature decreases, the axion field will 'roll down' to its final value and oscillate around it. Such oscillation sources the population of the axion (recall that the field value is related to the expected value of the particle number). To get a basic impression of this mechanism, we first write down the Klein-Gordon equation for the axion field in an expanding universe:

$$\partial_t^2 a + 3H\partial_t a - \frac{1}{R^2(t)}\nabla^2 a + m_a^2(t)a = 0, \tag{5.5}$$

where $R(t)$ is the scale factor of FLRW metric and $H = \dot{R}/R$ is the Hubble parameter. When the temperature is very high such that $m_a(t) > 3H$, the oscillation does not occur. The axion field oscillates once the temperature decreases with time such that $m_a(t) < 3H$. The energy density is then given by [107]

$$\Omega_a h^2 \simeq 0.4 \times \left(\frac{6\mu eV}{m_a}\right)^{7/6} \langle\theta_0^2\rangle. \tag{5.6}$$

Therefore, initial value θ_0 and mass m_a contribute to the abundance of dark matter. For θ_0, we have to consider two scenarios due to casual connectivity:

(1) PQ symmetry breaking occurs before inflation (pre-inflation).

(2) PQ symmetry breaking occurs after or during inflation (post-inflation).

For the pre-inflation scenario, only one casual patch influences θ_0, so it picks a random value and is homogeneous in the universe. For the post-inflation scenario, several casual patches contribute to θ_0, and we must take the average $\langle\theta_0^2\rangle = \pi^2/3$.

Thermal production

The thermal production of axions refers to the generation of axions during the early universe when it was in a state of thermal equilibrium. When the temperature of the primordial plasma is sufficiently high, axions are produced from the thermal bath of the QCD plasma [110, 111].

The Boltzmann equation governs the number density n_a:

$$\frac{dn_a}{dt} + 3Hn_a = \Gamma(n_{eq} - n_a), \tag{5.7}$$

where Γ is the total interaction rate at which the axion interacts with other particles. There are three main processes contributing to Γ [112, 113]:

(1) $a + g \rightleftharpoons q + \bar{q}$

(2) $a + q \rightleftharpoons g + q$ and $a + \bar{q} \rightleftharpoons g + \bar{q}$

(3) $a + g \rightleftharpoons g + g$,

where where $q/\bar{q}$ is quark/anti-quark and g is gulon. The density of axions from thermal production reads [112, 113]

$$\Omega_a h^2 \approx \frac{m_a n_a h^2}{\rho_{c,0}} = 4.4 \times 10^{-9} \left(\frac{100}{g_*(T_D)}\right)\left(\frac{10^{12} GeV}{f_a}\right), \tag{5.8}$$

where $\rho_{c,0}$ is the critical density today, $g_*(T_D)$ is degree of freedom when axion is decoupled and $f_a \sim 10^{9-12} GeV$. As the universe expanded and cooled down, the axion's number density was diluted, but its population was not changed significantly due to rather weak interactions.

Topological defects

When symmetry breaking occurs in the early universe, axion fields in different regions may take different vacuum expectation values, forming topological defects, such as strings, domain walls, and monopoles.

(1) *Monopoles*: A monopole is a hypothetical point-like topological defect, not homotopic to a point, meaning it cannot be smoothly deformed into a single point without breaking the structure. A monopole can decay or annihilate like strings and domain walls to produce axions.

(2) *Strings*: Strings can be considered one-dimensional tubes where the points all have the same vacuum states. Strings can oscillate and decay, producing axions.

(3) *Domain walls*: Domain walls are formed when PQ symmetry breaking occurs so that different regions take different vacuum expectation states. Domain walls are two-dimensional and separate different vacuum states. Domain walls store energy

and, if stable, can persist throughout the universe's evolution. Energy can be released as axions when domain walls collide and annihilate.

CHAPTER 6

Companion axions

In the first few chapters, we have seen how instanton gives rise to QCD θ-term in QCD Lagrangian and the strong CP problem caused by it. A surprising and understandable fact is that the nEDM also takes contribution from gravity [**60**, **114**, **115**] due to the gravitational topological term. This gravitational topological term also generates another cosine potential for the axion if one requires PQ mechanism. When minimizing the potential, a simple calculation shows the potential is not minimized at a CP-conserving value, leading to a new *strong-gravity-CP* problem. A reasonable way out of this dilemma is to introduce a new axion such that two cosine functions attain their minimum value simultaneously, which is the origin of the *companion-axion model*.

6.1 Theoretic framework

Recall that the divergence of the chiral current is

$$\partial^\mu j_\mu^5 = -\frac{g^2}{32\pi^2}\epsilon^{\mu\nu\alpha\beta}F^a_{\mu\nu}F^a_{\alpha\beta}, \tag{6.1}$$

where $SU(3)$ gluon field $F^a_{\mu\nu}$ is assumed. When gravity is involved, the divergence in curved spacetime reads [**44**, **45**, **46**, **47**]:

$$\nabla^\mu j_\mu^5 = -\frac{g^2}{32\pi^2}\epsilon^{\mu\nu\alpha\beta}F^a_{\mu\nu}F^a_{\alpha\beta} - \frac{1}{384\pi^2}\epsilon^{\mu\nu\alpha\beta}R^{\lambda\tau}{}_{\mu\nu}R_{\alpha\beta\lambda\tau}, \tag{6.2}$$

where ∇_μ is the Levi-Civita connection, and $R^\mu_{\alpha\beta\lambda}$ is the corresponding Riemann curvature. The term $\epsilon^{\mu\nu\alpha\beta}R^{\lambda\tau}{}_{\mu\nu}R_{\alpha\beta\lambda\tau}$ is also a topological term, known as *Pontryagin density*. The integral of Pontryagin density is an integer called the *Pontryagin index*:

$$\begin{aligned} p &= \frac{1}{16\pi^2}\int d^4x\sqrt{g} * R_{\mu\nu\lambda\tau}R^{\mu\nu\lambda\tau}, \\ *R_{\mu\nu\lambda\tau} &= \frac{1}{2}\sqrt{g}\epsilon_{\mu\nu\alpha\beta}R^{\alpha\beta}{}_{\lambda\tau}. \end{aligned} \tag{6.3}$$

The Pontryagin index is related to the topology of background spacetime, and the vacuum state should be labeled by two integers: one is the winding number of gauge field A, and the other is the Pontryagin index. This leads to a second θ-term in the Lagrangian in addition to $*FF$ or $*GG$:

$$\mathcal{L}_\theta = \frac{\theta_{QCD}}{32\pi^2}\int d^4x\sqrt{g} * F^a_{\mu\nu}F^{a\mu\nu} + \frac{\theta_{EH}}{48\pi^2}\int d^4x\sqrt{g} * R_{\mu\nu\alpha\beta}R^{\mu\nu\alpha\beta}. \tag{6.4}$$

Now both θ-terms violate CP, and the true θ that contributes to nEDM is a combination of them, called θ_{CEH}:

$$\theta_{CEH} = \frac{3}{2}\theta_{QCD} + \theta_{EH}, \tag{6.5}$$

where we have normalized the coefficients, $3/2$ comes from the fact that the Pontryagin index of Eguchi-Hanson metric is 3 and the range of ψ angle is halved (see Eq.3.74).

In the presence of fermions, the vacuum-to-vacuum transition amplitude is proportional to the determinant of the Dirac operator $i\gamma^\mu\nabla_\mu$. When the Dirac operator has zero modes, the amplitude vanishes trivially. These zero modes can be classified by eigenvalues ± 1 of γ^5, which is anti-commuting with $i\gamma^\mu\nabla_\mu$. The modes of eigenvalue -1 are called left-handed, and $+1$ is called right-handed. Only those amplitudes that violate the same chiral charge $\Delta Q_5 = 2(n_+ - n_-)$ are non-vanishing, where $n_\pm$ is the number of right/left-handed zero modes. The quantity $n_+ - n_-$ is also called the *index* of the Dirac operator and can be computed analytically via characteristic class according to index theorems [116]. For the CEH instanton Eq.3.70 and Eq.3.84, the index of Dirac operator $i\gamma^\mu\nabla_\mu = i\gamma^\mu(\partial_\mu - \Gamma_\mu - iA_\mu)$ has been computed exactly in [66] for generic representation of $SU(2)$ of dimension d_R:

$$\nu^{CEH}_{1/2} = \begin{cases} \frac{1}{4}d_R(d_R^2-2), & d_R = 2, 4... \\ \frac{1}{4}d_R(d_R^2-1), & d_R = 1, 3... \end{cases} \tag{6.6}$$

So pure EH gravitational instantons ($d_R = 1$) do not mediate chiral-symmetry breaking transitions for gauge-singlet fermions. For $SU(2)$-coloured fermions, the Dirac operator has index $\nu_{1/2}^{CEH} = 1$. Therefore, the induced effective interaction [52] is proportion to $e^{-\frac{8\pi^2}{g^2}\times\frac{3}{2}} \det\big(\bar{\psi}_L^i \psi_R^j\big) = e^{-\frac{12\pi^2}{g^2}} \det\big(\bar{\psi}_L^i \psi_R^j\big)$, while the one induced by BPST instanton is just $\propto e^{-\frac{8\pi^2}{g^2}} \det\big(\bar{\psi}_L^i \psi_R^j\big)$. On the other hand, it is known there are 16 collective coordinates (bosonic zero modes)[1] [117, 48] for CEH instanton, but it is hard to find them explicitly. An educated guess is that each bosonic zero mode contributes a factor $(8\pi^2/g^2)^{1/2}$, and the dimension of the Jacobian requires a factor $\rho^{-5} d\rho$, where ρ is the size of instanton. Finally, the renormalisation gives a factor $(\rho\Lambda)^{3b/2}$, where $b = 11 - \frac{2}{3}N_f$ is the one-loop beta-function and Λ is the regularisation scale. Collecting everything, the effective interaction [52, 118] induced by BPST and CEH instantons reads

$$\begin{aligned}\Delta L = &-d\left(\frac{2\pi}{\alpha_s(\Lambda)}\right)^6 \exp\left[-\frac{2\pi}{\alpha_s(\Lambda)} + iN\frac{a}{f_a} + i\theta_{QCD}\right]\\ &\times \frac{d\rho}{\rho^5}(\rho\Lambda)^b \det(q_{iL}\bar{q}_{iR})\\ &-\bar{d}\left(\frac{2\pi}{\alpha_s(\Lambda)}\right)^8 \exp\left[-\frac{3\pi}{\alpha_s(\Lambda)} + iN_g\frac{a}{f_a} + i\theta_{CEH}\right]\\ &\times \frac{d\rho}{\rho^5}(\rho\Lambda)^{3b/2} \det(q_{iL}\bar{q}_{iR}) + h.c.,\end{aligned} \tag{6.7}$$

where, N and N_g are anomaly coefficients, $\alpha_s(\Lambda = 1GeV) = 0.4 - 0.6$ [119] and $d \approx 0.017$ [52] (we expect $d \simeq \bar{d}$). Integrating out fermions loops (each pair $q_{iL}q_{iR}$ gives a factor $m_i\rho$) [48], we get the axion potential

$$V(a) = -2K_{QCD}\cos\left(N\frac{a}{f_a} + \theta_{QCD}\right) - 2K_{CEH}\cos\left(N_g\frac{a}{f_a} + \theta_{CEH}\right), \tag{6.8}$$

where

$$K_{QCD} = \frac{d}{8}\left(\frac{2\pi}{\alpha_s(\Lambda)}\right)^6 e^{-\frac{2\pi}{\alpha_s(\Lambda)}} m_u m_d m_s \Lambda \tag{6.9}$$

Evidently, minimizing this potential depends on the ratio $\kappa = K_{CEH}/K_{QCD}$:

$$\kappa = \frac{16}{25}\left(\frac{2\pi}{\alpha(\Lambda)}\right)^2 e^{-\pi/\alpha(\Lambda)} \in (0.06, 0.4) \gg 10^{-10}, \tag{6.10}$$

[1] we embed this $SU(2)$ gauge field into $SU(3)$, so there are 4 additional bosonic zero modes

where $\alpha(\Lambda = 1GeV) = 0.4{-}0.6$ is the running coupling evaluated at energy scale $\Lambda = 1GeV$. The potential is not minimized at the CP-conserving point unless $N/N_g = \theta_{QCD}/\theta_{CEH}$. Therefore original single axion does not work, and we call this issue *strong-gravity-CP* problem. One way out of this is to introduce the existence of another axion a', with symmetry breaking scale f_a' and anomaly coefficients N' and N_g' so that θ_{QCD} and θ_{CEH} can be canceled simultaneously. The potential now reads:

$$V(a,a') = -2K_{QCD}\cos\left(N\frac{a}{f_a} + N'\frac{a'}{f_a'} + \theta_{QCD}\right) - 2K_{CEH}\cos\left(N_g\frac{a}{f_a} + N_g'\frac{a'}{f_a'} + \theta_{CEH}\right). \tag{6.11}$$

The solution, which consists of two axions, is called *companion-axion model*. We also reasonably assume $N/N' \neq N_g/N_g'$, which implies these two cosine functions can be minimized at the same time

$$\begin{aligned} N\frac{a}{f_a} + N'\frac{a'}{f_a'} + \theta_{QCD} &= 0 \\ N_g\frac{a}{f_a} + N_g'\frac{a'}{f_a'} + \theta_{CEH} &= 0. \end{aligned} \tag{6.12}$$

Therefore, the strong-gravity-CP problem is solved. The next step is to read masses from the potential. We can diagonalize the mass matrix by defining the states

$$\begin{aligned} a_1 &= a\cos\alpha - a'\sin\alpha \\ a_2 &= a\sin\alpha + a'\cos\alpha, \end{aligned} \tag{6.13}$$

where the mixing angle α is given by

$$\tan 2\alpha = \frac{2\epsilon(NN' + \kappa N_g N_g')}{N^2 + \kappa N_g^2 - \epsilon^2 N'^2 - \kappa\epsilon^2 N_g'^2}, \tag{6.14}$$

and $\epsilon = f_a/f_a'$, $\kappa = K_{CEH}/K_{QCD}$. Without loss of generality, we assume a_1 is the heavier one so that $\epsilon \leq 1$. The axion masses are given by

$$m_1^2 = \frac{\Delta m^2}{2} + \frac{K_{QCD}}{f_a^2}\left[(N^2 + \kappa N_g^2) + \epsilon^2(N'^2 + \kappa N_g'^2)\right], \tag{6.15}$$

where Δm^2 is the difference of mass square $\Delta m^2 = m_1^2 - m_2^2$:

$$\Delta m^2 = \frac{2K_{QCD}}{f_a^2}\left[4\epsilon^2(NN' + \kappa N_g N_g')^2 + \left((N^2 + \kappa N_g^2) - \epsilon^2(N'^2 + \kappa N_g'^2)\right)^2\right]^{1/2}. \tag{6.16}$$

We do not need such complicated expressions and will perform some approximations. We consider two cases: (1) hierarchical regime: $f'_a \gg f_a$ and (2) a strong-mixing regime: $f'_a \sim f_a$. We also assume all anomaly coefficients are in the same order and ignore terms $\mathcal{O}(\kappa^2)$. For hierarchical case, we have

$$m_1^2 \sim \frac{2K_{QCD}}{f_a^2}, \;\; m_2^2 \sim \kappa\epsilon^2 m_1^2. \tag{6.17}$$

The second axion a_2 acquires mass due to CEH instanton effect κ but is suppressed by ϵ. Meanwhile, the first axion's mass is the same as the single-axion case. The mixing angle is also tiny:

$$\alpha \approx \frac{NN' + \kappa N_g N'_g}{N'^2 + \kappa N_g'^2}\epsilon \sim \epsilon \ll 1. \tag{6.18}$$

For mixing case $\epsilon \sim 1$, we have

$$\begin{aligned} m_1^2 &\approx \frac{2K_{QCD}}{f_a^2}\left[N^2 + N'^2 + \kappa\frac{N^2N_g^2 + N'^2N_g'^2}{N^2 + N'^2}\right] \\ m_2^2 &\approx \frac{2\kappa K_{QCD}}{f_a^2}\frac{N^2N_g^2 + N'^2N_g'^2}{N^2 + N'^2} \sim \kappa m_1^2. \end{aligned} \tag{6.19}$$

We see that a_1 is still of the same order of magnitude as the mass of the standard QCD axion, but a_2's mass is purely generated from CEH instanton effect κ. Below, we plot the parameter space of the companion axion model.

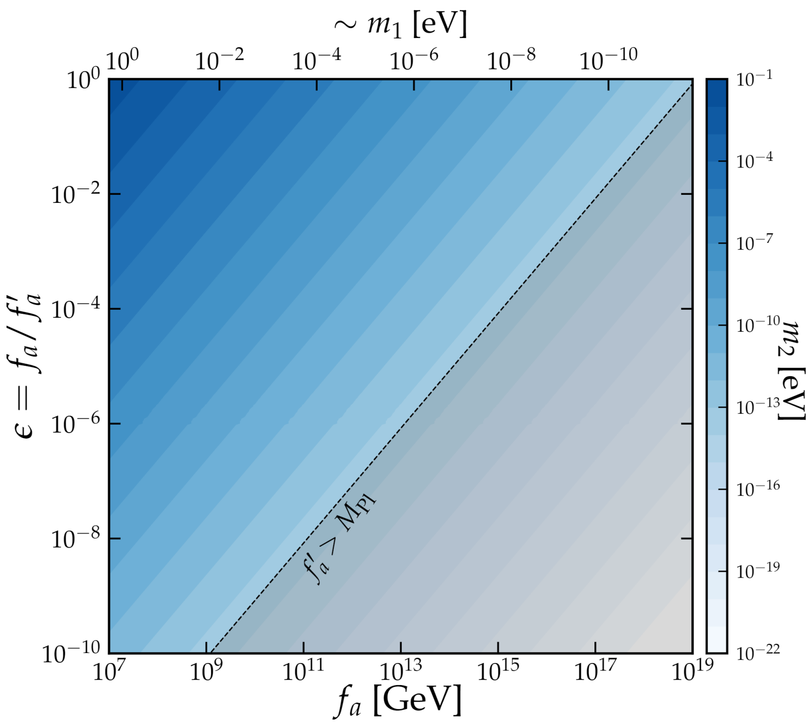

FIGURE 6.1: The parameter space of companion-axiom model.

As shown in Fig.6.1, the lower vertical axis represents ϵ, and the upper and lower horizontal axis represents f_a and the mass of the first axion m_1. The second axion mass m_2 is demonstrated by color. In this plot, each point $(\epsilon, f_a, m_1, m_2)$ corresponds to a solution to the strong-gravity CP problem. We also require f'_a less than Planck scale M_{PI}, so the grey part has been ruled out. Notice that when one axion is excluded, the other is excluded because they are coupled. At the end of this chapter, we would like to point out that the multi-axions model is not new. In particular, the string axiverse scenario [120, 121, 122, 123, 124, 125, 126, 127, 128, 129] led to the birth of many studies of systems of coupled axions [130, 131, 132, 133, 134]. In the next two chapters, we will investigate some phenomenological aspects of companion axion model.

CHAPTER 7

Phenomenology of the companion-axion model: photon couplings

This chapter is based on publications [135, 136]. The figures from this chapter can be reproduced using the code available at github.com/cajohare/CompAxion.

7.1 Phtoton constraints from companion-axion model

In laboratory experiments and astrophysical observations to search for axions, the Primakoff effect is a notable mechanism where axions can convert into photons in a strong electromagnetic field. Thus the axion-photon interaction is an important subject to study. For single axion case, the interaction reads [119, 137, 138]

$$\mathcal{L}_{a\gamma\gamma} = \frac{1}{4} a g_{a\gamma} * F_{\mu\nu} F^{\mu\nu}. \tag{7.1}$$

It is straightforward to write down companion-axion coupling to photon

$$\mathcal{L}_{a\gamma\gamma} = \frac{1}{4}(a g_{a\gamma} + a' g'_{a\gamma}) * F_{\mu\nu} F^{\mu\nu}, \tag{7.2}$$

where the coupling $g_{a\gamma}$ and $g'_{a\gamma}$ are given by

$$g_{a\gamma} = -\frac{\alpha_{EM} N}{2\pi f_a}\zeta, \quad g_{a\gamma} = -\frac{\alpha_{EM} N'}{2\pi f'_a}\zeta. \tag{7.3}$$

$\zeta = 1.92$ is fixed to avoid mixing axions with QCD mesons [139]. We can also get the couplings g_1, g_2 of mass eigenstates (a_1, a_2):

$$\begin{aligned} g_1 &= \frac{\alpha_{EM}}{2\pi f_a}\zeta(N\cos\alpha - \epsilon N' \sin\alpha), \\ g_2 &= \frac{\alpha_{EM}}{2\pi f_a}\zeta(N\sin\alpha + \epsilon N' \cos\alpha). \end{aligned} \tag{7.4}$$

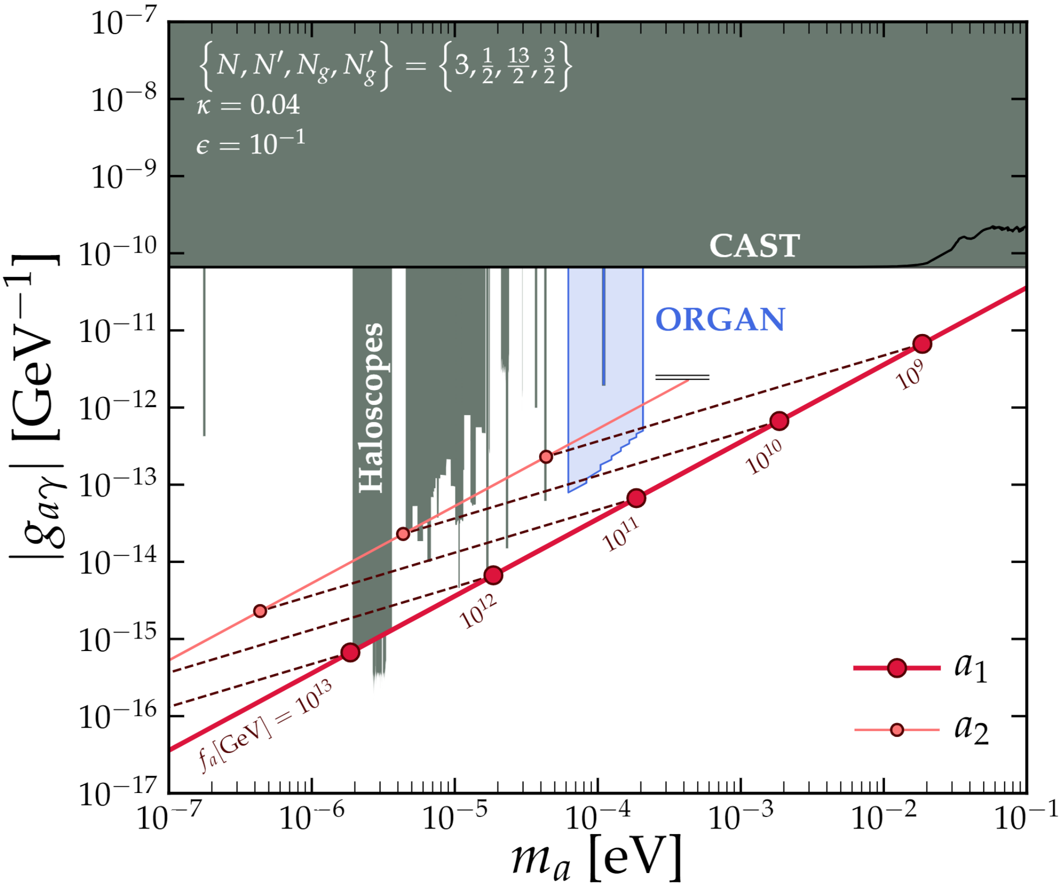

FIGURE 7.1: Photon coupling-mass relation for the two axion mass eigenstates. We connect the larger axion with its partner which is required to solve the strong-gravity CP problem. Both axions must be constrained when the haloscopes bounds [12, 14, 141, 142] reach the lighter axion band, similarly for the stellar cooling and helioscope [143, 144]. This figure is plotted to illustrate the non-trivial constraints and must be recast.

To plot the coupling and mass, we choose a representative set of the anomaly coefficients $\{N, N', N_g, N'_g\} = \{3, 1/2, 13/2, 3/2\}$ and CEH instanton effect $\kappa = 0.04$ [140]. In Fig.7.1, we plot the coupling-mass relation for the two axion mass eigenstates for mixing regime $\epsilon = 0.1$, and the existing haloscope and helioscope constraints on the single-axion are overlaid as well. As shown in Fig.7.2, we again use a color scale to represent the lighter axion a_2's mass, and the mass of the heavier one a_1 is given by the upper horizontal axis (hierarchical approximation). The shaded area of solution space is excluded. Later we will show how to derive these bounds.

Stella cooling

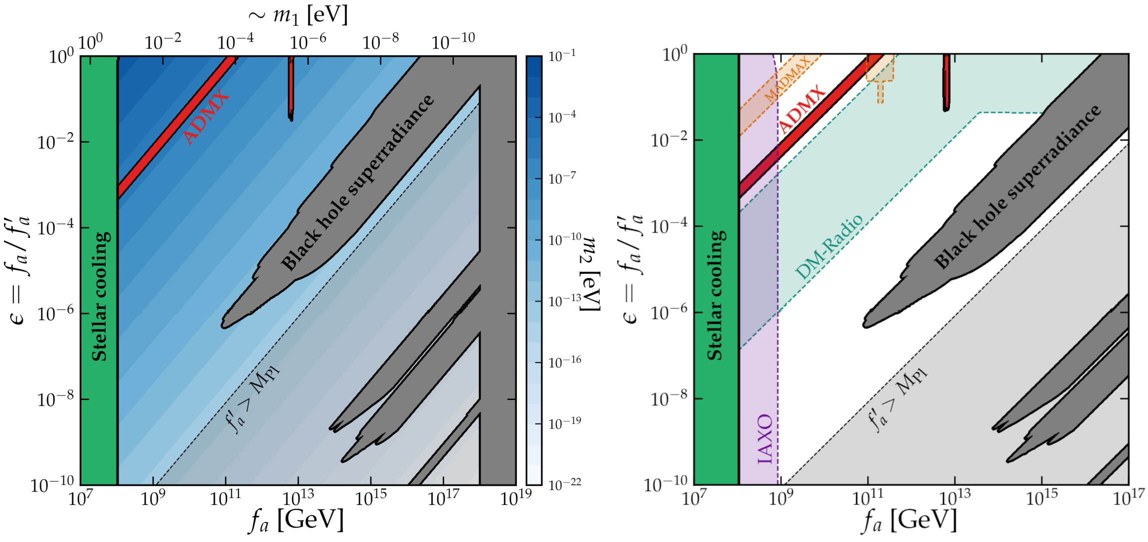

FIGURE 7.2: **Left**: Current bounds on the companion-axion model. The color scale shows the lighter axion a_2's mass, while the upper horizontal axis shows the heavier axion a_1's mass. **Right**: MADMAX [145], IAXO [146], and DMRadio/ABRACADABRA [147, 148] constraints.

As introduced in the previous chapter, the lifetime of a horizontal branch star is shortened by the Primakoff effect. The most strict upper bound on the photon coupling is given by [149]:

$$|g_{a\gamma}| < 6.6 \times 10^{-11}\text{GeV}^{-1}, \tag{7.5}$$

which holds independently of the axion mass up to around 30keV. For recasting the bound to our companion axion model case, we first point out that it is necessary to define an *active* state a^A that couples to photon and a *hidden* a^H state [130] that does not:

$$\begin{aligned}
\mathcal{L}_{a\gamma} &= \frac{1}{4}(a_1 g_1 + a_2 g_1) * F_{\mu\nu}F^{\mu\nu} \\
&= \frac{1}{4}\tilde{g}a^A * F_{\mu\nu}F^{\mu\nu}, \;\; \tilde{g} = \sqrt{g_1^2 + g_2^2} \\
a^A &= \frac{g_1}{\sqrt{g_1^2 + g_2^2}}a_1 + \frac{g_2}{\sqrt{g_1^2 + g_2^2}}a_2, \\
a^H &= \frac{g_2}{\sqrt{g_1^2 + g_2^2}}a_1 - \frac{g_1}{\sqrt{g_1^2 + g_2^2}}a_2.
\end{aligned} \tag{7.6}$$

For the hierarchical case, $g_2 \ll g_1$, we have $\tilde{g} \sim g_2$, and the bound would be the same as the single axion model. For mixing case, $g_2 \sim g_1$, the bound gets a overall factor $\sqrt{N^2 + N'^2}/N$.

Helioscopes

Helioscopes [150] are used to detect the axions produced in the sun. A typical helioscope consists of a long magnetic bore pointed to the sun, an X-ray optics system, and detectors that are used to capture the axions converting to photons in the magnetic field. When the axion mass is equal or below 0.02eV, the axion and photon oscillate coherently, enhancing the signal significantly. For the heavier axion, the momentum mismatch between the massive axion and the massless photon oscillates the conversion probability at a shorter length scale than the experiment. Therefore, the bore must be filled with a buffer gas such as Helium [151, 152] by which the photon acquires an effective mass to eliminate this mismatch. There are two phases we have to take into account [130]. The first phase is the axions leave the sun and reach the Earth. The second is the time when axions pass the magnetic field. For the first phase, we must consider the conversion between active and hidden states and calculate the survival probability of the active axions. The second phase gives rise to a three-body oscillation problem which is quite tricky to solve, and we will show that the axion-photon coupling is small compared to the coupling between the active and hidden states.
The mixing angle between active and hidden states is given by

$$\cos\theta = \frac{g_1}{\sqrt{g_1^2 + g_2^2}}, \tag{7.7}$$

leading to two equal non-vanishing off-diagonal terms in mass matrix $M_{12},\ M_{21}$:

$$M_{12} = -\Delta m^2 \frac{\cos^2\alpha}{1+\epsilon^2}\left(\tan\alpha + \epsilon(1-\tan^2\alpha) - \epsilon^2\tan\alpha\right). \tag{7.8}$$

The survival probability P of the active axion of energy ω after travelling distance L is given by

$$P = 1 - \sin^2 2\theta \sin^2\left(\frac{\Delta m^2 L}{4\omega}\right). \tag{7.9}$$

The first sine is approximated as

$$\sin^2 2\theta = \begin{cases} 4\epsilon^2, & \epsilon \ll 1 \\ \cos^2 2\alpha, & \epsilon \sim 1, \end{cases} \tag{7.10}$$

and the second sine is averaged to be $1/2$. Choosing $L = 1$AU, $\omega \sim$ keV we see that when $\Delta m^2 \gtrsim 10^{-12}$GeV^2, it is guaranteed that axion-axion oscillation length is shorter than the Earth-Sun distance.

When the axions enter the magnetic field B of the helioscope, the active axions can be converted to hidden axions and photons, with $\tilde{g}B\omega$ and $\Delta m^2\epsilon$ strength, respectively. Using Eq.7.8, we have

$$\frac{\tilde{g}B\omega}{\Delta m^2\epsilon} = \frac{\alpha_{EM}\zeta B\omega}{4\pi K_{QCD}} f_a' \lesssim 10^{-2}, \tag{7.11}$$

where $f_a' < M_{PL}$ is assumed. A similar calculation can be done for the mixing regime. Because of Eq.7.11, we can detect photon flux as in a single-axion case. The number of photons we observe on the earth is proportional to $g_{a\gamma}^4$. Considering survival probability, the old bound for $g_{a\gamma}$ gets an overall factor P^{-4}. The result of this calculation is plotted in the right panel of Fig.7.2, where The CAST bounds [141] are less sensitive than the stellar cooling bounds, and therefore, we haven't shown it. Instead, we plot bounds from helioscope IAXO [146] in the right panel of Fig.7.2.

Haloscopes

Haloscopes are used to detect axions constituting the dark matter halo of the Milky Way. We assume both axions are produced by the misalignment mechanism, neglecting topological defects. We also assume axion darker matter has no additional structures like miniclusters, which form via gravitational attraction and are dense. Dealing with two axions is relatively more complicated than the single axion case. To make progress, we have crudely estimated the abundance ratio of a_1 and a_2 (Eq.8.8), so rescaling the constraints from experiments such as ADMX for the single axion case is straightforward. Eq.8.8 also indicates that the lighter axion dominates the abundance unless $\epsilon \approx 1$. Here, we assume $\theta_1 = \theta_2$, but if one or both PQ symmetries are broken before inflation, these angles could need manual modification. Therefore, our haloscope bounds for companion-axion depend on a specific cosmological scenario and are more model-dependent than the single-axion case.

Resonance-based haloscopes, when searching for signals, have to scan through the axion mass range slowly. Thus, in the standard axions case, they have only been able to search in a small area near the classic preferred dark matter mass range. The haloscope's optimal region for the companion axion would be the lighter axion since its abundance dominates. This means we must extend the haloscope experiment beyond the classical axion region, to a much smaller mass range than the previous one.

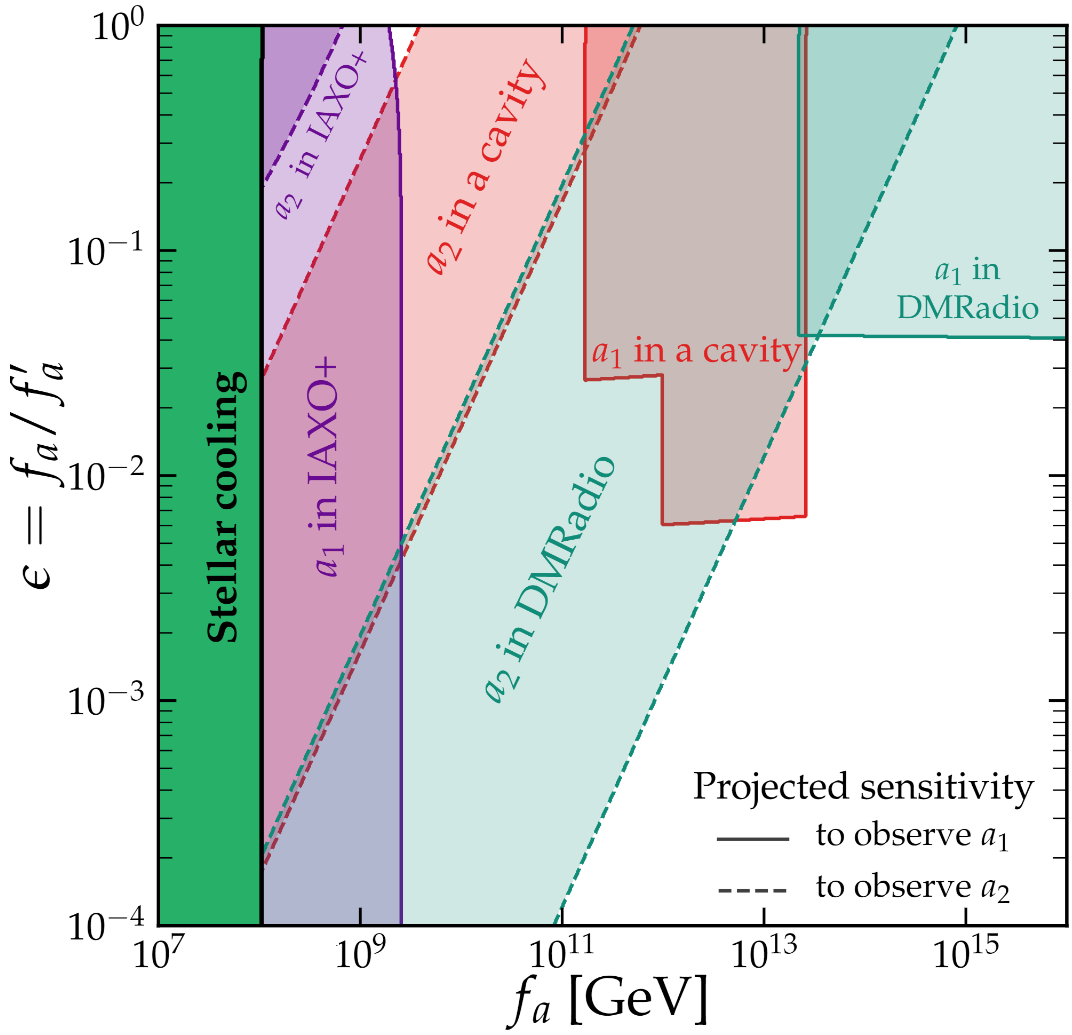

FIGURE 7.3: Projected sensitivity for future axion experiments: IAXO+, resonant cavity experiments ($1-100\mu$eV region) and DMRadio-like experiments (neV $-$ μeV region). Both axions can be seen in the region where a_1 and a_2 overlap. We can even see both axions in one experiment in the region where the same color overlap.

Another interesting feature of haloscope bounds is that we do not know whether it is a_1 or a_2. But once one axion gets constrained, another can be constrained immediately ($\epsilon f_a' = f_a$) because CP-conserving requires both. Thus we expect two bands in (f_a, ϵ) space. We have shown the ADMX [10] and future MADMAX [145] haloscopes constraints in the right panel of Fig.7.2.

Black hole superradiance

Black hole superradiance [153, 154, 155, 156, 157, 158, 159, 160, 161] is a booming topic.

Even if there is only one axion field, the solution of the perturbation equation is extremely complicated, let alone two coupled axions. Here we assume the off-diagonal term does not affect the bound states of two axions, so the existing constraints [162, 163, 164] are easily mapped to the companion axions case. But remember that the constraint may be incorrect for $\epsilon \approx 1$. We plot four bands corresponding to the black hole superradiance in Fig.7.2.

Unique signal in experiments

Judging the single axion or one of the two companion axions is usually tricky when detecting signals. We conclude this section by estimating how much of our companion-axion parameter space would leave a unique signature in experiments. We have plotted some of the regions, using relatively ambitious projections for these experiments, including IAXO+ [165, 146, 166], resonant-cavity [167, 168, 142, 169, 170, 171] and LC-circuit-based haloscopes [172, 147, 173, 174]. As shown in Fig.7.3, both signals will be seen in the regions where two axions overlap. We can even observe two axions in the same experiment.

CHAPTER 8

Cosmological implications

This chapter is based on publications [135, 136]. The figures from this chapter can be reproduced using the code available at `github.com/cajohare/CompAxion`.

8.1 Companion axions as dark matter

In this section, we investigate companion axions as dark matter. In particular, we focus on misalignment mechanism [103, 13, 105]. The previous discussion on the single-axion case shows two scenarios where the PQ symmetry was broken before or after inflation. For the companion axions, we have to deal with three scenarios:

(1) Both PQ symmetries are broken before the end of inflation (two pre-inflationary axions). Both $\theta_{1,2}$ are ranging from $-\pi$ to π.

(2) The heavier one a' symmetry is broken before the end of inflation, while the lighter one a is post-inflationary. In this scenario, θ_2 is a random variable, while θ_1 is the stochastic average $\pi/\sqrt{3}$.

(3) Both axions are post-inflationary (equivalently, no inflation), and we use the average $\pi/\sqrt{3}$ for both angles.

We still need to explicitly calculate the abundance of each axion since their ratio will be significant for implications. The zero-mode evolution equations for the two axions as a linearized system of coupled oscillators reads

$$\begin{aligned}\partial_t^2 a + \frac{3}{2t}\partial_t a + M_{11} a + M_{12} a' &= 0 \\ \partial_t^2 a' + \frac{3}{2t}\partial_t a' + M_{22} a' + M_{21} a &= 0,\end{aligned} \tag{8.1}$$

where we have assumed a radiation-dominated universe $H = 1/2t$ and ignored non-linear terms in the potential [8, 175, 176, 177, 178]. To calculate the abundance more precisely, we must include thermal effects on the mass. The temperature-dependent mass of axions obeys the power law [9]

$$m_i^2(T) = \min\left[m_i^2, m_i^2\left(\frac{T_c}{T}\right)^n\right], \quad i = 1, 2, \tag{8.2}$$

where $n = 6.68$ and $T_c = 103$MeV. The mass matrix is then given by

$$M_{ij}(T) = m_1^2(T)\begin{pmatrix} 1 & -\epsilon^2 \\ -\epsilon^2 & \kappa\epsilon^2. \end{pmatrix} \tag{8.3}$$

Since the temperature dependence has been factored out, we can diagonalize the mass matrix Eq.8.1 to rewrite the equations under mass eigenstates:

$$\begin{aligned}\partial_t^2 a_1 + \frac{3}{2t}\partial_t a_1 + m_1^2(T) a_1 &= 0 \\ \partial_t^2 a_2 + \frac{3}{2t}\partial_t a_2 + \kappa\epsilon^2 m_1^2(T) a_2 &= 0.\end{aligned} \tag{8.4}$$

We would like to know the temperature $T_{1,2}$ at which the condition $m_i(T_i) = 3H(T_i)$ is satisfied so that the oscillations start. Solving $m_i(T_i) = 3H(T_i)$, we have

$$T_i = \left(\frac{m_i M_{PL}\sqrt{90}}{24\pi^2\sqrt{g_*^i}}\right)^{2/(n+4)} T_c^{n/(n+4)} \tag{8.5}$$

where g_*^i is the relativistic degrees of freedom at temperature T_i, M_{PL} is the Planck mass. In hierarchical regime $\epsilon \ll 1$, the the temperature at the onset of oscillations for the lighter axion is smaller by a factor,

$$\frac{T_2}{T_1} = (\kappa\epsilon^2)^{1/(n+4)}. \tag{8.6}$$

The oscillation equations are solved by Wentzel–Kramers–Brillouin (WKB) approximation, giving the energy density for each axion (assuming entropy conservation):

$$\rho_i|_{\text{today}} = m_i(T_i) m_i \left(\frac{T_0}{T_i}\right)^3 \frac{g^0_{*s}}{g^i_{*s}}, \tag{8.7}$$

where $T_0 = 2.7K$, and g^i_{*s} are the entropy degrees of freedom. The total axion abundance Ω_a is the sum of two components $\Omega_a = \Omega_{a_1} + \Omega_{a_2}$. The ratio of two abundances reads:

$$\frac{\Omega_{a_2}}{\Omega_{a_1}} \sim \frac{\theta_2^2}{\theta_1^2}\kappa^{0.41}\epsilon^{-1.19} \quad (\epsilon \ll 1), \tag{8.8}$$

and

$$\frac{\Omega_{a_2}}{\Omega_{a_1}} \sim \frac{\theta_2^2}{\theta_1^2}\kappa^{0.41} \quad (\epsilon \lesssim 1), \tag{8.9}$$

where misalignment angles θ_i's are given by

$$\begin{aligned} \theta_1 &= \frac{\langle a_1(t_1)\rangle}{f_a}, \\ \theta_2 &= \frac{\langle a_2(t_2)\rangle\epsilon}{f_a}. \end{aligned} \tag{8.10}$$

In the hierarchical case, the lighter axion a_2 dominates relic abundance due to the factor $\epsilon^{-1.19}$, unless $\theta_2 \ll \theta_1$, which could occur in scenarios (1) and (2). However, when the misalignment angles are of the same order in the strong mixing case, the heavier axion a_1 dominates slightly. The relative abundances are plotted in Fig.8.1. As we can see, the axion abundance is generally always dominated by the lighter axion a_2 unless ϵ approaches 1. A few bounds are shown, where helioscope bounds from ADMX [**10**] are shown in red, while the projected SKA [**179**, **180**, **181**] bounds on gravitational waves from axion domain wall collapse are shown in pink. Black hole superradiance bounds are in dark grey. It is worth mentioning that Scenario (3) is a special case of scenario (2) when $\theta = \pi/\sqrt{3}$, so a thin straight line represents it.

8.2 Isocurvature bounds

The massless axion fields experience large amplitude quantum fluctuations during the universe inflation. Still, the energy density of these fluctuations does not contribute to

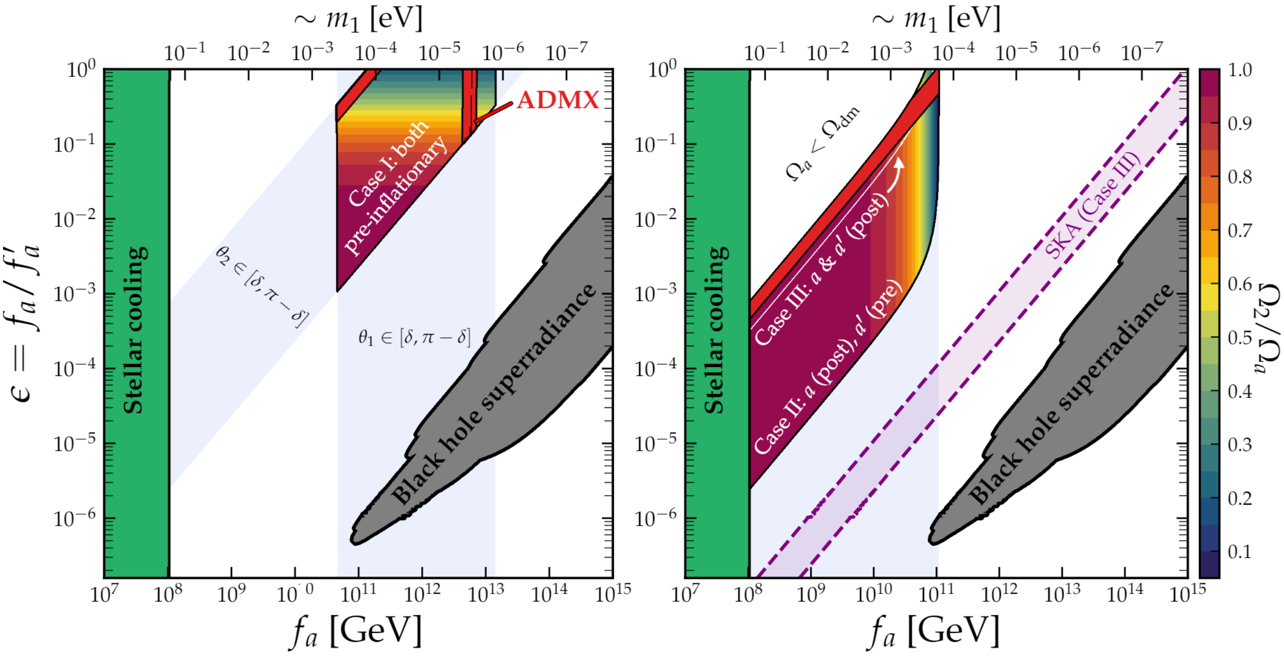

FIGURE 8.1: The range of companion axion parameter space for which the two axions represent viable dark matter candidates. Scenario (1), when both axions are pre-inflationary, is shown in the colored region of the left panel. Scenarios (2), when only f_a is post-inflationary, are shown in the colored region right panel. Scenario (3), when both axions are post-inflationary, is shown by the white line of the right panel.

the perturbations of the total energy density. Because they are negligible compared to the inflaton field's energy density which dominates the inflation, however, this kind of fluctuation contributes to the perturbations of the ratio of axion number density to entropy, giving rise to the so-called entropy, or *isocurvature* perturbations [182, 183, 184, 185]. One important characteristic of isocurvature perturbation is that it does not perturb the background geometry. Unlike isocurvature perturbation, the *adiabatic* perturbation has a non-vanishing net perturbation of matter content. As the axions would survive after recombination in the form of dark matter, the isocurvature perturbations contribute to the temperature and polarisation fluctuations in the cosmic microwave background radiation and are uncorrelated with the adiabatic fluctuations.

Assuming both the companion axion fluctuations are uncorrelated, the perturbation power spectrum at the pivot scale $k_{low} \approx 0.002\text{Mpc}^{-1}$ is:

$$\Delta^2_{a_1} = \Delta^2_{a_2}\epsilon^2\frac{\theta_2^2}{\theta_1^2} \simeq \frac{H_I^2}{\pi^2 f_a^2\theta_1^2}, \tag{8.11}$$

where H_I is the Hubble expansion rate during inflation. For scenario (1), where both axions are pre-inflationary, the isocurvature power spectrum ratio reads

$$\beta = \frac{\Delta^2_{a_1}}{A_s}\left(1+\epsilon^{-2}\frac{\theta_2^2}{\theta_1^2}\right), \tag{8.12}$$

where $A_s \simeq H_I^2/(\pi^2 M_{PL}\eta) = 2\times 10^{-9}$ is the adiabatic power spectrum evaluated at the pivot scale, and η is the 'slow roll' parameter. The Planck constraint $\beta < \beta_*$ (95% C.L.) [186] gives

$$H_I \lesssim \frac{\sqrt{\beta_*}A_s\pi f_a\theta_1}{(1+\epsilon^{-2}\theta_2^2/\theta_1^2)^{1/2}}, \quad \text{senario } (1). \tag{8.13}$$

In Fig.8.2, we have illustrated how the constraint depends on (θ_1, θ_2) for a particular choice f_a and ϵ. We see that when θ_1 must be tuned very close to 0, we get a very low scale of inflation. In scenario (2), the isocurvature bounds on the pre-inflationary axion are the same as in the literature, with $f_a \to f'_a$.

8.3 Domain Walls

Without the CEH instanton, the companion-axion model has a $Z_N \times Z_{N'}$ discrete symmetry from the first cosine term in the potential Eq.6.11. The vacuum state is not invariant under this symmetry. Therefore $Z_N \times Z_{N'}$ is spontaneously broken, and uncorrelated casual patches choose one of the $N \times N'$ states via the $Z_N \times Z_{N'}$ symmetry, leading to the formation of the domain wall. The energy density in these domain walls decays slower than cold matter as well as radiations and can easily overclose the universe, which is known as the *domain wall problem* [187, 188, 189]. Now the CEH instanton induces a second cosine term (known as bias term) in the potential 6.11, breaking the symmetry explicitly and vice-versa. The degeneracy of these axion vacuum states is therefore lifted, and the bias term induces the energy difference between the vacua [190, 191, 192, 193, 194, 195, 196, 197, 198]:

$$V_{bias} \sim \kappa K_{QCD}. \tag{8.14}$$

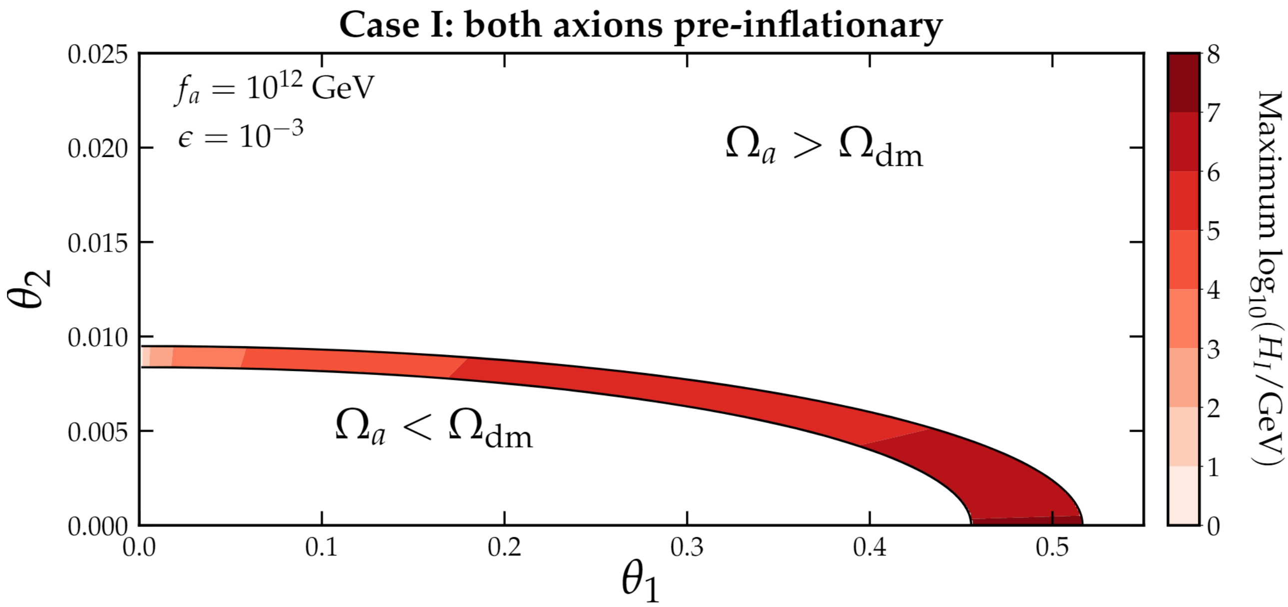

FIGURE 8.2: Isocurvature bounds for a particular choice of f_a and ϵ. The red band shows where the dark matter abundance is correct, while the shade illustrates the constraints on the inflationary scale. The position of the bend depends on the choice of vacuum scales. For different vacuum scales, the red band would occupy a different portion of the $\theta_1 - \theta_2$ plane

Bias term can destroy the domain walls, and we can explicitly estimate the temperature at which this destruction will occur and show that for most of the companion axion solution space. This temperature is higher than temperature T_i at which the axions pick up their masses. The interpretation of this scenario is that bias terms annihilate the domain walls before causing the problem. We assume here that two domain walls of the two axions form independently at the QCD phase transition via the Kibble mechanism [199, 200]. The width of each wall scales like the Compton wavelength:

$$\delta_i \sim \frac{1}{m_i}. \tag{8.15}$$

Surface tensions σ_i can be written in terms of the energy barrier that separates discrete vacua V_0:

$$\sigma_i \sim V_0 \delta_i, \;\; V_0 \sim K_{QCD}(1+\kappa). \tag{8.16}$$

The energy density difference V_{bias} acts as a volume pressure p_V on the walls. When this pressure becomes comparable to their tension $p_T \sim \sigma/t$, a domain wall of size $r \sim t$ gets annihilated. In the radiation-dominated era, the temperature T_{ann} at the time t_{ann} when annihilation occurs is estimated as

$$T_{ann} \sim 13.5\text{MeV}\left(\frac{m_i}{10^{-12}\text{eV}}\right)^{1/2}\left(\frac{11\kappa}{1+\kappa}\right)^{1/2}\left(\frac{10}{g_*}\right)^{1/4}. \tag{8.17}$$

The domain walls must annihilate before Big Bang nucleosynthesis at temperature $T_{bbn} = 1\text{MeV}$, so it is required $T_{ann} < T_i$, where T_i is defined in Eq.8.5, giving an upper bound for axion mass

$$m_i \lesssim 10^{-9}\text{eV}. \tag{8.18}$$

When $m_i \lesssim 10^{-9}\text{eV}$ is violated, it implies that the bias term is large enough to prevent the domain wall formation. We also require that the domain walls not be thicker than the horizon size: $m_i \gtrsim H(T)$, giving a lower bound:

$$m_i \gtrsim 10^{-10}\text{eV}. \tag{8.19}$$

Hence, we conclude that domain walls are relevant for a very narrow mass range $10^{-10}\text{eV} - 10^{-9}\text{eV}$, and the misalignment production is not significantly impacted.

8.4 Gravitational Waves

The decay of domain walls will strongly perturb the spacetime and thus result in a gravitational Wave (GW). The power spectrum of GW goes like k^3, up to its comoving wavenumber k_{peak}, above which it falls off as k^{-1} with a cut-off set by the thickness of the domain wall [**201**, **202**, **203**, **204**]. The peak frequency f_{peak} is estimated as

$$f_{peak} = \frac{k_{peak}}{R(t)} \sim 1.1 \times 10^{-8}\text{Hz}\left(\frac{m_i}{10^{-10}\text{eV}}\right)^{1/2}\left(\frac{11\kappa}{1+\kappa}\right)^{1/2}, \tag{8.20}$$

where we have taken $g_*(T_{ann}) = g_{*s}(T_{ann}) = 10$. The relic density at the peak reads

$$(\Omega_{gw}h^2)_{peak} \sim 3 \times 10^{-10}\left(\frac{10^{-10}\text{eV}}{m_i}\right)^4\left(\frac{(1+\kappa)^2}{12.1\kappa}\right)^2. \tag{8.21}$$

In Fig.8.3, we have plotted the predicted signals of GWs expressed in terms of the relic density as a function of frequency. The bands for each mass span are due to the uncertainty of the

CEH instanton effect κ. We also present power-law integrated exclusion curves from previous pulsar timing array experiment IPTA (comprising EPTA [205, 206, 207], NANOGrav-11 yr [208, 209, 210, 211], PPTA [212, 213]) and the future sensitivities of LISA [214] and SKA [215]. In addition, the strong signal reported by NANOGrav-12.5 yr [216, 217] (orange curves) recently is also shown and is very close to our largest prediction. Classifying this signal as gravitational waves is too early, although it touches our largest prediction.

Although current gravitational wave observations are not quite sensitive enough to see such a signal, future pulsar timing arrays are expected to probe this range. The diagonal band in Fig.8.1 corresponds to the case where the second axion has mass 10^{-9}eV so that the domain wall can form, which would occur when both axions are post-inflationary (scenario (3)). A vertical stripe to the right of the diagram corresponds to the case where the larger axion a_1 forms the domain walls.

8.5 Primordial Black Holes

Primordial Black Holes (PBHs) [220] can be formed from the collapse of closed domains containing a false vacuum, which start shrinking once their radii approach the Hubble horizon $\sim 1/H$. The energy is comprised of the wall tension (surface effect) and the interior false vacuum energy (volume effect), so it gives the mass

$$M_i = 4\pi r_i^2 \sigma_i + \frac{4\pi}{3} r_i^3 V_{bias}. \tag{8.22}$$

The domain will collapse into a black hole if its radius is smaller than the Schwarzschild radius $2M_i/M_{PL}^2$ [220]. For the small range of relevant masses, the bias term dominates, giving the black hole mass after the collapse

$$M_{PBH} = \frac{\sqrt{3}}{4\sqrt{2}} \frac{M_{PL}^3}{\sqrt{\pi\kappa K_{QCD}}} \sim 150 M_\odot \sqrt{\frac{0.1}{\kappa}}, \tag{8.23}$$

and the temperature at the collapse

$$T_{coll} \sim 25\text{MeV} \left(\frac{\kappa}{0.1}\right)^{1/4} \left(\frac{g_*}{10}\right)^{-1/4}. \tag{8.24}$$

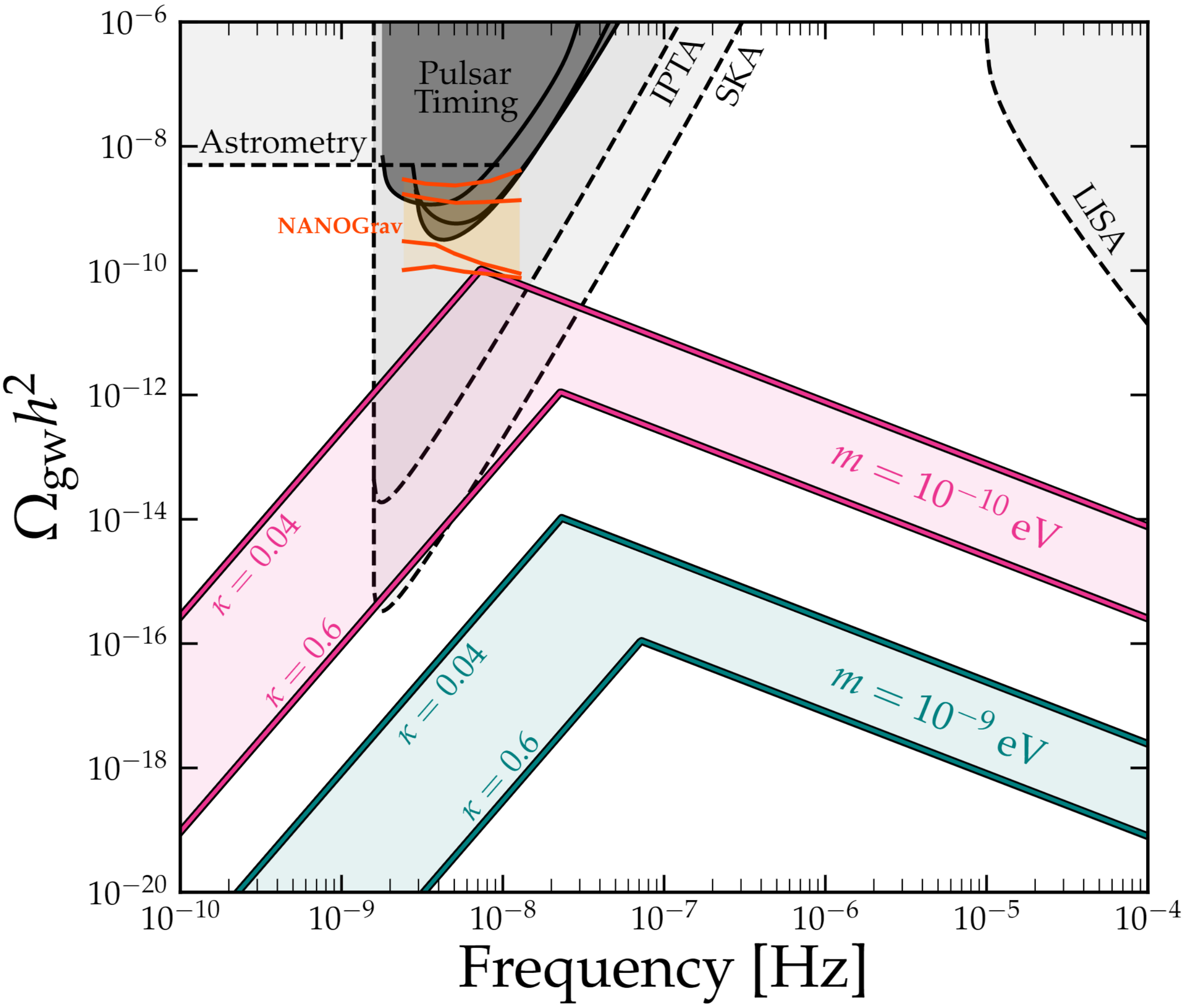

FIGURE 8.3: Relic abundance of GWs from domain wall decay. Previous pulsar timing array searches for GWs background EPTA, NANOGrav-11 yr, and PPTA are shown. We make use of the power-law integrated curves presented in [218] with the exception of the sensitivity to gravitational waves with astrometric data from [219].

In previous consideration [221] of PBHs, to preserve a single-axion solution to the strong CP problem, only a small bias term is allowed (equivalent to $\kappa \sim 10^{-12}$ in our model). Therefore, the PBHs could only be formed by having long-lasting $N > 1$ domain wall networks. For the single-axion model, the survival probability of domain walls can be estimated via numerical simulations [221, 222]. But using these results for the companion-axion model would be unreliable due to the complexity of the domain wall network and the large bias potential. Instead, we make a very crude analytical estimate as follows. We treat this process as the decay of a false vacuum with mean lifetime t_{ann}. Since the tunneling processes which destroy false vacuums have exponential time dependence, we can estimate that the fraction of closed domains which survive until the collapse temperature T_{coll} would be:

$$p_{coll} \sim e^{-(T_{ann}/T_{coll})^2} \sim 10^{-22} - 10^{-9}. \tag{8.25}$$

The considerable uncertainty in the prediction comes from $\kappa \in [0.06, 0.4]$. We also choose the axion mass to be 10^{-10}eV because a larger mass will make the survival probability negligibly small. The present-day PBH energy density then reads.

$$\rho_{PBH} \sim p_{coll} \frac{M_{PBH}}{r_i^3} \left(\frac{T_0}{T_{coll}} \right)^3 = p_{coll} \frac{M_{PL}^6}{M_{PBH}^2} \left(\frac{T_0}{T_{coll}} \right)^3, \tag{8.26}$$

giving a fraction of the dark matter density they constitute

$$f_{PBH} \sim 34.9 p_{coll} \frac{M_{PL}^6}{H_0^2 M_{PBH}^2} \left(\frac{T_0}{T_{coll}} \right)^3. \tag{8.27}$$

We see that the dramatic uncertainty of the dark matter fraction for $m = 10^{-10} eV$ goes from $\mathcal{O}(10^{-13})$ to $\mathcal{O}(1)$ inherited from κ. For heavier axions, PBH abundance is negligibly small. Although this calculation has many inaccuracies, it still explains the formation of a subdominant population of LIGO-sized PBHs.

CHAPTER 9

Conclusion

In this thesis, we have studied quantum gravity effects through the Yang-Mill-gravitational instantons that define the global structure of the vacuum and have unsuppressed effects on CP violation in strong interactions. The analysis in Chapter 6 has revealed a new source of CP violation that is bundled with the standard strong CP phase via coloured gravitational instantons (CEHs). Hence the vacuum structure of non-Abelian gauge theories, such as QCD, is more complicated when the gravitational effects are included than it is widely assumed based on the analysis that excludes gravity. We have stressed that this violation is an infrared topological effect and, hence, is unsuppressed by the Planck scale as it would naively be expected. Consequently, the size of the additional CP violation is only marginally smaller than the standard CP violation in flat spacetime and provides a sizable contribution to the relevant physical observables, most notably, to the electric dipole moment of the neutron. Therefore, the strong CP problem involves two, *a* priori unrelated, CP violating phases, that cannot be removed by the standard Peccei-Quinn mechanism to make the theory CP invariant to a level dictated by the observations.

We have introduced an axion extension to the standard Peccei-Quinn mechanism, offering fresh perspectives in axion phenomenology and cosmology.

In Chapter 6, we first computed the effective interaction induced by CEH instantons (in the dilute instanton gas approximation) and confirmed quantitatively that the standard Peccei–Quinn solution to the strong CP problem is compromised due to the new source of CP violation in the gravity-QCD sector. We proposed a simple remedy that extends the Peccei-Quinn symmetry to incorporate two axion fields.

The phenomenology of the companion axion model has been studied in Chapter 7, focusing on axion-photon couplings. The analysis is complicated relative to the one-axion model as it involves axion-axion interactions that may be relevant when two axion decay constants are of the same order of magnitude. In all cases though we find that the standard QCD axion state is accompanied with the lighter companion axion. We carefully re-evaluate the existing bounds on axion-photon couplings as well as present projections for future experiments. Most remarkably, we predict that future axion searches with haloscopes and helioscopes may well discover two QCD axions, perhaps even within the same experiment.

The companion axion model offers an interesting and lively cosmology as well. We have estimated the abundance of axions in all possible cosmological scenarios: where both axions are produced before inflation, after inflation or when the lighter axion is produced before and the heavier axion after inflation. In a large range of parameters, both axions can contribute to dark matter with in most cases the highest of them having a higher abundance.

The companion axion model naturally resolves the infamous axion domain wall problem once the two different contributions to the axion potential exhibit non-overlapping residual discrete symmetries. This is expected in a generic model. The cosmological consequences of this are quite interesting for a very small range of the theory parameters. In particular, we predict the generation of stochastic ~ 10 nHz gravitational wave background with large enough amplitude to be observable in pulsar timing arrays. In addition, the collision of fastly decaying unstable axion walls can produce primordial black holes of $\sim 100\ M_{\odot}$. Remarkably, there is tantalizing preliminary evidence of these effects reported in current astrophysical observations.

The identification of quantum gravity effects and their relevance for particle physics is a fascinating area of research. In this thesis, we just discussed one such object, the CEH instanton, that links quantum gravity with particle phenomenology. It is clear that further study of this area, in conjunction with theoretical and experimental aspects, can greatly enhance our understanding of particle physics.

References

[1] A. A. Belavin, A. M. Polyakov, A. S. Schwartz, and Y. S. Tyupkin, "Pseudoparticle solutions of the yang-mills equations," *Physics Letters B*, vol. 59, no. 1, pp. 85–87, 1975.

[2] S. W. Hawking, "Gravitational instantons," *Physics Letters A*, vol. 60, no. 2, pp. 81–83, 1977.

[3] C. A. Baker *et al.*, "An improved experimental limit on the electric dipole moment of the neutron," *Physical Review Letters*, vol. 97, no. 13, p. 131801, 2006.

[4] R. D. Peccei and H. R. Quinn, "Constraints imposed by CP conservation in the presence of instantons," *Physical Review D*, vol. 16, no. 6, p. 1791, 1977.

[5] R. D. Peccei and H. R. Quinn, "CP conservation in the presence of instantons," *Physical Review Letters*, vol. 38, no. 25, p. 1440, 1977.

[6] A. Ringwald and K. Saikawa, "Axion dark matter in the post-inflationary peccei-quinn symmetry breaking scenario," *Physical Review D*, vol. 93, no. 8, p. 085031, 2016.

[7] P. Sikivie, "Axion cosmology," *Axions: Theory, Cosmology, and Experimental Searches*, pp. 19–50, 2008.

[8] L. Visinelli and P. Gondolo, "Dark matter axions revisited," *Physical Review D*, vol. 80, no. 3, p. 035024, 2009.

[9] O. Wantz and E. P. S. Shellard, "Axion cosmology revisited," *Physical Review D*, vol. 82, no. 12, p. 123508, 2010.

[10] C. Bartram *et al.*, "Search for invisible axion dark matter in the 3.3–4.2 μ ev mass range," *Physical review letters*, vol. 127, no. 26, p. 261803, 2021.

[11] C. Boutan *et al.*, "Piezoelectrically tuned multimode cavity search for axion dark matter," *Physical Review Letters*, vol. 121, no. 26, p. 261302, 2018.

[12] R. Bradley, J. Clarke, D. Kinion, L. J. Rosenberg, K. van Bibber, S. Matsuki, M. Muck, and P. Sikivie, "Microwave cavity searches for dark-matter axions," *Reviews of Modern Physics*, vol. 75, no. 3, p. 777, 2003.

[13] T. Braine *et al.*, "Extended search for the invisible axion with the axion dark matter experiment," *Physical review letters*, vol. 124, no. 10, p. 101303, 2020.

[14] N. Du *et al.*, "Search for invisible axion dark matter with the axion dark matter experiment," *Physical review letters*, vol. 120, no. 15, p. 151301, 2018.

[15] A. A. Michelson and E. W. Morley, "On the relative motion of the earth and the luminiferous ether," *The London, Edinburgh, and Dublin Philosophical Magazine and Journal of Science*, vol. 24, no. 151, pp. 449–463, 1887.

[16] A. Einstein, "On the electrodynamics of moving bodies," *Annalen der physik*, vol. 17, no. 10, pp. 891–921, 1905.

[17] A. Einstein, "Zur elektrodynamik bewegter körper," *Annalen der physik*, vol. 4, 1905.

[18] J. B. Hartle, "Gravity: An introduction to einstein's general relativity," 2003.

[19] C. W. Misner, K. S. Thorne, and J. A. Wheeler, *Gravitation*. Freeman San Francisco, CA, 2000.

[20] R. M. Wald, *General relativity*. University of Chicago press, 2010.

[21] S. Weinberg, "Gravitation and cosmology: principles and applications of the general theory of relativity," 1972.

[22] S. S. Schweber, *QED and the men who made it: Dyson, Feynman, Schwinger, and Tomonaga*. 1994.

[23] J. S. Schwinger, "On gauge invariance and vacuum polarization," *Phys. Rev.*, vol. 82, pp. 664–679, 1951.

[24] J. S. Schwinger, "Quantum electrodynamics. 2. Vacuum polarization and selfenergy," *Phys. Rev.*, vol. 75, p. 651, 1948.

[25] S.-I. Tomonaga and J. R. Oppenheimer, "On Infinite Field Reactions in Quantum Field Theory," *Phys. Rev.*, vol. 74, pp. 224–225, 1948.

[26] F. J. Dyson, "Divergence of perturbation theory in quantum electrodynamics," *Phys. Rev.*, vol. 85, pp. 631–632, 1952.

[27] F. J. Dyson, "The Radiation theories of Tomonaga, Schwinger, and Feynman," *Phys. Rev.*, vol. 75, pp. 486–502, 1949.

[28] R. P. Feynman, "Relativistic cutoff for quantum electrodynamics," *Phys. Rev.*, vol. 74, pp. 1430–1438, 1948.

[29] J. Schwinger, "On Radiative Corrections to Electron Scattering," *Phys. Rev.*, vol. 75, pp. 898–899, 1949.

[30] A. Salam, "Weak and Electromagnetic Interactions," *Conf. Proc. C*, vol. 680519, pp. 367–377, 1968.

[31] S. Weinberg, "A Model of Leptons," *Phys. Rev. Lett.*, vol. 19, pp. 1264–1266, 1967.

[32] T. Nakano and K. Nishijima, "Charge Independence for V-particles," *Prog. Theor. Phys.*, vol. 10, pp. 581–582, 1953.

[33] K. Nishijima, "Charge Independence Theory of V Particles," *Prog. Theor. Phys.*, vol. 13, no. 3, pp. 285–304, 1955.

[34] M. Gell-Mann, "The interpretation of the new particles as displaced charge multiplets," *Nuovo Cim.*, vol. 4, no. S2, pp. 848–866, 1956.

[35] N. Cabibbo, "Unitary Symmetry and Leptonic Decays," *Phys. Rev. Lett.*, vol. 10, pp. 531–533, 1963.

[36] M. Kobayashi and T. Maskawa, "CP Violation in the Renormalizable Theory of Weak Interaction," *Prog. Theor. Phys.*, vol. 49, pp. 652–657, 1973.

[37] B. Pontecorvo, "Inverse beta processes and nonconservation of lepton charge," *Zh. Eksp. Teor. Fiz.*, vol. 34, p. 247, 1957.

[38] Z. Maki, M. Nakagawa, and S. Sakata, "Remarks on the unified model of elementary particles," *Prog. Theor. Phys.*, vol. 28, pp. 870–880, 1962.

[39] B. Pontecorvo, "Mesonium and anti-mesonium," *Sov. Phys. JETP*, vol. 6, p. 429, 1957.

[40] B. Pontecorvo, "Neutrino Experiments and the Problem of Conservation of Leptonic Charge," *Zh. Eksp. Teor. Fiz.*, vol. 53, pp. 1717–1725, 1967.

[41] S. L. Adler, "Axial-vector vertex in spinor electrodynamics," *Physical Review*, vol. 177, no. 5, p. 2426, 1969.

[42] J. S. Bell and R. Jackiw, "A pcac puzzle: $\pi^0 \to \gamma\gamma$ in the σ-model," *Nuovo cimento*, vol. 60, no. CERN-TH-920, pp. 47–61, 1969.

[43] M. D. Schwartz, *Quantum field theory and the standard model*. Cambridge university press, 2014.

[44] K. Fujikawa and H. Suzuki, *Path integrals and quantum anomalies*. No. 122, Oxford University Press, 2004.

[45] K. Fujikawa, "Path-integral measure for gauge-invariant fermion theories," *Physical Review Letters*, vol. 42, no. 18, p. 1195, 1979.

[46] K. Fujikawa, "Erratum: Path integral for gauge theories with fermions," *Phys. Rev. D*, vol. 22, pp. 1499–1499, Sep 1980.

[47] K. Fujikawa, "Path integral for gauge theories with fermions," *Physical Review D*, vol. 21, no. 10, p. 2848, 1980.

[48] A. I. Vainshtein, V. I. Zakharov, V. A. Novikov, and M. A. Shifman, "ABC of instantons," *Soviet Physics Uspekhi*, vol. 25, no. 4, p. 195, 1982.

[49] S. Coleman, *Aspects of symmetry: selected Erice lectures*. Cambridge University Press, 1988.

[50] S. Weinberg, "The $U(1)$ problem," *Physical Review D*, vol. 11, no. 12, p. 3583, 1975.

[51] G. 't Hooft, "How instantons solve the $U(1)$ problem," *Physics Reports*, vol. 142, no. 6, pp. 357–387, 1986.

[52] G. 't Hooft, "Computation of the quantum effects due to a four-dimensional pseudo-particle," *Physical review: D*, vol. 14, no. 12, pp. 3432–3450, 1976.

[53] G. W. Gibbons and S. W. Hawking, "Gravitational multi-instantons," *Physics Letters B*, vol. 78, no. 4, pp. 430–432, 1978.

[54] G. W. Gibbons and S. W. Hawking, "Classification of gravitational instanton symmetries," *Communications in Mathematical Physics*, vol. 66, pp. 291–310, 1979.

[55] T. Eguchi and A. J. Hanson, "Asymptotically flat self-dual solutions to euclidean gravity," *Physics letters B*, vol. 74, no. 3, pp. 249–251, 1978.

[56] T. Eguchi and A. J. Hanson, "Self-dual solutions to euclidean gravity," *Annals of Physics*, vol. 120, no. 1, pp. 82–106, 1979.

[57] E. Calabi, "Métriques kählériennes et fibrés holomorphes," in *Annales scientifiques de l'École normale supérieure*, vol. 12, pp. 269–294, 1979.

[58] T. Eguchi, P. B. Gilkey, and A. J. Hanson, "Gravitation, gauge theories and differential geometry," *Physics reports*, vol. 66, no. 6, pp. 213–393, 1980.

[59] H. Kim and Y. Yoon, "Yang–mills instantons in the gravitational instanton backgrounds," *Physics Letters B*, vol. 495, no. 1-2, pp. 169–175, 2000.

[60] S. Arunasalam and A. Kobakhidze, "Charged gravitational instantons: extra CP violation and charge quantisation in the standard model," *The European Physical Journal C*, vol. 79, pp. 1–5, 2019.

[61] H. Boutaleb-Joutei, A. Chakrabarti, and A. Comtet, "Gauge field configurations in curved spacetimes. i," *Physical Review D*, vol. 20, no. 8, p. 1884, 1979.

[62] H. Boutaleb-Joutei, A. Chakrabarti, and A. Comtet, "Gauge field configurations in curved spacetimes. ii," *Physical Review D*, vol. 20, no. 8, p. 1898, 1979.

[63] H. Boutaleb-Joutei, A. Chakrabarti, and A. Comtet, "Gauge field configurations in curved space-times. iii. self-dual su(2) fields in eguchi-hanson space," *Physical Review D*, vol. 21, no. 4, p. 979, 1980.

[64] H. Boutaleb-Joutei, A. Chakrabarti, and A. Comtet, "Gauge field configurations in curved space-times. iv. self-dual su(2) fields in multicenter spaces," *Physical Review D*, vol. 21, no. 8, p. 2280, 1980.

[65] H. Boutaleb-Joutei, A. Chakrabarti, and A. Comtet, "Gauge field configurations in curved space-times. v. regularity constraints and quantized actions," *Physical Review D*, vol. 21, no. 8, p. 2285, 1980.

[66] M. Bianchi, F. Fucito, G. Rossi, and M. Martellini, "Explicit construction of yang-mills instantons on ale spaces," *Nuclear Physics B*, vol. 473, no. 1-2, pp. 367–404, 1996.

[67] J. S. Schwinger, "The Theory of quantized fields. 1.," *Phys. Rev.*, vol. 82, pp. 914–927, 1951.

[68] G. Luders, "On the Equivalence of Invariance under Time Reversal and under Particle-Antiparticle Conjugation for Relativistic Field Theories," *Kong. Dan. Vid. Sel. Mat. Fys. Med.*, vol. 28N5, no. 5, pp. 1–17, 1954.

[69] J. H. Christenson, J. W. Cronin, V. L. Fitch, and R. Turlay, "Evidence for the 2π decay of the k_2^0 meson," *Physical Review Letters*, vol. 13, no. 4, p. 138, 1964.

[70] M. Abramczyk, S. Aoki, T. Blum, T. Izubuchi, H. Ohki, and S. Syritsyn, "Lattice calculation of electric dipole moments and form factors of the nucleon," *Physical Review D*, vol. 96, no. 1, p. 014501, 2017.

[71] V. Baluni, "CP-nonconserving effects in quantum chromodynamics," *Physical Review D*, vol. 19, no. 7, p. 2227, 1979.

[72] L. Bartolini, F. Bigazzi, S. Bolognesi, A. L. Cotrone, and A. Manenti, "Neutron electric dipole moment from gauge-string duality," *Physical Review Letters*, vol. 118, no. 9, p. 091601, 2017.

[73] R. J. Crewther, P. Di Vecchia, G. Veneziano, and E. Witten, "Chiral estimate of the electric dipole moment of the neutron in quantum chromodynamics," *Physics Letters B*, vol. 88, no. 1-2, pp. 123–127, 1979.

[74] E. de Rafael, "Strong CP-violation in an effective chiral lagrangian approach," *Nuclear Physics B*, vol. 367, no. 2, pp. 313–333, 1991.

[75] M. Pospelov and A. Ritz, "Theta vacua, QCD sum rules, and the neutron electric dipole moment," *Nuclear Physics B*, vol. 573, no. 1-2, pp. 177–200, 2000.

[76] E. M. Purcell and N. F. Ramsey, "On the possibility of electric dipole moments for elementary particles and nuclei," *Physical Review*, vol. 78, no. 6, p. 807, 1950.

[77] J. M. Pendlebury *et al.*, "Revised experimental upper limit on the electric dipole moment of the neutron," *Physical Review D*, vol. 92, no. 9, p. 092003, 2015.

[78] S. Weinberg, "A new light boson?," *Physical Review Letters*, vol. 40, no. 4, p. 223, 1978.

[79] F. Wilczek, "Problem of strong P and T invariance in the presence of instantons," *Physical Review Letters*, vol. 40, no. 5, p. 279, 1978.

[80] J. E. Kim, "Weak-interaction singlet and strong CP invariance," *Physical Review Letters*, vol. 43, no. 2, p. 103, 1979.

[81] M. A. Shifman, A. I. Vainshtein, and V. I. Zakharov, "Can confinement ensure natural CP invariance of strong interactions?," *Nuclear Physics B*, vol. 166, no. 3, pp. 493–506, 1980.

[82] A. R. Zhitnitsky, "On possible suppression of the axion-hadron interactions," *Yadernaya Fizika*, vol. 31, no. 2, pp. 497–504, 1980.

[83] M. Dine, W. Fischler, and M. Srednicki, "A simple solution to the strong CP problem with a harmless axion," *Physics letters B*, vol. 104, no. 3, pp. 199–202, 1981.

[84] Y. Asano, E. Kikutani, S. Kurokawa, T. Miyachi, M. Miyajima, Y. Nagashima, T. Shinkawa, S. Sugimoto, and Y. Yoshimura, "Search for a rare decay mode k+$\rightarrow \pi$+ νv and axion," *Physics Letters B*, vol. 107, no. 1-2, pp. 159–162, 1981.

[85] W. A. Bardeen, R. D. Peccei, and T. Yanagida, "Constraints on variant axion models," *Nuclear Physics B*, vol. 279, no. 3-4, pp. 401–428, 1987.

[86] J. E. Kim, "Light pseudoscalars, particle physics and cosmology," *Physics Reports*, vol. 150, no. 1-2, pp. 1–177, 1987.

[87] K. Mimasu and V. Sanz, "ALPs at colliders," *Journal of High Energy Physics*, vol. 2015, no. 6, pp. 1–25, 2015.

[88] K. van Bibber, P. M. McIntyre, D. E. Morris, and G. G. Raffelt, "A Practical Laboratory Detector for Solar Axions," *Phys. Rev. D*, vol. 39, p. 2089, 1989.

[89] K. Zioutas *et al.*, "A Decommissioned LHC model magnet as an axion telescope," *Nucl. Instrum. Meth. A*, vol. 425, pp. 480–489, 1999.

[90] K. Zioutas *et al.*, "First results from the CERN Axion Solar Telescope (CAST)," *Phys. Rev. Lett.*, vol. 94, p. 121301, 2005.

[91] I. G. Irastorza *et al.*, "Towards a new generation axion helioscope," *JCAP*, vol. 06, p. 013, 2011.

[92] I. G. Irastorza, F. Avignone, A. Liolios, S. Russenschuck, H. t. Kate, K. van Bibber, T. Geralis, O. Limousin, J. Villar, H. Gomez, *et al.*, "The international axion observatory iaxo. letter of intent to the cern sps committee," tech. rep., 2013.

[93] N. Du *et al.*, "A Search for Invisible Axion Dark Matter with the Axion Dark Matter Experiment," *Phys. Rev. Lett.*, vol. 120, no. 15, p. 151301, 2018.

[94] B. M. Brubaker *et al.*, "First results from a microwave cavity axion search at 24 μeV," *Phys. Rev. Lett.*, vol. 118, no. 6, p. 061302, 2017.

[95] C. M. Adair *et al.*, "Search for Dark Matter Axions with CAST-CAPP," *Nature Commun.*, vol. 13, no. 1, p. 6180, 2022.

[96] A. A. Melcón *et al.*, "First results of the CAST-RADES haloscope search for axions at 34.67 μeV," *JHEP*, vol. 21, p. 075, 2020.

[97] R. Ballou *et al.*, "New exclusion limits on scalar and pseudoscalar axionlike particles from light shining through a wall," *Phys. Rev. D*, vol. 92, no. 9, p. 092002, 2015.

[98] G. Raffelt and A. Weiss, "Red giant bound on the axion - electron coupling revisited," *Phys. Rev. D*, vol. 51, pp. 1495–1498, 1995.

[99] J. Isern and E. Garcia-Berro, "White dwarf stars as particle physics laboratories," *Nucl. Phys. B Proc. Suppl.*, vol. 114, pp. 107–110, 2003.

[100] G. G. Raffelt, "Astrophysical axion bounds," *LECTURE NOTES IN PHYSICS-NEW YORK THEN BERLIN-*, vol. 741, p. 51, 2008.

[101] J. R. Ellis and K. A. Olive, "Constraints on Light Particles From Supernova Sn1987A," *Phys. Lett. B*, vol. 193, p. 525, 1987.

[102] J. Engel, D. Seckel, and A. C. Hayes, "Emission and detectability of hadronic axions from SN1987A," *Phys. Rev. Lett.*, vol. 65, pp. 960–963, 1990.

[103] L. F. Abbott and P. Sikivie, "A cosmological bound on the invisible axion," *Physics Letters B*, vol. 120, no. 1-3, pp. 133–136, 1983.

[104] R. L. Davis, "Cosmic axions from cosmic strings," *Physics Letters B*, vol. 180, no. 3, pp. 225–230, 1986.

[105] M. Dine and W. Fischler, "The Not So Harmless Axion," *Physics Letters B*, vol. 120, no. 1-3, pp. 137–141, 1983.

[106] J. Ipser and P. Sikivie, "Are galactic halos made of axions?," *Physical Review Letters*, vol. 50, no. 12, p. 925, 1983.

[107] D. J. E. Marsh, "Axion cosmology," *Physics Reports*, vol. 643, pp. 1–79, 2016.

[108] C. A. J. O'Hare, *Detecting WIMPs, neutrinos and axions in the next generation of dark matter experiment*. PhD thesis, University of Nottingham, 2017.

[109] J. Preskill, M. B. Wise, and F. Wilczek, "Cosmology of the invisible axion," *Physics Letters B*, vol. 120, no. 1-3, pp. 127–132, 1983.

[110] E. W. Kolb and M. S. Turner, "The early universe," *Nature*, vol. 294, no. 5841, pp. 521–526, 1981.

[111] M. S. Turner, "Thermal production of not so invisible axions in the early universe," tech. rep., Fermi National Accelerator Lab., 1986.

[112] E. Masso, F. Rota, and G. Zsembinszki, "Axion thermalization in the early universe," *Physical Review D*, vol. 66, no. 2, p. 023004, 2002.

[113] K. Saikawa, *Production and evolution of axion dark matter in the early universe*. PhD thesis, Ph. D. thesis, University of Tokyo, 2013.

[114] S. Deser, M. J. Duff, and C. J. Isham, "Gravitationally induced CP effects," *Physics Letters B*, vol. 93, no. 4, pp. 419–423, 1980.

[115] R. Holman, T. W. Kephart, and S.-J. Rey, "Semiclassical gravity and invisible axions," *Physical review letters*, vol. 71, no. 3, p. 320, 1993.

[116] M. F. Atiyah, V. K. Patodi, and I. M. Singer, "Spectral asymmetry and riemannian geometry. i," in *Mathematical Proceedings of the Cambridge Philosophical Society*, vol. 77, pp. 43–69, Cambridge University Press, 1975.

[117] C. W. Bernard, "Gauge zero modes, instanton determinants, and quantum-chromodynamic calculations," *Physical Review D*, vol. 19, no. 10, p. 3013, 1979.

[118] G. 't Hooft, "Symmetry breaking through bell-jackiw anomalies," *Phys. Rev. Lett.*, vol. 37, pp. 8–11, Jul 1976.

[119] A. Deur, S. J. Brodsky, and G. F. de Teramond, "The qcd running coupling," *Progress in Particle and Nuclear Physics*, vol. 90, pp. 1–74, 2016.

[120] B. S. Acharya, K. Bobkov, and P. Kumar, "An M theory solution to the strong CP-problem, and constraints on the axiverse," *Journal of High Energy Physics*, vol. 2010, no. 11, pp. 1–31, 2010.

[121] A. Arvanitaki, S. Dimopoulos, S. Dubovsky, N. Kaloper, and J. March-Russell, "String axiverse," *Physical Review D*, vol. 81, no. 12, p. 123530, 2010.

[122] M. Cicoli, M. Goodsell, and A. Ringwald, "The type iib string axiverse and its low-energy phenomenology," *Journal of High Energy Physics*, vol. 2012, no. 10, pp. 1–65, 2012.

[123] J. Jaeckel and A. Ringwald, "The low-energy frontier of particle physics," *Annual Review of Nuclear and Particle Science*, vol. 60, pp. 405–437, 2010.

[124] E. Masso, "Axions and axion-like particles," *Nuclear Physics B-Proceedings Supplements*, vol. 114, pp. 67–73, 2003.

[125] E. Masso and R. Toldra, "Light spinless particle coupled to photons," *Physical Review D*, vol. 52, no. 4, p. 1755, 1995.

[126] A. Ringwald, "Exploring the role of axions and other WISPs in the dark universe," *Physics of the Dark Universe*, vol. 1, no. 1-2, pp. 116–135, 2012.

[127] A. Ringwald, "Searching for axions and alps from string theory," in *Journal of Physics: Conference Series*, vol. 485, p. 012013, IOP Publishing, 2014.

[128] M. J. Stott, D. J. E. Marsh, C. Pongkitivanichkul, L. C. Price, and B. S. Acharya, "Spectrum of the axion dark sector," *Physical Review D*, vol. 96, no. 8, p. 083510, 2017.

[129] P. Svrcek and E. Witten, "Axions in string theory," *Journal of High Energy Physics*, vol. 2006, no. 06, p. 051, 2006.

[130] F. Chadha-Day, "Axion-like particle oscillations," *Journal of Cosmology and Astroparticle Physics*, vol. 2022, no. 01, p. 013, 2022.

[131] D. Cyncynates, T. Giurgica-Tiron, O. Simon, and J. O. Thompson, "Friendship in the axiverse: Late-time direct and astrophysical signatures of early-time nonlinear axion dynamics," *arXiv preprint arXiv:2109.09755*, 2021.

[132] N. Kitajima and F. Takahashi, "Resonant conversions of qcd axions into hidden axions and suppressed isocurvature perturbations," *Journal of Cosmology and Astroparticle Physics*, vol. 2015, no. 01, p. 032, 2015.

[133] D. J. E. Marsh and W. Yin, "Opening the 1Hz axion window," *Journal of High Energy Physics*, vol. 2021, no. 1, pp. 1–30, 2021.

[134] M. Reig, "The stochastic axiverse," *Journal of High Energy Physics*, vol. 2021, no. 9, pp. 1–40, 2021.

[135] Z. Chen, A. Kobakhidze, C. A. J. O'Hare, Z. S. C. Picker, and G. Pierobon, "Cosmology of the companion-axion model: dark matter, gravitational waves, and primordial black holes," *arXiv preprint arXiv:2110.11014*, 2021.

[136] Z. Chen, A. Kobakhidze, C. A. J. O'Hare, Z. S. C. Picker, and G. Pierobon, "Phenomenology of the companion-axion model: photon couplings," *The European Physical Journal C*, vol. 82, no. 10, p. 940, 2022.

[137] L. Di Luzio, M. Giannotti, E. Nardi, and L. Visinelli, "The landscape of QCD axion models," *Physics Reports*, vol. 870, pp. 1–117, 2020.

[138] M. Srednicki, “Axion couplings to matter: (I). CP-conserving parts,” *Nuclear Physics B*, vol. 260, no. 3-4, pp. 689–700, 1985.

[139] W. A. Bardeen and S. H. H. Tye, “Current algebra applied to properties of the light higgs boson,” *Physics Letters B*, vol. 74, no. 3, pp. 229–232, 1978.

[140] Z. Chen and A. Kobakhidze, “Coloured gravitational instantons, the strong CP problem and the companion axion solution,” *The European Physical Journal C*, vol. 82, no. 7, pp. 1–6, 2022.

[141] A. A. Melcón *et al.*, “First results of the cast-rades haloscope search for axions at 34.67 μev,” *Journal of High Energy Physics*, vol. 2021, no. 10, pp. 1–16, 2021.

[142] B. T. McAllister, G. Flower, J. Kruger, E. N. Ivanov, M. Goryachev, J. Bourhill, and M. E. Tobar, “The ORGAN experiment: An axion haloscope above 15 GHz,” *Physics of the dark universe*, vol. 18, pp. 67–72, 2017.

[143] S. Andriamonje *et al.*, “An Improved limit on the axion-photon coupling from the CAST experiment,” *JCAP*, vol. 04, p. 010, 2007.

[144] V. Anastassopoulos *et al.*, “New CAST Limit on the Axion-Photon Interaction,” *Nature Phys.*, vol. 13, pp. 584–590, 2017.

[145] S. Beurthey *et al.*, “MADMAX status report,” *arXiv preprint arXiv:2003.10894*, 2020.

[146] E. Armengaud *et al.*, “Physics potential of the international axion observatory (IAXO),” *Journal of Cosmology and Astroparticle Physics*, vol. 2019, no. 06, p. 047, 2019.

[147] Y. Kahn, B. R. Safdi, and J. Thaler, “Broadband and resonant approaches to axion dark matter detection,” *Physical review letters*, vol. 117, no. 14, p. 141801, 2016.

[148] https://irwinlab.sites.stanford.edu/dark-matter-radio-dmradio.

[149] A. Ayala, I. Domínguez, M. Giannotti, A. Mirizzi, and O. Straniero, “Revisiting the bound on axion-photon coupling from globular clusters,” *Physical review letters*, vol. 113, no. 19, p. 191302, 2014.

[150] P. Sikivie, “Experimental tests of the" invisible" axion,” *Physical Review Letters*, vol. 51, no. 16, p. 1415, 1983.

[151] M. Arik *et al.*, “Search for solar axions by the CERN axion solar telescope with He 3 buffer gas: Closing the hot dark matter gap,” *Physical review letters*, vol. 112, no. 9, p. 091302, 2014.

[152] M. Arik *et al.*, “New solar axion search using the cern axion solar telescope with ^{4}he filling,” *Physical Review D*, vol. 92, no. 2, p. 021101, 2015.

[153] S. R. Dolan, "Instability of the massive klein-gordon field on the kerr spacetime," *Physical Review D*, vol. 76, no. 8, p. 084001, 2007.

[154] A. Arvanitaki and S. Dubovsky, "Exploring the string axiverse with precision black hole physics," *Physical Review D*, vol. 83, no. 4, p. 044026, 2011.

[155] P. Pani, V. Cardoso, L. Gualtieri, E. Berti, and A. Ishibashi, "Black hole bombs and photon mass bounds," *Physical review letters*, vol. 109, no. 13, p. 131102, 2012.

[156] R. Brito, V. Cardoso, and P. Pani, *Superradiance*, vol. 10. Springer, 2020.

[157] A. Arvanitaki, M. Baryakhtar, and X. Huang, "Discovering the qcd axion with black holes and gravitational waves," *Physical Review D*, vol. 91, no. 8, p. 084011, 2015.

[158] A. Arvanitaki, M. Baryakhtar, S. Dimopoulos, S. Dubovsky, and R. Lasenby, "Black hole mergers and the qcd axion at advanced ligo," *Physical Review D*, vol. 95, no. 4, p. 043001, 2017.

[159] H. F. Rúnarsson, "Kerr black holes with proca hair," *Classical and Quantum Gravity*, vol. 33, no. 15, p. 154001, 2016.

[160] V. Cardoso, O. J. C. Dias, G. S. Hartnett, M. Middleton, P. Pani, and J. E. Santos, "Constraining the mass of dark photons and axion-like particles through black-hole superradiance," *Journal of Cosmology and Astroparticle Physics*, vol. 2018, no. 03, p. 043, 2018.

[161] M. J. Stott and D. J. E. Marsh, "Black hole spin constraints on the mass spectrum and number of axionlike fields," *Physical Review D*, vol. 98, no. 8, p. 083006, 2018.

[162] V. M. Mehta, M. Demirtas, C. Long, D. J. E. Marsh, L. Mcallister, and M. J. Stott, "Superradiance exclusions in the landscape of type iib string theory," *arXiv preprint arXiv:2011.08693*, 2020.

[163] V. M. Mehta, M. Demirtas, C. Long, D. J. E. Marsh, L. McAllister, and M. J. Stott, "Superradiance in string theory," *Journal of Cosmology and Astroparticle Physics*, vol. 2021, no. 07, p. 033, 2021.

[164] M. J. Stott, "Ultralight bosonic field mass bounds from astrophysical black hole spin," *arXiv preprint arXiv:2009.07206*, 2020.

[165] A. Abeln *et al.*, "Conceptual design of BabyIAXO, the intermediate stage towards the International Axion Observatory," *Journal of High Energy Physics*, vol. 2021, no. 5, pp. 1–80, 2021.

[166] E. Armengaud *et al.*, "Conceptual design of the international axion observatory (IAXO)," *Journal of Instrumentation*, vol. 9, no. 05, p. T05002, 2014.

[167] D. Alesini, D. Babusci, D. Di Gioacchino, C. Gatti, G. Lamanna, and C. Ligi, "The KLASH proposal," *arXiv preprint arXiv:1707.06010*, 2017.

[168] J. Jeong, S. Youn, S. Ahn, J. E. Kim, and Y. K. Semertzidis, "Concept of multiple-cell cavity for axion dark matter search," *Physics Letters B*, vol. 777, pp. 412–419, 2018.

[169] A. A. Melcón *et al.*, "Axion searches with microwave filters: the RADES project," *Journal of Cosmology and Astroparticle Physics*, vol. 2018, no. 05, p. 040, 2018.

[170] A. Álvarez Melcón *et al.*, "Scalable haloscopes for axion dark matter detection in the 30 μeV range with RADES," *Journal of High Energy Physics*, vol. 2020, no. 7, pp. 1–28, 2020.

[171] I. Stern and A. Status, "PoS ICHEP2016, 198 (2016)."

[172] J. L. Ouellet *et al.*, "First results from ABRACADABRA-10 cm: a search for sub-μ eV axion dark matter," *Physical review letters*, vol. 122, no. 12, p. 121802, 2019.

[173] N. Crisosto, P. Sikivie, N. S. Sullivan, D. B. Tanner, J. Yang, and G. Rybka, "ADMX SLIC: results from a superconducting LC circuit investigating cold axions," *Physical Review Letters*, vol. 124, no. 24, p. 241101, 2020.

[174] J. A. Devlin *et al.*, "Constraints on the coupling between axionlike dark matter and photons using an antiproton superconducting tuned detection circuit in a cryogenic penning trap," *Physical Review Letters*, vol. 126, no. 4, p. 041301, 2021.

[175] M. S. Turner, "Cosmic and local mass density of "invisible" axions," *Physical Review D*, vol. 33, no. 4, p. 889, 1986.

[176] D. H. Lyth, "Axions and inflation: Sitting in the vacuum," *Phys. Rev. D*, vol. 45, no. 3394, p. 44, 1992.

[177] K. Strobl and T. J. Weiler, "Anharmonic evolution of the cosmic axion density spectrum," *Physical Review D*, vol. 50, no. 12, p. 7690, 1994.

[178] K. J. Bae, J.-H. Huh, and J. E. Kim, "Update of axion CDM energy density," *arXiv preprint arXiv:0806.0497*, 2008.

[179] C. Carilli and S. Rawlings, "Science with the Square Kilometer Array: Motivation, key science projects, standards and assumptions," *arXiv preprint astro-ph/0409274*, 2004.

[180] G. Janssen *et al.*, "Gravitational wave astronomy with the SKA," *arXiv preprint arXiv:1501.00127*, 2014.

[181] A. Weltman *et al.*, "Fundamental physics with the square kilometre array," *Publications of the Astronomical Society of Australia*, vol. 37, p. e002, 2020.

[182] M. Beltran, J. Garcia-Bellido, and J. Lesgourgues, "Isocurvature bounds on axions revisited," *Physical Review D*, vol. 75, no. 10, p. 103507, 2007.

[183] M. Beltran, J. Garcia-Bellido, J. Lesgourgues, A. R. Liddle, and A. Slosar, "Bayesian model selection and isocurvature perturbations," *Physical Review D*, vol. 71, no. 6, p. 063532, 2005.

[184] P. Crotty, J. Garcia-Bellido, J. Lesgourgues, and A. Riazuelo, "Bounds on isocurvature perturbations from cosmic microwave background and large scale structure data," *Physical Review Letters*, vol. 91, no. 17, p. 171301, 2003.

[185] T. Kobayashi, R. Kurematsu, and F. Takahashi, "Isocurvature constraints and anharmonic effects on qcd axion dark matter," *Journal of Cosmology and Astroparticle Physics*, vol. 2013, no. 09, p. 032, 2013.

[186] Y. Akrami *et al.*, "Planck 2018 results-X. Constraints on inflation," *Astronomy & Astrophysics*, vol. 641, p. A10, 2020.

[187] Y. B. Zeldovich, "Cosmological fluctuations produced near a singularity," *Monthly Notices of the Royal Astronomical Society*, vol. 192, no. 4, pp. 663–667, 1980.

[188] P. Sikivie, "Axions, domain walls, and the early universe," *Physical Review Letters*, vol. 48, no. 17, p. 1156, 1982.

[189] A. Vilenkin, "Cosmic strings and domain walls," *Physics reports*, vol. 121, no. 5, pp. 263–315, 1985.

[190] S. M. Barr, X. C. Gao, and D. Reiss, "Peccei-quinn symmetries without domains," *Physical Review D*, vol. 26, no. 8, p. 2176, 1982.

[191] G. Lazarides and Q. Shafi, "Axion models with no domain wall problem," *Physics Letters B*, vol. 115, no. 1, pp. 21–25, 1982.

[192] G. R. Dvali, Z. Tavartkiladze, and J. Nanobashvili, "Biased discrete symmetry and domain wall problem," *Physics Letters B*, vol. 352, no. 3-4, pp. 214–219, 1995.

[193] C. Hagmann, S. Chang, and P. Sikivie, "Axions from string decay," *Nuclear Physics B-Proceedings Supplements*, vol. 72, pp. 81–86, 1999.

[194] B. Rai and G. Senjanovic, "Gravity and the domain-wall problem," *Physical Review D*, vol. 49, no. 6, p. 2729, 1994.

[195] S. M. Barr and J. E. Kim, "New confining force solution of the qcd axion domain-wall problem," *Physical Review Letters*, vol. 113, no. 24, p. 241301, 2014.

[196] M. Reig, "On the high-scale instanton interference effect: axion models without domain wall problem," *Journal of High Energy Physics*, vol. 2019, no. 8, pp. 1–13, 2019.

[197] A. Caputo and M. Reig, “Cosmic implications of a low-scale solution to the axion domain wall problem,” *Physical Review D*, vol. 100, no. 6, p. 063530, 2019.

[198] G. B. Gelmini, M. Gleiser, and E. W. Kolb, “Cosmology of biased discrete symmetry breaking,” *Phys. Rev. D*, vol. 39, pp. 1558–1566, Mar 1989.

[199] T. W. B. Kibble, G. Lazarides, and Q. Shafi, “Walls bounded by strings,” *Physical Review D*, vol. 26, no. 2, p. 435, 1982.

[200] T. W. B. Kibble, “Topology of cosmic domains and strings,” *Journal of Physics A: Mathematical and General*, vol. 9, no. 8, p. 1387, 1976.

[201] M. Kawasaki and K. Saikawa, “Study of gravitational radiation from cosmic domain walls,” *JCAP*, vol. 09, p. 008, 2011.

[202] T. Hiramatsu, M. Kawasaki, and K. Saikawa, “Gravitational Waves from Collapsing Domain Walls,” *JCAP*, vol. 05, p. 032, 2010.

[203] T. Hiramatsu, M. Kawasaki, and K. Saikawa, “On the estimation of gravitational wave spectrum from cosmic domain walls,” *JCAP*, vol. 02, p. 031, 2014.

[204] K. Saikawa, “A review of gravitational waves from cosmic domain walls,” *Universe*, vol. 3, no. 2, p. 40, 2017.

[205] M. Kramer and D. J. Champion, “The European Pulsar Timing Array and the Large European Array for Pulsars,” *Class. Quant. Grav.*, vol. 30, p. 224009, 2013.

[206] L. Lentati *et al.*, “European Pulsar Timing Array Limits On An Isotropic Stochastic Gravitational-Wave Background,” *Mon. Not. Roy. Astron. Soc.*, vol. 453, no. 3, pp. 2576–2598, 2015.

[207] S. Babak *et al.*, “European Pulsar Timing Array Limits on Continuous Gravitational Waves from Individual Supermassive Black Hole Binaries,” *Mon. Not. Roy. Astron. Soc.*, vol. 455, no. 2, pp. 1665–1679, 2016.

[208] M. A. McLaughlin, “The North American Nanohertz Observatory for Gravitational Waves,” *Class. Quant. Grav.*, vol. 30, p. 224008, 2013.

[209] Z. Arzoumanian *et al.*, “The NANOGrav 11-year Data Set: Pulsar-timing Constraints On The Stochastic Gravitational-wave Background,” *Astrophys. J.*, vol. 859, no. 1, p. 47, 2018.

[210] K. Aggarwal *et al.*, “The NANOGrav 11-Year Data Set: Limits on Gravitational Waves from Individual Supermassive Black Hole Binaries,” *Astrophys. J.*, vol. 880, p. 2, 2019.

[211] A. Brazier *et al.*, “The NANOGrav Program for Gravitational Waves and Fundamental Physics,” 8 2019.

[212] R. N. Manchester *et al.*, “The Parkes Pulsar Timing Array Project,” *Publ. Astron. Soc. Austral.*, vol. 30, p. 17, 2013.

[213] R. M. Shannon *et al.*, “Gravitational waves from binary supermassive black holes missing in pulsar observations,” *Science*, vol. 349, no. 6255, pp. 1522–1525, 2015.

[214] P. Amaro-Seoane *et al.*, “Laser Interferometer Space Antenna,” 2 2017.

[215] C. L. Carilli and S. Rawlings, “Science with the Square Kilometer Array: Motivation, key science projects, standards and assumptions,” *New Astron. Rev.*, vol. 48, p. 979, 2004.

[216] Z. Arzoumanian, P. T. Baker, H. Blumer, B. Bécsy, A. Brazier, P. R. Brook, S. Burke-Spolaor, S. Chatterjee, S. Chen, J. M. Cordes, *et al.*, “The nanograv 12.5 yr data set: search for an isotropic stochastic gravitational-wave background,” *The Astrophysical Journal Letters*, vol. 905, no. 2, p. L34, 2020.

[217] K. Kohri and T. Terada, “Solar-Mass Primordial Black Holes Explain NANOGrav Hint of Gravitational Waves,” *Phys. Lett. B*, vol. 813, p. 136040, 2021.

[218] K. Schmitz, “New Sensitivity Curves for Gravitational-Wave Signals from Cosmological Phase Transitions,” *JHEP*, vol. 01, p. 097, 2021.

[219] J. Darling, A. E. Truebenbach, and J. Paine, “Astrometric Limits on the Stochastic Gravitational Wave Background,” *Astrophys. J.*, vol. 861, no. 2, p. 113, 2018.

[220] S. W. Hawking, I. G. Moss, and J. M. Stewart, “Bubble Collisions in the Very Early Universe,” *Phys. Rev. D*, vol. 26, p. 2681, 1982.

[221] F. Ferrer, E. Masso, G. Panico, O. Pujolas, and F. Rompineve, “Primordial Black Holes from the QCD axion,” *Phys. Rev. Lett.*, vol. 122, no. 10, p. 101301, 2019.

[222] M. Kawasaki, K. Saikawa, and T. Sekiguchi, “Axion dark matter from topological defects,” *Phys. Rev. D*, vol. 91, no. 6, p. 065014, 2015.